December 2019

The Effects of Indirubin Derivative E804 on Inflammatory Profiles in Glioblastoma Multiforme Cell Lines and Subsequent Crosstalk Effect on Tumor Associated THP-1 Macrophages

Micaela Ro Scobie
Clemson University, micaela.scobie@gmail.com

THE EFFECTS OF INDIRUBIN DERIVATIVE E804 ON INFLAMMATORY PROFILES IN GLIOBLASTOMA MULTIFORME CELL LINES AND SUBSEQUENT CROSSTALK EFFECT ON TUMOR ASSOCIATED THP-1 MACROPHAGES

A Dissertation
Presented to
the Graduate School of
Clemson University

In Partial Fulfillment
of the Requirements for the Degree
Doctor of Philosophy
Biological Sciences

---

by
Micaela Ro Scobie
December 2019

Accepted by:
Dr. Charles D. Rice, Committee Chair
Dr. Vincent S. Gallicchio
Dr. Vincent P. Richards
Dr. Yanzhang Wei

ABSTRACT

Glioblastoma Multiforme (GBM) is a highly invasive brain tumor that affects approximately 18,000 people annually in the USA alone yet remains without curative treatment. Median survival with treatment is 14 months, with most treatments only prolonging life for several months while causing severe adverse side effects. There is a need for new therapeutic modalities. Herein I explore two small molecules that show promise in modulating inflammatory signaling in an *in vitro* GBM model. Indirubins E804 (indirubin-3'-(2,3 dihydroxypropyl)-oximether) and 7BIO (7-Bromoindirubin-3'-oxime) are synthetic derivatives of natural indirubin. Natural indirubin is a bisindole alkaloid derived from tryptophan precursors and is an agonist for the ligand-activated transcription factor aryl hydrocarbon receptor (AHR). Indirubin has been shown to disrupt important cancer-driving signaling such as JAK/STAT3, GSK3, and CDKs. To determine AHR pathway significance in my results, I added a selective AHR antagonist, 6,2',4'-trimethoxyflavone (TMF), in addition to indirubins. Herein I show that E804 modulates a large array of inflammatory genes, including down-regulation of important autocrine GBM signaling molecules like IL-6 and VEGF, which help drive tumor development. 7BIO, but not E804, increased the expression of STAT3, suggesting that this compound is not suitable for glioma therapy. Additional studies showed that E804 does not fully activate the unfolded protein response (UPR). The UPR is an ER stress pathway that can induce

indiscriminate apoptosis - an undesirable side effect in an area as sensitive as the brain. Finally, using transcriptomics combined with pathway analysis, I examined the effects that E804- or E804+TMF-treated glioblastoma cells have on differentiated THP-1 macrophages to model the effects that gliomas may have on glioma-associated macrophages. Glioma-associated macrophages can comprise up to 30% of GBM mass, and, if activated by certain glioma-derived signals, have been implicated in tumor promotion. I found that treated-GBM supernatants inhibited gene profiles in THP-1 macrophages that are linked to tumor progression, such as the Wnt, TLR, and Cell Cycle pathways; enriched gene ontology (GO) terms in up-regulated gene lists involving vascularization and hormone metabolism; and modulated expression of genes associated with macrophage polarization. Taken together, the results of this study demonstrate that E804 and E804 + TMF modulate signaling in GBM cells, with the ability to influence macrophages. These treatments hold promise as an alternative to current modalities using very toxic nitrosourea compounds, and future work should continue to investigate crosstalk between macrophages and GBM, both *in vitro* and *in vivo.*

DEDICATION

To my parents, Jill and Bill Scobie, and to Mike Knoerr,

for their unwavering love, a profound belief in my abilities,

and nurturing that cannot be overestimated.

ACKNOWLEDGMENTS

I would like to express my deepest appreciation for my advisor, mentor, and friend, Dr. Charles D. Rice, for his guidance through each stage of the dissertation process - from when I was first considering a PhD at Clemson, through to completion of this degree. Dr. Rice's assistance was instrumental in my success. I would also like to extend my sincere thanks to my committee, Dr. Vincent S. Gallicchio, Dr. Vincent P. Richards, and Dr. Yanzhang Wei, for their support and guidance throughout my project.

I very much appreciate the insight, encouragement, and support that Dr. Lisa Bain and Dr. William Baldwin gave freely. I'd also like to recognize mentors early on in my journey, Bebe Tarleton, Dr. Thomas E. Meigs, and Dr. Timothy Forrest, who helped to solidify my love of Biology.

TABLE OF CONTENTS

LIST OF TABLES

LIST OF FIGURES

LITERATURE REVIEW

Glioblastoma Multiforme (GBM) and current state of the field

Gliomas account for 30% of all primary brain and central nervous system (CNS) cancers (National Brain Tumor Society , Goodenberger and Jenkins 2012). Of the four WHO-defined malignancy grades, Glioblastoma Multiforme (GBM) ranks as the most aggressive and fatal of the gliomas (grade IV) and boasts 17,000 new diagnoses in the US per year (Holland 2000, National Cancer Institute). Found mainly in the cerebral hemispheres, GBM may arise from astrocytes, but other cell types may contribute as well, including neuronal and oligodendrocyte precursors (Zong, Verhaak, and Canoll 2012, Zong, Parada, and Baker 2015, Alcantara Llaguno and Parada 2016), which may determine the origin and nature of glioma stem cells (Jackson, Hassiotou, and Nowak 2014). While GBM rarely metastasizes to other organs (Hamilton et al. 2014), it is a diffuse tumor and can spread to any region of the spinal cord or brain (American Brain Tumor Association 2014, Alifieris and Trafalis 2015). Diagnosis rarely occurs prior to the onset of severe neurological symptoms due to brain pressure. Even with treatment GBM has a dismal prognosis, at 25% overall survival after 2 years (van Tellingen et al. 2015). While many experimental drugs exist, none have achieved a cure for GBM.

The pathogenesis of GBM is the subject of intense debate, and may depend on the subtype. Based on intrinsic transcriptional profiles, pro-neural,

neural, mesenchymal, and classical types are recognized (Verhaak et al. 2010). Genotypic classification seems to determine phenotypic constitution seen upon histopathological examination (Wang et al. 2017, Joo et al. 2013) and molecular lesions can vary widely among these subtypes. Multiple copies of endothelial growth factor receptor (EGFR) and alterations in both chromosome 10 and 7 characterize the classical subtype (Kuehn 2010). Mutations in p53, platelet-derived growth factor receptor alpha (PDGFRA), and isocitrate dehydrogenase 1 (IDH1) are more typical of the pro-neural subtype, while high rates of mutation in both 0-6-methylguanine-DNA methyltransferase (MGMT) and IDH1 are typical of the neuronal subtype (Molenaar et al. 2014). High rates of mutation in neurofibromatosis type 1 (NF1) are typical of the mesenchymal subtype.

Although glioblastoma cannot be cured surgically, the first management step is to debulk as much of the tumor as possible. Following surgery, GBM is often treated using radiotherapy, chemotherapy, and possibly immunotherapy with the goal of slowing tumor growth. No current treatments are completely curative (Young et al. 2015). Chemotherapy options include alkylating agents such as temozolomide (TMZ), delivered orally, and carmustine, delivered as an infused wafer directly to the brain (Ramirez et al. 2013). Oral medications such as TMZ have difficulty crossing the blood-brain barrier, and implantation of carmustine-infused biodegradable polymers has limited success with high risk of brain edema and infection (Omuro and DeAngelis 2013). The work presented

herein may lead to an alternative, or at least concomitant, treatment plan that could be applied to infusible biodegradable polymers.

GBM are highly vascularized tumors, thus anti-angiogenic treatments have long been pursued (McNamara and Mason 2012). Bevacizumab is a monoclonal antibody targeting vascular endothelial growth factor (VEGF) and is usually used in tandem with temozolomide. However, new evidence implies that anti-VEGF therapies alone are insufficient, and may in fact contribute to later tumor invasion (Keunen et al. 2011). Anti-VEGF Bevacizumab in combination with glycolytic pathway targeting therapies have been suggested as a potential solution. Ultimately it is the persistent, rather than transient, normalization of vasculature hypothesized to decrease tumor growth and perhaps aid in therapeutic efficacy (Huang et al. 2013). Regardless, Bevacizumab is often used only as a salvage treatment, as its efficacy lies in slowing the progression of GBM but not in overall survival time increase (Chamberlain 2011). In addition to being highly vascularized, the enlarging mass is often associated with a necrotic center resulting from hypoxia and lack of nutrients, and there may be interplay between insulin signaling and induction of hypoxia mediated by UGFBP2-HIF1α interactions (Lin, Liao, and Qutub 2015, Dunn et al. 2012).

Multiple studies have been focused on immunotherapy as a viable treatment modality, with limited positive results as clearly pointed out in a recent review (Lim et al. 2018). Standard clinical approaches of surgery, chemotherapy, and radiation are each, and in combination, immunosuppressive. Vaccination

and chimeric antigen receptor (CAR) T-cell approaches to GBM reached a wall in Phase II and III trials, but oncolytic viruses such as PVS-RIPO show promise in a few patients (Bigner 2011, 2017). Injection of PVS-RIPO into the tumor not only directly lyses cancer cells, but also alerts the immune system to the tumor's presence (Goetz et al. 2011). Consequently, this approach must be carefully monitored to prevent excessive brain swelling (Cavallo 2015). In addition to PVS-RIPO therapy, other viral therapies targeting GBM are in earlier stages of development, such as measles, herpes and zika (Duebgen et al. 2014, MayoClinic 2017, Zhu et al. 2017). These viruses preferentially target and kill glioblastoma stem cells. Immune checkpoint inhibitors (targeting CTLA-4, PD-L1, others) show some promise until the inevitable tumor recurrence. Many of the issues associated with GBM immunotherapy are linked to the well-documented local and systemic immunosuppression in patients with the disease, such as limited number of tumor infiltrating lymphocytes (TILs) and compromised cell-mediated immunity (Roszman, Elliott, and Brooks 1991).

Glioma cells also express high levels of indoleamine 2,3-deoxygenases (IDO) that metabolize tryptophan to kynurenine, which drives T-cell suppression and immune tolerance (Guastella et al. 2018). Moreover, kynurenine is a potent ligand for the aryl hydrocarbon receptor (AHR), which, when activated, up-regulates expression of immunosuppressive TGF-β (Gramatzki et al. 2009). The AHR is a member of the basic helix-loop-helix (bHLH-PAS) superfamily of proteins and functions as a ligand-activated transcription factor (Gu, Hogenesch,

and Bradfield 2000) for multiple responsive gene products. Most notable of these genes include phase I and II drug-metabolizing enzymes and transporters (Denison et al. 2002, Hu et al. 2007, Nebert et al. 2000, Köhle and Bock 2007). Other gene products include proteins associated with cell cycle arrest, such as p21, p57, and p27 (Knockaert et al. 2004).

Indirubins and the Aryl Hydrocarbon Receptor (AHR)

Successful control of glioma cell proliferation (inhibition, induced apoptosis), including the targeting of glioma stem cells and promotion of a favorable microenvironment to immunologically combat the tumor, is a goal of virtually all researchers in the field of brain cancer research. To that end, a class of small molecules, natural indirubin and its derivatives, are being explored as promising anti-tumor and immunomodulatory agents (Moon et al. 2006, Kim et al. 2009). Originally used in Chinese medicine to treat chronic myelogenous leukemia, the indigo plant's active compound has since been identified as indirubin and has been synthesized in the lab to create increasingly bioavailable derivatives such as indirubin-3'-(2,3 dihydroxypropyl)-oximether (E804) and 7-bromoindirubin-3'-oxime (7BIO) (Moon et al. 2006). Indirubin is a bis-indole alkaloid derived from tryptophan precursors. Indirubin has been shown to inhibit angiogenesis in prostate cancer by way of VEGFR2-mediated JAK/STAT3 pathway disruption (Zhang et al. 2011), decrease inflammatory cytokine signaling (interferon gamma and IL6) (Kunikata et al. 2000), and induce cancer cell

apoptosis via inhibition of cyclin-dependent kinases (CDKs) (Kim et al. 2009, Knockaert et al. 2004, Hoessel, Leclerc, Endicott, Nobel, et al. 1999). Additionally, E804 has been shown to inhibit angiogenesis in human umbilical vein endothelial cells (HUVECs) *in vivo* (Shin and Kim 2012), modulate inflammatory processes (Babcock, Anderson, and Rice 2013), and inhibit STAT3 (Nam et al. 2005). The bromo-substituted indirubin 7BIO has been found to induce apoptosis in both breast cancer and thyroid carcinoma cell lines (Nicolaou et al. 2012).

In addition to effects on CDK activity, indirubins also bind and activate AHR (Adachi et al. 2001, Springs and Rice 2006, Faber et al. 2018, Kawanishi et al. 2003), though are metabolized very quickly (Guengerich et al. 2004) by phase I enzymes (CYP1A1, CY1B1) induced through AHR activation. However, AHR antagonist (e.g. 6, 2′, 4′-trimethoxyflavone – TMF) can inhibit metabolism, and spare other desirable functions of these compounds. Likewise, the AHR also binds indole-derived compounds found in many cruciferous vegetables (Murray, Patterson, and Perdew 2014). It is clear that the AHR plays a key role in a myriad of physiological roles; not only of drug metabolism, but also immune regulation, organogenesis, mucosal barier function, and cell cycle arrest (Hubbard, Murray, and Perdew 2015). AHR-indirubin structure activity relationships (SARs) vary depending upon specific indirubin derivative structure and bioavailability (Blažević et al. 2015). Further elucidation of how AHR versus CDK activity relates to indirubin derivatives is a promising avenue of GBM research. The two

derivatives of indirubin, E804 and 7BIO, have been chosen for their known anti-inflammatory and potential anti-tumor properties (Kim et al. 2009, Moon et al. 2006, Nicolaou et al. 2012, Shin and Kim 2012). While traditional treatment options for GBM should not be abandoned, the diversity of cancer diagnoses requires a multi-tier treatment approach. Additional complementary treatment options for GBM are needed. Less toxic compounds that can modulate the tumor immune and inflammatory environment are promising drug candidates that may displace current strategies such as carmustine-laden wafers.

The Unfolded Protein Response (UPR)

The endoplasmic reticulum (ER) is responsible for synthesizing, modifying and folding proteins within the cell. Proteostasis within the ER is maintained by a variety of factors and managed by a multipronged pathway termed the unfolded protein response (UPR), which surveys and responds to misfolded or unfolded proteins within the cellular environment (Hetz, Chevet, and Oakes 2015). ER stress may be induced by a multitude of reasons, including pathophysiologies such as tumor development (Vandewynckel et al. 2013). If proteostasis is disrupted, one or all three branches of the UPR can be activated to deal with the accumulation of misfolded proteins. The overlapping redundancies built into the UPR pathway ensure restoration of normal cellular function, or if unable to restore homeostasis, induction of apoptosis. If too many misfolded proteins are detected, translation is halted and misfolded proteins simultaneously destroyed.

Additionally, chaperone proteins are increased to help with proper folding of other proteins (Obacz et al. 2017).

The three major arms activated within the UPR are regulated by the membrane bound sensors protein kinase R–like ER kinase (PERK), inositol-requiring enzyme 1α (IRE1) and activating transcription factor 6α (ATF6). These can be distinctively active, but are also commonly co-regulated. Considered the master regulator of the UPR, glucose-regulated protein 78 (GRP78) keeps these three transcription factors in an inactive state under normal conditions. During ER stress, GRP78 will dissociate from PERK, IRE1, and/or ATF6, and tag the misfolded protein, signaling for the pathway to commence (Chaudhari et al. 2014). Therefore, GRP78 supports cell survival by inhibiting UPR-induced apoptosis. GRP78 is upregulated in some chemoresistant cancers, and thus is associated with chemo-resistance (Roller and Maddalo 2013).

Although not wholly understood, the UPR appears to play a supporting role in tumorigenesis and tumor progression in many cancer types, including Glioblastoma Multiforme (GBM) (Ma and Hendershot 2004). Tumorigenesis induces ER stress, which if prolonged can further aid in tumor progression. Due to mutation, hypoxic conditions, glucose deprivation, low pH, and rapid growth, tumor cells are exposed to many factors that heighten the risk of protein misfolding. These stressors, combined with increased protein requirements, lead to induction of the UPR (Ma and Hendershot 2004). The adaptive healing and anti-apoptotic responses of the UPR are first induced in order to process the

accumulation of misfolded proteins. If unsuccessful, later responses may lead to induction of apoptosis. However, tumors appear able to exploit these stress response pathways to benefit from initial pathway protective mechanisms, while avoiding later-stage apoptosis (Luo and Lee 2013). Constitutive UPR activation has been reported in many tumors, including GBM. Specifically the IRE1 and PERK arms of the UPR have been implicated in GBM growth and progression (Doultsinos et al. 2019). Prolonged, chronic activation of the UPR pathways has been implicated in tumor progression, thus targeted down-regulation of certain UPR-related genes is a likely therapeutic target for GBM and other cancers. The increase in UPR activity during glioma initiation and progression provides a fresh avenue of exploration for potential cancer therapeutics. It is my hope that new therapeutic targets may be identified from work such as described here.

UPR regulation is investigated herein by E804. Indole compounds are documented regulators of the UPR system (Chakraborty et al. 2016). Additionally, the bis-indole alkaloid compound indirubin has been well studied for its immune-modulatory properties (Qi, Li, and Li 2017, Cheng and Merz 2016). Synthetic indirubins such as E804 used herein are designed to increase bioavailability via substitution group alterations. Certain indirubin derivatives are posited to have neuro-protective effects via down-regulation of apoptosis-inducing genes in the UPR pathway such as CHOP (Kosuge et al. 2017). Indirubin-induced CHOP down-regulation may work via inhibition of glycogen synthase kinase 3 (GSK-3) (Meares et al. 2011). Additionally, GSK-3 is a major

regulator of numerous and diverse pathways. Dysregulation of these pathways are implicated in many disease types, including cancer (Mancinelli et al. 2017). GSK-3 regulates the STAT3 pathway, which is implicated in glioma development (Ganguly et al. 2018) and which has been found to be down-regulated by E804 treatment in prior work (cite my paper).

Much of the UPR pathway remains unexplored with regards to indirubin treatment. Herein I explore the effect E804 treatment on UPR pathway modulation in two GBM cell lines that show high, yet variable, AHR expression. This study identifies E804 as a modulator of the UPR pathway in GBM cells, with therapeutic implications.

Macrophages

While GBM are astrocyte in cellular origin, a malignant GBM tumor can be comprised of up to 50% microglia (Hambardzumyan, Gutmann, and Kettenmann 2016). Microglia are CNS macrophages that are present under normal circumstances in the brain and spine, but have been found at higher percentage in association with low-grade gliomas. Additionally, during a traumatic brain event such as brain cancer other immune cells can cross the blood brain barrier. Monocyte-derived macrophages have also been found to associate with glioma tumors at higher percentages (15-30%) than in normal non-neoplastic brains (10-15%) (Simmons et al. 2011).

This influx of macrophages may be due to the fact that macrophages and microglial are important to tumor survival and growth. Often referred to as glioma-associated macrophages (GAMs), they can assist in neo-vascularization and general tumor growth (Hambardzumyan, Gutmann, and Kettenmann 2016). Even in normal tissue macrophages are heterogeneous; consequently GAMs follow more than just one phenotype, according to *in vitro* studies (Kennedy et al. 2013). Depending on what cytokine and cognate stimulation the GAM receives, these macrophages will express different cellular markers that can be used to polarize them into different phenotypes (M1 and M2). The M1 phenotype is a T-helper 1 (Th1) driven macrophage. M1 cells are polarized by LPS and IFN-gamma, and release pro-inflammatory cytokines such as IL-12, IL-23, and iNOS (Hambardzumyan, Gutmann, and Kettenmann 2016, Bygd, Forsmark, and Bratlie 2014). By contrast, the M2 phenotype is a T-helper 2 (Th2) driven macrophage, that can be further divided into M2a, M2b, and M2c subsets. In general, M2 cells are polarized by IL-4, IL-10 and IL-13, and release anti-inflammatory cytokines such as IL-10, IL-1Rα, TGF- β, and TNF-α (Hambardzumyan, Gutmann, and Kettenmann 2016, Bygd, Forsmark, and Bratlie 2014).

Although the easy dichotomy of this classification is somewhat misleading given the plasticity of myelomonocytic cell populations, the general categorization may be helpful in directing new lines of GBM treatment research. Previous studies suggest that the M2 phenotype correlates with increased glioma growth (Feng et al. 2015). It has also been demonstrated that inhibition of M2-like

macrophages can slow glioma growth (Pyonteck et al. 2013). It is possible that by inducing a switch from M2 to M1 polarization, a new immunotherapy for GBM may be identified (Prinz and Priller 2014).

Wnt pathway crosstalk with TLR and AHR pathways

The Wingless-related integration site (Wnt) pathway plays a major role in embryonic development, cell proliferation, cell migration, and tissue homeostasis. Abberant Wnt signaling has been implicated in human colorectal, breast, pancreatic ductal adenocarcinoma (PDAC), endometrial, and brain cancers (Zhan, Rindtorff, and Boutros 2017). Due to demonstrated tumor promoting characteristics in many cancer types including GBM, members of the Wnt pathway are logical therapeutic targets (Suwala et al. 2016, McCord et al. 2017).

In GBM, Wnt activation has been linked to radio-resistance *in vivo (Kim et al. 2012),* glioma stem cell (GSC) persistence (Wu et al. 2017), and proliferation, survival, and clonogenicity of GBM cells (Kahlert et al. 2015). Not only is Wnt implicated in GBM progression, elevated Wnt proteins aid in microglial recruitment and perhaps M2 polarization (Matias et al. 2019), thus contributing to GBM tumor expansion via immune cell reprogramming. Through dispatch of Wnt signals, M2 macrophages may engage in matrix remodeling that could have significant ramifications for GBM tumor structure. Conversely, inhibition of Wnt

signaling can prevent M2 macrophage polarization that would otherwise be induced by IL-4 or TGF-β (Feng et al. 2018).

Of special relevance to the body of work presented herein, the Wnt pathway is functionally connected to both Toll-Like Receptor (TLR) (Casili et al. 2018, Zolezzi and Inestrosa 2017) and AHR (Mathew, Simonich, and Tanguay 2009, Procházková et al. 2011) signaling. As master regulator of inflammation, NF-κB provides a link between pathways involved with innate immune system inflammatory signaling, such as the Wnt and TLR pathways. Particularly important in neuroinflammatory diseases such as Alzheimer's disease (AD) or GBM, inflammatory signaling mediated by NF-κB is a central component in brain dysregulation. Compounded by the high percentage of innate immune cells such as macrophages present in the GBM environment, the TLR pathway is an important target with regards to immunomodulation. Not only do Wnt and TLR inflammatory signaling overlap; crosstalk has been demonstrated between Wnt and AHR pathways as well. Both the AHR and Wnt pathway are evolutionarily conserved and important in normal development (Schneider, Branam, and Peterson 2014). AHR activation has been shown to antagonize the Wnt pathway in multiple models. Evidence for crossover signaling between Wnt and the AHR has been found in zebrafish via R-spondin1 (Mathew et al. 2008), in mouse embryonic stem cells via binding of dioxin (Wang et al. 2015), in mouse hepatoma cells via the *cyp1a1* promoter (Schulthess et al. 2015), and beyond.

Thus, targeting of the AHR in GBM may induce modulation of other key pathways that aid in brain development and inflammatory regulation.

The model

LN-18 and T98G cell lines (ATCC), initially collected from grade IV astrocytomas in Caucasian males ages 65 and 61 respectively, were chosen for their sensitivity to indirubin compounds, such as E804, due to high expression of the aryl hydrocarbon receptor (AHR) (Gramatzki et al. 2009). To date, both cell lines have been used extensively in both brain cancer and ER stress research (Weatherbee, Kraus, and Ross 2016, Nguyen et al. 2019). Both cell lines are documented as susceptible to ER stress, especially via PERK signaling (Jia et al. 2010). Therefore, LN-18 and T98G cell lines are good models to study the potential neuro-protective effects of indirubins via immunomodulation and alleviation of ER stress.

Not only do these cell lines have an active protein stress response, they also express high levels of tumor suppressor genes that respond to genotoxic stress such as *p53* and *p21*. T98G cells typically have higher levels of p53 protein, as they are homozygous mutant at 237, while LN-18 cells are heterozygous mutant at 238. Both cell lines express high levels of p21 and do not express p16 *(Weller et al. 1998)*. T98G cells have higher protein levels of BCL-2 apoptotic family proteins, including BCL-2, MCL-1, BCL-X, and BAX. Additionally,

the LN-18 cell line is generally more sensitive to drug-induced cytotoxicity than the T98G line (Weller et al. 1998).

The peripheral blood monocyte cell line THP-1 (ATCC) was initially collected from a 1-year old male with acute monocytic leukemia. THP-1 cells were chosen for their common use as differentiated macrophages in inflammation and cancer studies. The THP-1 cell line is an established model mimicking monocyte-derived macrophages *in vitro*. Additionally, THP-1 macrophages differentiated with PMA are easily polarized along the continuum of M1 and M2 phenotypes (Wang et al. 2014, Genin et al. 2015). Stimulation of THP-1 monocytes and macrophages with LPS also demonstrates this cell line is an ideal candidate for studying inflammation and immunomodulation (Chanput et al. 2010, Robertson et al. 2015, Wang, Pham, and Kim 2018).

Conclusion

The goal of this research is to characterize the effects that E804 and 7BIO have on the inflammatory environment of human GBM and THP-1 cell lines as mediated by the AHR pathway. The two derivatives of indirubin, E804 and 7BIO, have been chosen for their known immunomodulatory properties (Kim et al. 2009, Moon et al. 2006, Nicolaou et al. 2012, Shin and Kim 2012). AHR antagonist TMF will be used to investigate the impact of indirubin treatments on the AHR pathway specifically. While current avenues of GBM research hold promise, complementary treatment options for GBM are needed. Small

molecules like indirubin that can target inflammatory signaling, UPR signaling, or influence immune cell recruitment in the tumor microenvironment are promising drug candidates. To my knowledge, the studies proposed herein are the first as of this writing to explore the mechanisms of the AHR signaling pathway upon indirubin binding in GBM *in vitro* models. In addition to the furtherance of the neuro-onocology body of knowledge, elucidation of indole-AHR signaling in GBM will benefit the field of immunotoxicoogy. Importantly, the questions outlined herein will help to better understand AHR-targeted therapy, and perhaps outline future GBM drug development and inquiry.

MODULATION OF GLIOMA-INFLAMMATION CROSSTALK PROFILES IN HUMAN GLIOBLASTOMA CELLS BY INDIRUBIN-3'-(2,3 DIHYDROXYPROPYL)-OXIMETHER (E804) AND 7-BROMOINDIRUBIN-3'-OXIME (7BIO)

Micaela R. Scobie

Published in

Scobie, M. R., Houke, H. R., & Rice, C. D. (2019). Modulation of glioma-inflammation crosstalk profiles in human glioblastoma cells by indirubin-3'-(2,3 dihydroxypropyl)-oximether (E804) and 7-bromoindirubin-3′-oxime (7BIO). *Chemico-Biological Interactions*, 312, 108816.

Department of Biological Sciences

Clemson University, Clemson SC USA 29634

ABSTRACT

Indirubins E804 (indirubin-3'-(2,3 dihydroxypropyl)-oximether) and 7BIO (7-Bromoindirubin-3'-oxime) are synthetic derivatives of natural indirubin, the active compound in Danggui Longhui Wan, a traditional Chinese remedy for cancer and inflammation. Herein, I explore E804 and 7BIO for their potential to modulate key pro-inflammatory genes and cytokines in LN-18 and T98G glioblastoma cells. High grade gliomas typically secrete large amounts of inflammatory cytokines and growth factors that promote tumor growth in an autocrine fashion. Inflammation is emerging as a key concern in the success of new treatment modalities for glioblastomas. Studies indicate that select indirubin derivatives bind and activate signaling of the AHR pathway, as well as inhibit cyclin-dependent kinases and STAT3 signaling. AHR signaling is involved in hematopoiesis, immune function, cell cycling, and inflammation, and thus may be a possible target for glioma treatment. To determine the significance of the AHR pathway in LN-18 and T98G glioma inflammatory profiles, and on the effects of E804 and 7BIO on these profiles, I used 6,2′,4′-trimethoxyflavone (TMF), a putative selective AHR antagonist. It was confirmed that E804 and 7BIO activates the AHR leading to *cyp1b1* expression, and that TMF antagonizes expression. I then employed a commercial cancer inflammation and immunity crosstalk qRT-PCR array to screen for anti-inflammatory related properties. TMF alone inhibited expression of *ifng*, *ptsg2*, *il12b*, *tnfa*, *il10*, *il13*, the balance between *pd1* and *pdl1*, and even expression of *mhc1a/b*. E804 was very potent

in suppressing many pro-inflammatory genes, including *il1a, il1b, il12a, ptgs2, tlr4,* and others. E804 also affected expression of *il6, vegfa, and stat3*. Conversely, 7BIO induced *cox2*, but suppressed a different selection of pro-inflammatory genes including *nos2*, *tnfa*, and *igf1*. Secretion of IL-6 protein, an iconic inflammatory cytokine, was decreased by E804. VEGF (vascular endothelial growth factor) protein secretion was upregulated by 7BIO, yet downregulated by E804 and E804 plus TMF. Thus, E804 is both an AHR ligand and regulator of important pro-inflammatory cytokines such as IL-6 and oncogene STAT3, among others. These results point to the use of E804 and TMF in combination as a promising new treatment for glioblastoma.

Key words: Glioblastoma multiforme, Aryl hydrocarbon receptor, Indirubin, E804, 7BIO, Inflammation, Immunomodulation.

1.0. INTRODUCTION

Primary brain cancer and other central nervous system (CNS) cancers account for an estimated 16,830 deaths in 2018 in the US alone (Siegel, Miller, and Jemal 2018). Out of all brain and CNS malignancies, 30% are gliomas (National Brain Tumor Society , Goodenberger and Jenkins 2012). Of these gliomas, glioblastoma multiforme (GBM) (WHO grade IV) is the most aggressive and lethal subset (Holland 2000). Found mainly in the cerebral hemispheres, GBM may arise from astrocytes, but other cell types may contribute as well, including neuronal and oligodendrocyte precursors (Zong, Verhaak, and Canoll 2012, Zong, Parada, and Baker 2015, Alcantara Llaguno and Parada 2016), which may determine the origin and nature of glioma stem cells (Jackson, Hassiotou, and Nowak 2014). GBM can metastasize to any area of the brain or spinal cord (American Brain Tumor Association 2014, Alifieris and Trafalis 2015). Extra-CNS metastasis is extremely rare, but has been documented in a few cases (Hamilton et al. 2014). By the time of diagnosis, the highly malignant mass can be large, causing symptoms such as headache, nausea, vomiting, drowsiness, cognitive and personality changes, and seizures (Omuro and DeAngelis 2013). Median survival with treatment is only 14.6 months; fewer than 30% of patients survive 2 years (American Brain Tumor Association 2014, Alifieris and Trafalis 2015).

Glioma cells express high levels of indoleamine 2,3-deoxygenases (IDO) that metabolize tryptophan to kynurenine, which drives T-cell suppression and

immune tolerance (Guastella et al. 2018). Moreover, kynurenine is a potent ligand for the aryl hydrocarbon receptor (AHR), which, when activated, upregulates expression of TGF-β, which is immunosuppressive (Gramatzki et al. 2009). The AHR is a member of the basic helix-loop-helix (bHLH-PAS) superfamily of proteins and functions as a ligand-activated transcription factor (Gu, Hogenesch, and Bradfield 2000) for multiple responsive gene products. Most notable of these genes include phase I and II drug-metabolizing enzymes and transporters (Denison et al. 2002, Hu et al. 2007, Nebert et al. 2000, Köhle and Bock 2007). Other gene products include proteins associated with cell cycle arrest, such as *p21, p57*, and *p27* (Knockaert et al. 2004). The AHR is also involved in the polarization of T-cells towards T-regs, furthering the immunosuppressive tumor microenvironment, and influences the polarization of macrophages (Gabriely and Quintana 2019). AHR activation by tumor-derived kynurenine also suppresses *nfkb1* activation in glioma-associated macrophages, and promotes *ccl2* and *ccr2* expression, thereby driving these macrophages towards a M2 phenotype (Takenaka et al. 2019).

Mechanistically, there is evidence that signal transducer and activator of transcription 3 (STAT3), may be a key mediator of both glioma cell proliferation and negative effects on the tumor microenvironment, namely suppressing GAMs, while promoting T-regs and myeloid-derived suppressor cells (Chang et al. 2017). *Stat3* is constitutively activated in the majority of GBM patients, and the level of expression correlates well with histological grade and prognosis (Abou-

Ghazal et al. 2008, Matsebatlela et al. 2015, Tu et al. 2011, Ganguly et al. 2018). Moreover, glioma cells actively secrete growth factors to activate and maintain expression of *stat3* in glioma stem cells (Almiron Bonnin et al. 2017). Considering the key role of STAT3 in glioma growth and effects on the microenvironment, therapies targeting STAT3 should be of high priority. One small molecule (ibrutinib) inhibitor of bone marrow and X-linked (BMX) non-receptor tyrosine kinase that is linked to *stat3* upregulation in glioma stem cells is already receiving attention (Shi et al. 2018).

Natural indirubin and its derivatives have been explored as promising anti-tumor and immunomodulatory agents (Moon et al. 2006, Kim et al. 2009). Originally used in Chinese medicine to treat chronic myelogenous leukemia, the indigo plant's active compound has since been identified as indirubin and has been synthesized in the lab to create increasingly bioavailable derivatives such as indirubin-3'-(2,3 dihydroxypropyl)-oximether (E804) and 7-bromoindirubin-3'-oxime (7BIO) (Moon et al. 2006). Indirubin is a bis-indole alkaloid derived from tryptophan precursors. Indirubin has been shown to inhibit angiogenesis in prostate cancer by way of VEGFR2-mediated JAK/STAT3 pathway disruption (Zhang et al. 2011), decrease inflammatory cytokine signaling (interferon gamma and IL6) (Kunikata et al. 2000), and induce cancer cell apoptosis via inhibition of cyclin-dependent kinases (CDKS) (Kim et al. 2009, Knockaert et al. 2004, Hoessel, Leclerc, Endicott, Nobel, et al. 1999, Babcock, Anderson, and Rice 2013). E804 has also been shown to inhibit angiogenesis in human umbilical vein

endothelial cells (HUVECs) *in vivo* (Shin and Kim 2012), has potent anti-inflammatory properties (Babcock, Anderson, and Rice 2013), and inhibits STAT3 (Nam et al. 2005). The bromo-substituted indirubin 7BIO has been found to induce apoptosis in both breast cancer and thyroid carcinoma cell lines (Nicolaou et al. 2012).

In addition to their effects on CDK activity, indirubins also bind and activate AHR (Adachi et al. 2001, Springs and Rice 2006, Faber et al. 2018, Kawanishi et al. 2003), though are metabolized very quickly (Guengerich et al. 2004) by phase I enzymes induced through AHR activation. However, AHR antagonists, such as 6, 2′, 4′-trimethoxyflavone (TMF) can inhibit metabolism, and spare other desirable functions of these compounds. In the study described herein, indirubin derivatives E804 and 7BIO were chosen for their known anti-inflammatory and potential anti-tumor properties (Kim et al. 2009, Moon et al. 2006, Nicolaou et al. 2012, Shin and Kim 2012). Each compound, alone and in the presence of TMF, were examined for their effects on inflammatory profiles of two human glioblastoma cell lines, LN-18 and T98G, each differing in patient origin and in level of basal expression of the AHR (Gramatzki et al. 2009). Indirubin E804 was superior to 7BIO as an anti-inflammatory agent, and was shown to be a potent ligand for the AHR, though TMF was able to inhibit this effect. While traditional treatment options of GBM should not be abandoned, additional complementary treatment options for GBM are needed. Less toxic compounds that can modulate the tumor immune and inflammatory environment

are promising drug candidates that may displace current strategies like carmustine-laden wafers.

2.0. MATERIALS AND METHODS

2.1. Chemicals: Indirubin-3'-(2,3 dihydroxypropyl)-oximether (E804) and 7-Bromoindirubin-3'-oxime (7BIO) were obtained from Alexis Biochemical (CA, USA). The AHR antagonist 6,2',4'-trimethoxyflavone (TMF) was purchased from Sigma-Aldrich (MO, USA). Stock solutions at 10^{-2} M were prepared by solubilizing compounds in dimethyl sulfoxide (DMSO, Corning, NY, USA). Chemical structures for E804, 7BIO, and TMF are shown in Figure 1.

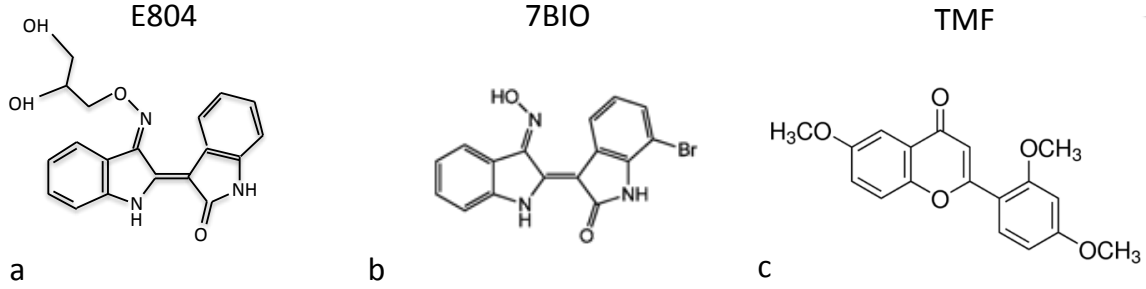

Figure 1. Chemical structures for a) Indirubin-3'-(2,3 dihydroxypropyl)-oximether (E804), b) 7-Bromoindirubin-3'-oxime (7BIO), and c) 6, 2′, 4′-trimethoxyflavone (TMF).

2.2. Cell culture: Human Glioblastoma Multiforme (GBM) cell lines, LN-18 (ATCC CRL-2610) and T98-G (ATCC CRL-1690), were obtained from ATCC (VA, USA) and cultured using Dulbecco's Modified Eagle's Medium (DMEM, Cellgro, MA, USA) as the base medium. Medium was supplemented with 10%

heat-inactivated fetal bovine serum (FBS) with iron (Hyclone, USA), 20 mM HEPES, 10 mM L-glutamine, 100 U/ml penicillin, 100 µg/ml streptomycin, 110 µg/ml sodium pyruvate, 1% non-essential amino acids (100 × stock), 4.5 g/l glucose, and 1.5 g/l of $NaHCO_3$, each from Sigma (Sigma Aldrich, MO, USA). Cells were typically grown and maintained at 37 °C with 5% CO_2 in Corning 75 cm^2 culture flasks.

2.3. Effects of E804 and 7BIO on cyp1b1 *and* stat3 *mRNA expression:*

LN-18 and T98G cells were seeded in 6-well plates (Corning Primaria™, NY, USA) at 2 x 10^6 cells per well in 2 ml, and allowed to adhere for 4 h. Wells were then treated with 10 µM E804 or 7BIO, with 0.1% DMSO as the carrier control, and with/without 10 µM TMF, in a total of 3 ml complete medium per well. Six and 24 h post-exposure, supernatants were removed from the wells and stored at -20 ºC for later cytokine analysis. The experiment was repeated three times. Messenger RNA was extracted using RNAzol (Molecular Research Center, OH, USA) according to the manufacturer's protocol. Complementary DNA was synthesized using qScript cDNA Supermix (Quantabio, MA USA). Each experiment was repeated three times. Gene expression was analyzed by quantitative real-time PCR with a BioRad iC5 detection system, RT^2 SYBR green/fluorescein master mix (Qiagen), and primer sets designed using Integrated DNA Technology (IDT) software, and validated prior to use (Table 1). The quantity of *cyp1b1* and *stat3* mRNA was expressed as fold-changes in gene

expression compared to *gapdh*. For data analysis, the ΔΔCt method was used. Expression data were compared between treatment groups using ANOVA, followed by a Bonferroni's post-test using GraphPad5 statistical package.

Table 1. Primer sets for qRT-PCR

Gene name	Accession #	Primer sequence (5' → 3')	Tm (°C)	Product size (bp)
Cyp1b1	NM_000104	F: ATG TCC TGG CCT TCC TTT ATG R: GTG TCC TTG GGA ATG TGG TAG	52	115
Gapdh	NM_001256799	F: AGC CTC AAG ATC ATC AGC AAT GCC R: TGT GGT CAT GAG TCC TTC CAC GAT	57	105
Stat3	NM_003150	F: GAG AAG GAC ATC AGC GGT AAG R: CAG TGG AGA CAC CAG GAT ATT G	52	138

2.4. *Focused commercial RT-qPCR Super-Arrays for cancer inflammation and immunity crosstalk:* LN-18 and T98G cell lines were grown and treated with E804, 7BIO, with/without TMF, or DMSO carrier control as described for RT-qPCR as above. RNAzol (Molecular Research Center, OH, USA) was added to each well and the mixture homogenized by gentle pipetting several times. This homogenate was passed to the second experimental exposure, and then to the third to pool all three treatments. mRNA was extracted according to manufacturer's instructions (Molecular Research). After collecting mRNA from each tube, genomic DNA contamination was removed using elimination mixture supplied by the manufacturer, and first strand cDNA synthesis was carried out using the RT^2 Easy First Strand Kit (Qiagen) as described by the manufacturer. A predesigned Cancer Inflammation & Immunity Crosstalk

Profiler™ array of 96 genes was purchased from Qiagen Corporation (cat # PAHS-181Z) for use with RT^2 Real-Timer SYBR Green/fluorescein qPCR master mixes purchased from the same supplier. Specific methods followed those suggested by the manufacturer. RT-qPCR was performed on a BioRad iQ5 real-time PCR detection system. For data analysis, the ΔΔCt method was used; for each gene fold-changes were calculated as difference in gene expression between untreated controls and treated cell cultures. Data were gathered and interpreted using software provided by Qiagen. Details on methods have been previously published (Matsebatlela et al. 2015, Babcock, Anderson, and Rice 2013).

2.5. Enzyme-linked immunosorbent assay (ELISA): An enzyme-linked immunosorbent assay (ELISA) was used to quantify interleukin-6 (IL-6) and vascular endothelial growth factor (VEGFA) secreted by LN-18 and T98G cells following treatment at 6 and 24 h. Supernatants from cells treated with E804 or 7BIO, carrier control, and with or without TMF for qPCR studies were used as the source. A commercially available ELISA kit from BioLegend (CA, USA) was used for both IL-6 and VEGFA cytokine assays. Three different experiments were examined independently. Cytokine levels were compared between treatment groups using ANOVA, followed by a Bonferroni's post-test using GraphPad5 statistical package.

3.0. RESULTS

3.1. E804 and 7BIO induce expression of cyp1b1 *and* stat3 *mRNA*

Cyp1b1 induction was used as a marker for relative AHR activity in LN-18 and T98G glioma cell lines after E804 and 7BIO treatment at 6 h and 24 h post-exposure. There was no response to either indirubin in LN-18 cells at 6 h, but by 24 h *cyp1b1* expression was 20-fold higher in E804 treated cells over the control, and was slightly less induced by 7BIO (Figure 2). TMF moderately induced *cyp1b1* in LN-18 cells at both 6 h and 24 h post-exposure. TMF also antagonized the AHR activity of E804, but not that of 7BIO. In contrast, 7BIO induced *cyp1b1* at 6 h post-exposure in T98G cells, but not by 24 h, while it took 24 h for E804 to induce expression. TMF antagonized *cyp1b1* induction by both E804 and 7BIO in T98G cells. *Stat3* mRNA expression in LN-18 cells was enhanced by 7BIO, but not by E804 at 6 h exposure, and TMF did not modify these responses (Figure 3). By 24 h exposure the combination of 7BIO and TMF increased *stat3* expression. In T98G cells, none of the treatments affected *stat3* expression at 6 h exposure. By 24 h exposure, 7BIO induced *stat3* expression, and this effect was not modified by TMF co-exposure. In comparison to E804, 7BIO induces *stat3* expression in both cell lines.

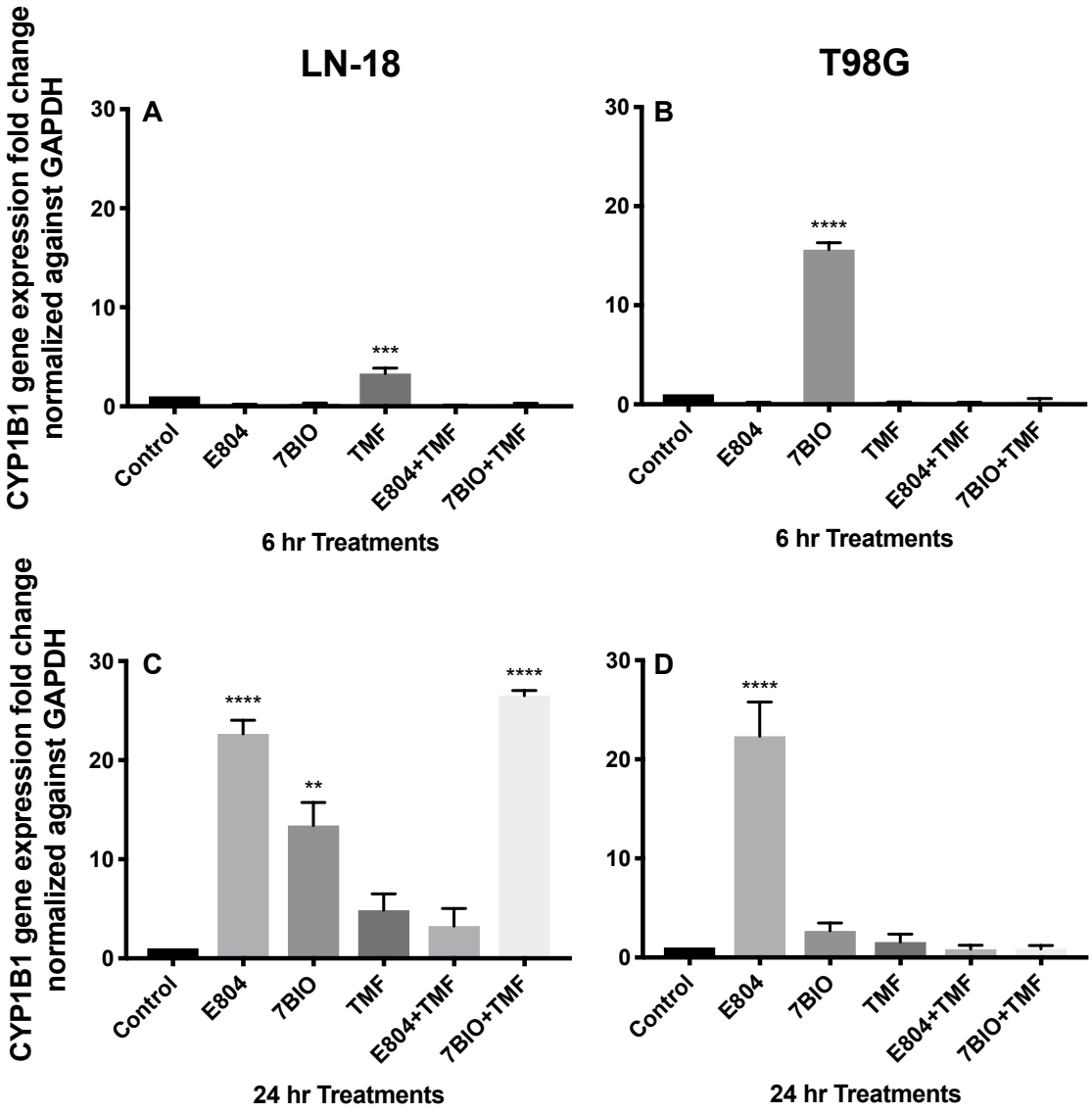

Figure 2. The effects of E804 or 7BIO, and/or TMF, on expression of *cyp1b1.* Data are represented as fold change compared to the control and normalized against house-keeping reference *gapdh*. All compounds treated at 10 μM. Gene expression in a, c) the LN-18 cell line and b, d) the T98G cell line, for 6 h (a and b) or 24 h (c and d). Data represent the mean fold expression $\pm$ S.E. of three different experiments. (**) indicates $p < 0.005$, (***), $p < 0.0005$, (****) $p < 0.001$.

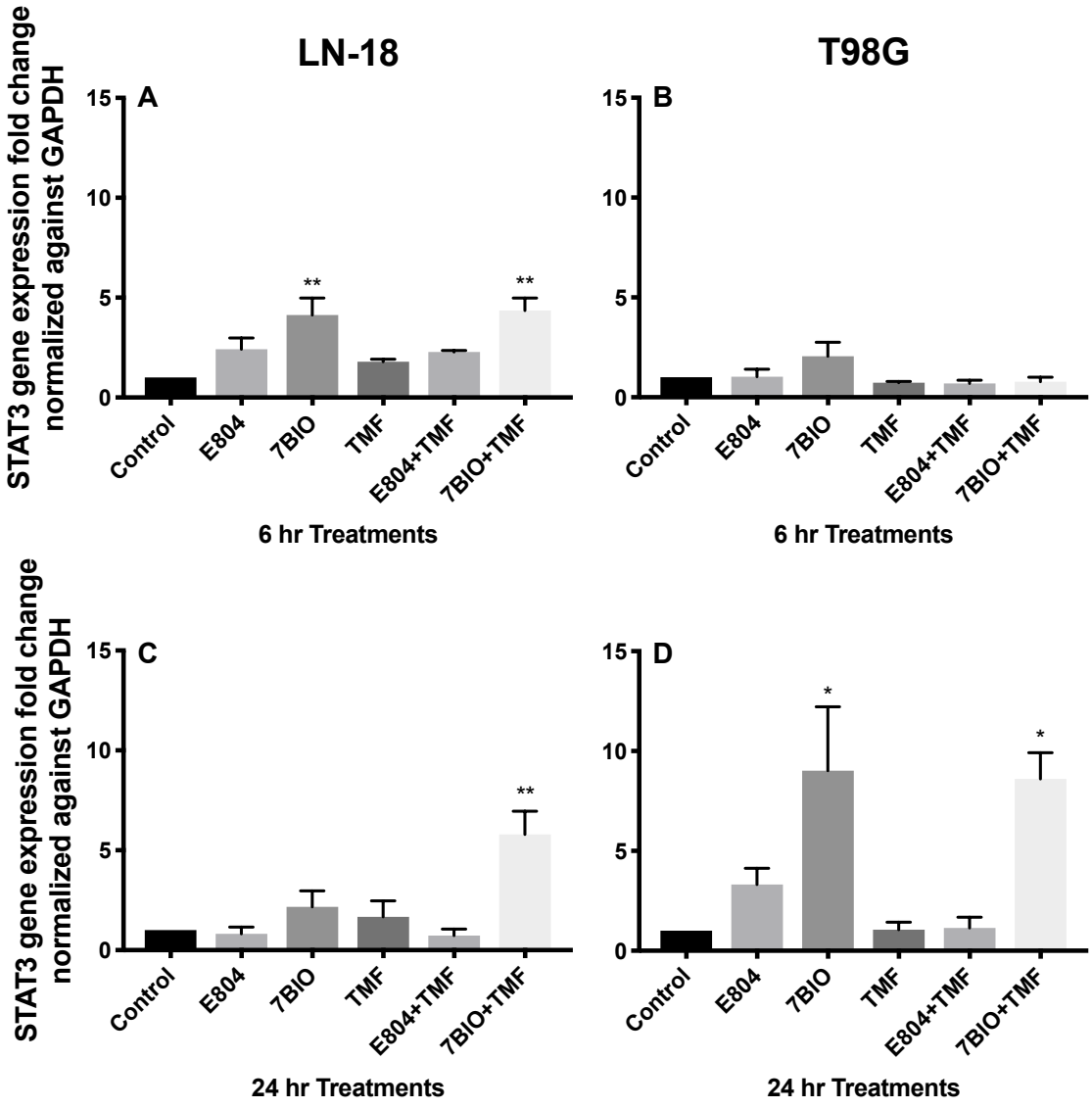

Figure 3. The effects of E804 or 7BIO, and/or TMF, on expression of *stat3.* Data are represented as fold change compared to the control and normalized against house-keeping reference *gapdh*. All compounds treated at 10 μM. Gene expression in a, c) the LN-18 cell line and b, d) the T98G cell line, for 6 h (a and b) or 24 h (c and d). Data represent the mean fold expression $\pm$ S.E. of three different experiments. (*) indicates $p < 0.05$, (**), $p < 0.005$.

3.2. Effects of treatments on cancer-inflammation cross-talk arrayed genes

Broadly, E804 treatment suppressed the expression of most pro-inflammatory genes, including cytokines *il1a* and *il1b*, *il12*, *nos2*, and *ifng* in LN-18 cells, with 7BIO having less of an effect (Table 2). Of particular note, E804 suppressed *egfr*, a key treatment target for some glioma subtypes. One of the most profound effects was that both compounds greatly suppressed *csf2* and *csf3* expression. *Pd1* and *pdl1* were suppressed by both indirubins, and especially in the presence of the AHR antagonist TMF. The combination of either E804 or 7BIO and TMF suppressed the expression of *tlr2* to a great degree at both 6 and 24 h. With a few of the inflammatory genes, treatment with TMF alone was suppressive in terms of gene expression. Of note, E804 treatment suppressed the expression of MHC-1 genes, as did TMF treatment.

T98G cells were more sensitive to the anti-inflammatory effects of E804 and 7BIO than LN-18 cells (Table 3). Most of the pro-inflammatory genes were suppressed, except that *il12b*, *il23a*, and *nos2* were induced. Treatment with E804 increased the expression of *il10* and *il13* at 24 h. However, *pdl1* is still a likely target, as is *ctla4* when in the presence of an AHR antagonist and either E804 or 7BIO. Of note, *igf1* expression was greatly impacted by both indirubins, as well as TMF, at 24 h. Unlike the effects of E804 and TMF on *mhc1a/b* expression invLN-18 cells, there was little effect on *mhc1a/b* expression in T98G cells. Also, in contrast to LN-18 cells, EGFR was not targeted by treatments.

Table 2. Select genes from commercial Human Cancer Inflammation and Immunity Crosstalk™ array displaying genes associated with inflammation, growth, signal transduction, and antigen presentation. All compounds treated at 10 μM. Treatments were compared to 0.1% DMSO as carrier control. LN-18 cells were treated for 6 h or 24 h, and triplicate samples pooled before mRNA extraction. Data represented as fold change compared to the appropriate time-point control and normalized against house-keeping gene expression.

Gene Name	Genbank No.	Symbol	LN18 gene expression change after 6 hr					LN18 gene expression change after 24 hr				
			E804	7BIO	TMF	E804 + TMF	7BIO + TMF	E804	7BIO	TMF	E804 + TMF	7BIO + TMF
PRO-INFLAMMATORY												
Chemokine ligand 2	NM_002982	CCL2	-1.57	-1.19	-2.94	-4.09	-2.46	-6.84	-1.36	-2.89	-1.89	-6.13
Chemokine ligand 10	NM_004591	CCL20	-6.30	-2.79	-1.25	1.68	1.40	-9.00	-4.42	-1.38	2.69	-2.97
Cyclooxygenase 2	NM_000963	COX2	1.64	2.25	-3.24	-1.48	2.69	-1.29	2.16	-5.27	-2.47	3.10
Interferon gamma	NM_000619	IFNG	1.13	-1.01	-4.50	1.00	-23.14	-2.14	-2.49	-4.44	-25.21	-3.51
Interleukin 1α	NM_000575	IL1A	-4.37	1.58	1.93	-2.91	3.32	-4.07	1.03	2.55	-4.29	-1.80
Interleukin 1β	NM_000576	IL1B	-2.84	1.18	2.70	1.76	8.33	-19.07	1.75	1.92	3.54	2.36
Interleukin 2	NM_000586	IL2	1.13	-1.01	1.00	-2.06	-1.73	-2.14	1.39	-1.08	-1.81	7.12
Interleukin 6	NM_000600	IL6	1.49	1.26	-1.17	2.73	1.84	-5.89	1.50	-2.43	1.05	-3.11
Interleukin 12α	NM_000882	IL12A	-10.43	-3.32	1.11	1.21	-2.43	-5.23	1.17	3.36	1.52	3.08
Interleukin 12β	NM_002187	IL12B	1.13	-1.01	-12.23	14.10	-13.09	-2.14	-2.49	-2.43	8.54	-1.55
Interleukin 23α subunit p19	NM_016584	IL23A	1.13	-1.01	-1.61	-16.70	1.52	1.69	2.58	1.43	2.35	9.22
Inducible nitric oxide synthase	NM_000625	INOS	-4.49	-4.26	-1.85	2.90	-1.55	4.00	-2.29	1.56	13.85	5.98
Toll like receptor 4	NM_138554	TLR4	-7.23	-2.30	1.02	-2.55	-1.85	-6.52	1.08	1.61	-6.51	-1.20
Tumor necrosis factor α	NM_000594	TNFA	3.52	-1.81	-6.92	10.94	-1.37	-2.99	-3.48	-3.07	2.50	-1.76
ANTI-INFLAMMATORY												
Cytotoxic T-lymphocyte-associated protein 4	NM_005214	CTLA4	1.13	-1.01	1.00	-27.66	-13.38	-2.14	-2.49	-14.46	-5.26	-4.57
Chemokine ligand 5	NM_002994	CXCL5	1.13	-1.01	-2.06	-6.53	1.04	-2.14	-2.49	-2.19	1.05	1.99
Chemokine ligand 12	NM_000609	CXCL12	-1.78	-4.02	-4.00	-7.85	-47.00	-5.57	1.04	-3.03	-5.48	-10.16
Indoleamine 2,3-dioxygenase 1	NM_002164	IDO1	1.94	-1.01	2.95	4.78	7.03	-4.03	1.46	-1.04	-2.08	11.98
Interleukin 4	NM_000589	IL4	5.45	-1.01	2.06	3.23	1.43	-2.14	-2.49	3.44	2.46	8.36
Interleukin 8	NM_000584	IL8	-1.12	2.03	2.31	1.46	3.51	-8.52	-3.10	-13.69	1.43	-8.83
Interleukin 10	NM_000572	IL10	1.13	-1.01	-1.74	-11.76	1.14	-2.14	-2.49	-2.15	-1.09	2.81
Interleukin 13	NM_002188	IL13	-1.95	-1.78	-3.72	-1.12	-1.90	-1.46	-2.38	-1.95	-1.89	3.83
Programmed cell death 1	NM_005018	PD1	1.13	-1.01	-6.96	1.00	1.00	-2.14	-2.49	1.00	1.00	-35.02
PD ligand 1	NM_014143	PDL1	-3.28	-3.80	2.94	1.02	1.02	-6.99	-2.10	3.12	-1.32	-1.06
Transforming growth factor β1	NM_000660	TGFB1	-1.70	-1.66	1.78	1.60	1.97	-1.16	-1.09	1.32	-1.09	5.73
CYTOKINES & GROWTH FACTORS												
Epidermal growth factor	NM_001963	EGF	-3.72	1.16	-1.71	-5.83	-2.16	1.24	2.42	4.46	2.89	5.49
EGF receptor	NM_005228	EGFR	-3.39	-1.61	1.31	-1.58	1.43	-5.84	1.04	1.45	-4.38	2.98
Insulin like growth factor 1	NM_000618	IGF1	-1.79	-1.41	2.65	-1.71	2.57	-1.14	2.15	6.51	1.53	14.92
IL-15	NM_000585	IL15	-2.27	1.52	-1.20	-2.81	-1.48	-2.71	1.15	-1.03	-6.58	1.16
Secreted phosphoprotein 1	NM_000582	SPP1	-1.32	-1.24	1.57	1.29	2.20	-1.10	-1.63	1.36	1.33	-86.08
SIGNAL TRANSDUCTION												
Granulocyte macrophage CSF-2	NM_000758	CSF2	-2.28	-2.12	-1.19	-1.07	-2.04	-11.63	-3.78	-3.68	-1.32	-5.01
Granulocyte CSF-3	NM_000759	CSF3	-20.76	-1.91	1.17	-1.88	2.07	-3.49	-3.20	-1.28	2.45	1.18
Signal transducer and activator of transcription 3	NM_003150	STAT3	-1.44	-1.76	1.71	1.32	1.73	-3.50	-1.30	1.23	-1.95	1.77
Toll like receptor 2	NM_003264	TLR2	-1.87	-2.14	-1.95	-115.20	-7.94	-3.06	1.85	-1.12	-254.96	-51.76
Toll like receptor 3	NM_003265	TLR3	-6.96	-2.05	3.38	2.30	2.94	-12.63	1.72	3.97	-1.94	8.19
ANTIGEN PRESENTATION												
Major histocompatibility complex, class I, A	NM_002116	HLA-B	1.13	-1.01	-42.84	-17.36	-3.38	-2.14	-2.49	-12.27	-50.65	1.26
Major histocompatibility complex, class I, B	NM_005514	HLA-C	1.13	-1.01	-23.10	-4.54	-9.91	-2.14	-2.49	-4.13	-10.02	1.27

Table 3. Select genes from commercial Human Cancer Inflammation and Immunity Crosstalk™ array displaying genes associated with inflammation, growth, signal transduction, and antigen presentation. All compounds treated at 10 μM. Treatments were compared to 0.1% DMSO as carrier control. T98G cells were treated for 6 h or 24 h, and triplicate samples pooled before mRNA extraction. Data represented as fold change compared to the appropriate time-point control and normalized against house-keeping gene expression.

Gene Name	Genbank No.	Symbol	T98G gene expression change after 6 hr					T98G gene expression change after 24 hr				
			E804	7BIO	TMF	E804 + TMF	7BIO + TMF	E804	7BIO	TMF	E804 + TMF	7BIO + TMF
PRO-INFLAMMATORY												
Chemokine ligand 2	NM_002982	CCL2	-6.29	-2.25	-9.35	-23.12	-17.97	-12.28	-1.41	-2.97	-61.80	-14.98
Chemokine ligand 10	NM_004591	CCL20	-4.65	1.92	1.19	-2.19	1.55	4.42	2.77	4.02	1.62	16.23
Cyclooxygenase 2	NM_000963	COX2	-2.06	11.23	5.85	8.53	54.11	13.98	10.06	8.78	5.60	76.77
Interferon gamma	NM_000619	IFNG	-2.06	-2.75	1.00	1.00	1.00	1.00	-1.15	-4.94	-3.28	-19.60
Interleukin 1α	NM_000575	IL1A	-8.28	2.13	2.39	-4.56	2.70	-8.20	-1.01	1.32	-3.45	2.41
Interleukin 1β	NM_000576	IL1B	-3.62	3.16	3.00	-1.35	4.48	-3.82	2.48	2.85	-1.34	9.09
Interleukin 2	NM_000586	IL2	-2.06	-1.40	1.00	-2.57	1.00	1.00	-1.15	-4.07	1.79	1.00
Interleukin 6	NM_000600	IL6	-2.11	-1.27	-1.58	-4.80	2.39	-1.62	1.94	-1.55	-3.80	4.72
Interleukin 12α	NM_000882	IL12A	-5.38	-2.58	-1.19	-9.13	-1.89	-1.03	1.00	-1.05	-6.65	-1.11
Interleukin 12β	NM_002187	IL12B	9.86	-1.16	1.00	60.43	1.00	1.00	-1.15	-1.78	190.64	-2.40
Interleukin 23α subunit p19	NM_016584	IL23A	7.50	8.65	2.78	8.12	4.27	1.38	1.36	2.23	7.59	1.94
Inducible nitric oxide synthase	NM_000625	INOS	17.19	1.48	-1.16	26.00	-5.29	21.99	4.21	7.35	99.05	34.46
Toll like receptor 4	NM_138554	TLR4	-6.79	-1.02	1.42	-4.02	-1.11	-2.20	1.92	2.81	-11.15	2.89
Tumor necrosis factor α	NM_000594	TNFA	-2.06	-2.75	1.00	1.65	1.00	1.00	-1.01	1.00	3.83	1.00
ANTI-INFLAMMATORY												
Cytotoxic T-lymphocyte-associated protein 4	NM_005214	CTLA4	-2.06	-2.75	1.00	1.00	1.00	1.00	-1.15	-37.81	-1.16	2.68
Chemokine ligand 5	NM_002994	CXCL5	-1.71	1.16	1.30	1.14	2.65	7.41	5.57	4.68	2.68	5.21
Chemokine ligand 12	NM_000609	CXCL12	-1.13	-1.19	-1.67	-2.08	-2.39	-1.96	-3.05	-1.63	-2.74	-5.80
Indoleamine 2,3-dioxygenase 1	NM_002164	IDO1	-2.06	2.35	1.94	3.77	4.28	4.81	7.05	4.76	-2.26	5.90
Interleukin 4	NM_000589	IL4	2.75	-1.26	1.52	4.91	1.20	1.16	-2.57	1.93	11.46	2.16
Interleukin 8	NM_000584	IL8	-15.24	1.60	-1.04	-8.76	1.90	-1.21	5.55	-1.95	-4.63	3.11
Interleukin 10	NM_000572	IL10	2.71	-1.59	1.53	1.55	1.00	15.45	-1.15	-1.86	3.92	5.88
Interleukin 13	NM_002188	IL13	2.16	1.07	-1.43	3.28	-3.08	15.63	2.01	3.60	11.32	-1.34
Programmed cell death 1	NM_005018	PD1	-2.06	-2.75	1.00	1.00	-15.83	1.00	-1.15	-1.71	1.00	1.00
PD ligand 1	NM_014143	PDL1	1.15	1.58	6.85	1.20	-10.61	-1.17	1.92	3.01	1.64	2.44
Transforming growth factor β1	NM_000660	TGFB1	1.33	1.50	1.14	-1.35	-2.16	1.64	2.02	1.72	1.67	2.08
CYTOKINES & GROWTH FACTORS												
Epidermal growth factor	NM_001963	EGF	-1.66	-1.04	-2.02	-3.87	-1.46	-1.56	-1.52	-1.58	-4.20	-2.23
EGF receptor	NM_005228	EGFR	-4.11	-1.17	-1.41	-2.64	-1.72	-1.42	1.39	1.31	-3.00	2.00
Insulin like growth factor 1	NM_000618	IGF1	-1.37	-2.31	-4.52	1.60	-7.24	-14.96	-549.26	-106.83	-13.50	-98.33
IL-15	NM_000585	IL15	1.42	-1.04	-2.86	-5.20	-1.43	1.13	-1.47	-2.77	-9.13	-2.52
Secreted phosphoprotein 1	NM_000582	SPP1	1.01	-1.43	1.55	1.31	1.71	-1.15	-1.85	1.72	1.05	1.33
SIGNAL TRANSDUCTION												
Granulocyte macrophage CSF-2	NM_000758	CSF2	-45.27	-3.12	-1.76	-21.77	-12.08	1.42	8.75	1.48	-45.19	2.45
Granulocyte CSF-3	NM_000759	CSF3	6.86	2.11	-1.31	13.15	1.18	3.13	-1.02	1.29	134.99	1.94
Signal transducer and activator of transcription 3	NM_003150	STAT3	-1.22	-1.01	1.44	1.31	1.29	-2.42	1.11	1.46	-1.21	1.47
Toll like receptor 2	NM_003264	TLR2	1.92	-2.48	1.00	1.06	1.00	7.37	1.61	-2.16	6.04	5.19
Toll like receptor 3	NM_003265	TLR3	1.05	1.82	3.08	2.48	3.16	-22.82	1.72	1.03	-8.85	1.91
ANTIGEN PRESENTATION												
Major histocompatibility complex, class I, A	NM_002116	HLA-B	-1.02	1.06	-2.46	-1.47	-1.82	1.00	8.35	1.05	2.16	1.98
Major histocompatibility complex, class I, B	NM_005514	HLA-C	1.28	1.21	-2.27	-2.04	-2.06	1.59	1.09	-2.20	-3.16	-2.05

3.3. Indirubins E804 and 7BIO modulate IL-6 and VEGF-A secretion in glioblastoma cell lines

As a hallmark cytokine marker of a pro-inflammatory environment, IL-6 secretion by LN-18 and T98G glioma cells was quantified after 6 h and 24 h exposure to E804, 7BIO, and in combination with the AHR antagonist TMF. IL-6 secretion was modestly suppressed, and moderated increased in LN-18 cell by E804 and 7BIO, respectively (Figure 4). These effects were completely inhibited by TMF. By 24 h post exposure to E804, IL-6 secretion was modestly suppressed, and this effect was reversed by co-exposure to TMF. TMF alone also increased IL-6 secretion in LN-18 cells. Of note, IL-6 secretion in LN-18 cells receiving only the carrier control increased between 6 and 24 h. In contrast to LN-18 cells, T98G cells did not secrete more IL-6 between 6 and 24 h culture. As with LN-18 cells, E804 lowered IL-6 secretion during the 6 h exposure, while 7BIO increased secretion in T98G cells. Unlike with LN-18 cells, addition of TMF increased IL-6 secretion in T98G cells. By 24 h post-exposure, 7BIO was shown to increase IL-6 secretion, and TMF enhanced this effect.

Vascular endothelial growth factor-A (VEGF-A) secretion was higher in LN-18 cells than in T98G cells at both 6 and 24 h of culture (Figure 5). Indirubin E804 suppressed VEGF-A secretion in LN-18 cells at 6 h, but not by 24 h, while 7BIO increased secretion at 24 h. At 6 h, VEGF-A secretion was inhibited by the presence of TMF, and at 24 h the effect continued with cells also receiving E804. There was little effect of treatments on VEGF-A secretion in T98G cells at 6 h,

with a slight increase from cells treated with E804 and TMF, while 7BIO increased secretion alone, and in combination with TMF. The combination of E804 and TMF suppressed VEGF-A secretion.

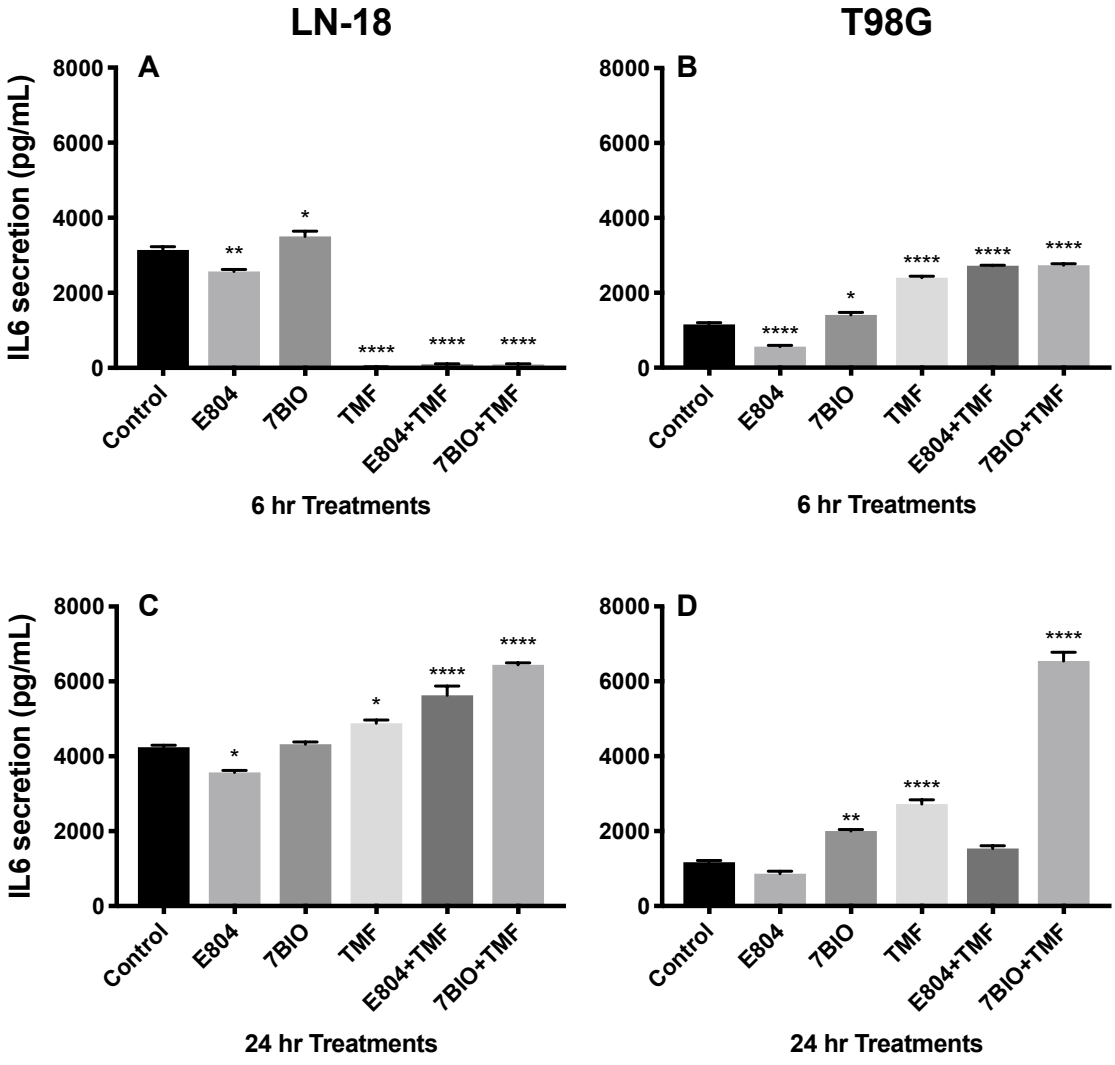

Figure 4. The effects of E804 or 7BIO, and/or TMF, on secretion of IL-6 as measured by ELISA. All compounds treated at 10 μM. Secretion in a, c) the LN-18 cell line and b, d) the T98G cell line, for 6 h (a and b) or 24 h (c and d). Data represent the mean fold expression $\pm$ S.E. of three different experiments. (*) indicates $p < 0.05$, (**) $p < 0.005$, (****) $p < 0.0001$.

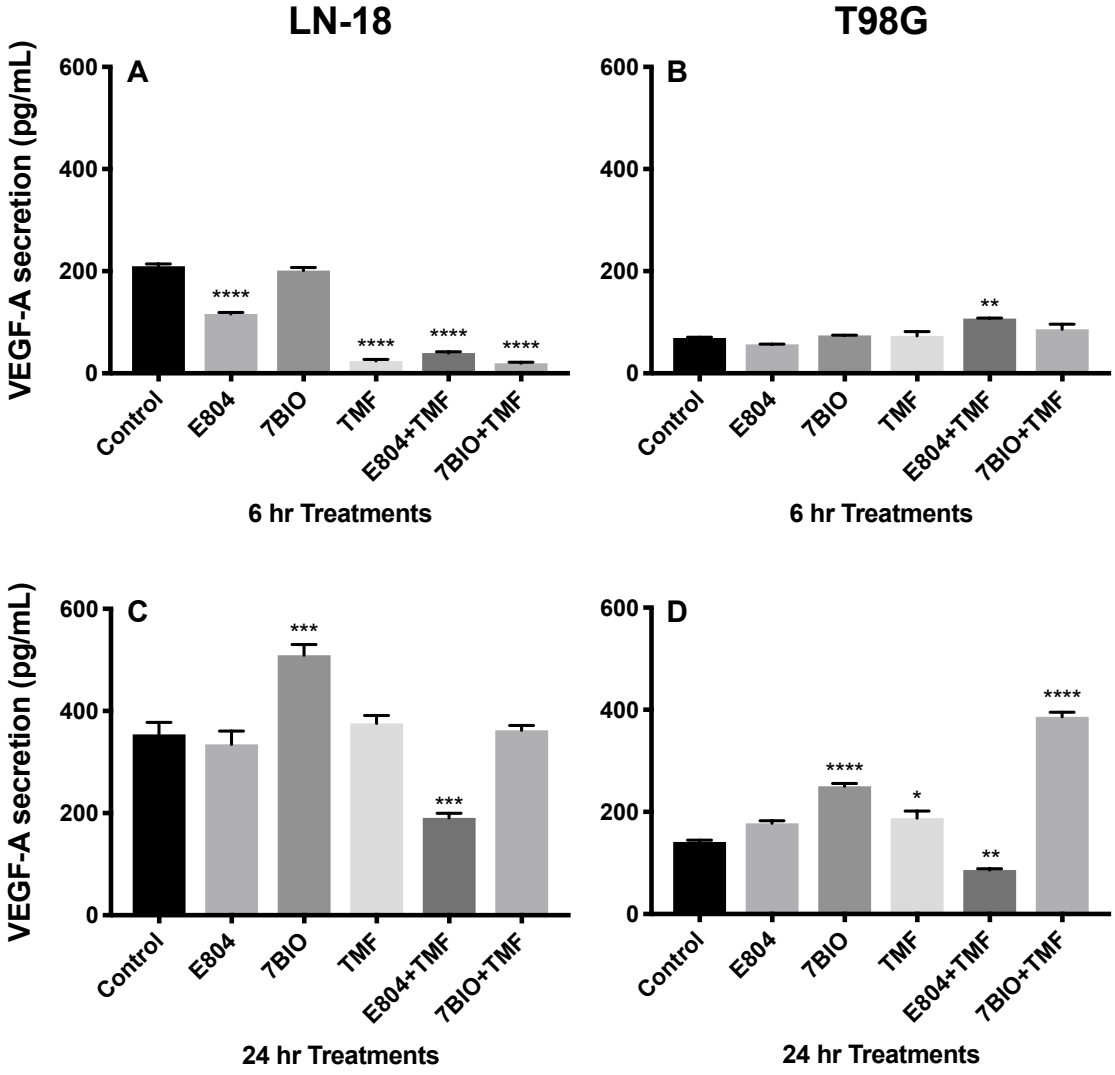

Figure 5. The effects of E804 or 7BIO, and/or TMF, on secretion of VEGF-A as measured by ELISA. All compounds treated at 10 μM. Secretion in a, c) the LN-18 cell line and b, d) the T98G cell line, for 6 h (a and b) or 24 h (c and d). Data represent the mean fold expression ± S.E. of three different experiments. (*) indicates $p < 0.05$, (**) $p < 0.005$, (***) $p < 0.0005$, (****) $p < 0.0001$.

4.0. DISCUSSION

In this study I found that, as with many other indirubins, E804 and 7BIO are ligands for the AHR, as demonstrated by the induction of *cyp1b1* in LN-18 and T98G glioma cells over the course of 6 to 24 h. Furthermore, this activity can be inhibited by AHR antagonism, depending on the time course and cell line. Although TMF is used to antagonize the activity of E804 and 7BIO, this flavonoid is also a partial agonist at early time points, as demonstrated herein with LN-18 cells, and by others (Murray et al. 2010). As a partial agonist, it induces *cyp1b1* minimally and continues to block the activity of E804, at least for up to 24 h. From observations with LN-18 cells, TMF is not an antagonist against the activity of 7BIO. The underlying differences in AHR activity between the two cell lines may be due to the observation that basal AHR protein levels are lower in LN-18 cells than in T98G cells, but the induction of CYPs by typical AHR ligands is higher in the former (Gramatzki et al. 2009).

The observation of AHR antagonism by TMF in these two glioma lines after treatment with E804 may bode well for clinical applications to impede the activity of endogenous ligands, namely kynurenines, produced during the metabolism of tryptophan by glioma associated TDO2 and IDO1/2. AHR activation by kynurenines in gliomas is associated with T-cell suppression and immune tolerance in the tumor microenvironment, and polarization of glioma associated macrophages towards the M2 phenotype, and thus a tumor-promoting environment (Guastella et al. 2018, Gabriely and Quintana 2019,

Takenaka et al. 2019). Flavonoid compounds like TMF, and many others, are common ingredients in plants used as a healthy diet, and pose no toxic threat to humans (Hubbard et al. 2017).

Previous studies have demonstrated anti-inflammatory properties of E804, and have shown that this compound targets STAT3 signaling (Chan et al. 2012, Miyoshi et al. 2012, Nam et al. 2005, Babcock, Anderson, and Rice 2013). Indirubin 7BIO has been shown to induce both caspase-dependent and independent cell death in several cancer cell lines, but to my knowledge has not been examined for anti-inflammatory or anti-STAT3 signaling activity (Nicolaou et al. 2012, Ribas et al. 2006). Herein, I demonstrate that 7BIO induces *stat3* gene expression in LN-18 and T98G cells, and therefore may not be suitable for glioma therapy because of the known pro-tumor role of STAT3 signaling in brain cancer. On the other hand, E804 does not induce *stat3* gene expression under the conditions examined herein. Taken together with aforementioned studies indicating its anti-STAT3 signaling properties, this compound may be better suited for future anti-glioma studies.

Gliomas comprise a highly pro-inflammatory neoplasia, secreting large amounts of IL-1β, IL-6, and IL-8 in human GBM cell lines and in cultured primary tumor cells (Yeung et al. 2013). The driver for these cytokines is typically NF-κB, which is expressed at high levels in some gliomas, and may be the cause of transitions from the pro-neural subtype to a mesenchymal state (Bhat et al. 2013). It has been suggested that IL-6 is an autocrine growth factor secreted by

gliomas, and this may be due to continued activation of NF-κB (Shan et al. 2015). However, glioma cells also secrete high levels of TGF-β, which contributes to T-reg activation and immunosuppression seen in the local and systemic environment of patients (Gramatzki et al. 2009, Vega, Graner, and Sampson 2008, Nduom, Weller, and Heimberger 2015).

The connection between TGF-β and NF-κB, and roles of IL-6 in glioma-inflammation cross-talk has been the subject of intense study. It has been suggested that TGF-β induces miR-182, and therefore suppresses the gene *cyld*, a deubiquination enzyme and negative regulator of NF-κB signaling components (Song et al. 2012). This leads to upregulation and sustained expression of NF-κβ. Furthermore, IL-6 secreted by gliomas activates the IL-6/JAK/STAT3 signaling pathway through an autocrine fashion (Johnson, O'Keefe, and Grandis 2018). This pathway, in turn, further activates NF-κB signaling, resulting in sustained IL-6 secretion (Hendrayani et al. 2016). This may explain the observed high background levels of IL-6 secreted by glioma cells in the absence of treatment, which were in the range of 3000 – 4000 pg/ml by LN-18 cells, and 1000 pg/ml by T98G cells. By comparison, LPS-activated macrophages typically secrete IL-6 in the range of 300 - 400 pg/ml (Matsebatlela et al. 2015).

Therefore, identifying small molecules to inhibit this pro-inflammatory cross talk in gliomas seems critical going forward. To that end, previous work from the Rice lab using the mouse macrophage cell line RAW264.7 demonstrated that E804 inhibits LPS-stimulated expression of NF-κB, along with

expression of *il6*, *il1*, *nos2*, and *csf2* (Babcock, Anderson, and Rice 2013). In this study I found that E804 slightly reduced IL-6 protein secretion, while other treatments, including AHR antagonism, increased production and secretion, and especially the combination of 7BIO and TMF at 24 h. It appears that AHR antagonism is anti-inflammatory early on following treatments in LN-18 cells, and slightly pro-inflammatory in T98G cells at the same time point. These data suggest that the potent effect of E804 and TMF on IL-6 protein production and secretion is short lived in LN-18 cells. At this point, it is unclear if these observations are due to differences in basal levels of AHR between the two cell lines.

The total anti-inflammatory properties of these treatments in glioma cells cannot be determined based solely on IL-6 secretion. To this point, the cancer-inflammation cross-talk gene array employed in this study yields more differences between LN-18 and T98G cells, and the effects of the two indirubins and the effects of AHR antagonism. The experimental design allowed us to observe the effects of TMF alone on the expression of select genes previously determined to have a role in cancer-inflammation cross-talk. From the array, it can be deduced that the AHR in LN-18 cells is involved in the expression of *ifng*, *ptsg2*, *il12b*, *tnfa*, *il10*, *il13*, the balance between *pd1* and *pdl1*, and even expression of *mhc1a/b*. The mechanisms associated with these changes in gene expression is not clear from this study, but LN-18 cells may provide an important platform for such future studies. Overall, the role of the AHR in the expression of

arrayed genes in T98G cells differed from LN-18 cells. AHR antagonism had the opposite effect on expression of *ptsg2*, *il12b*, *mhc1a/b*, and especially *igf1*, while maintaining high expression of *pdl1*. The downregulation of MHC-1 molecules on the surface of glioma cells may benefit natural killer cells because this is a major trigger for natural killer activation and target killing.

The observations that 7BIO induces expression of *stat3*, is a potent AHR agonist that is not antagonized with TMF, and promotes IL-6 and VEGF-A secretion to such a high degree, make it unlikely that 7BIO could be used to modulate glioma cells in future studies. On the other hand, E804 has broad anti-inflammatory properties, is an AHR ligand that can be antagonized in terms of AHR activities, and can target not only inflammatory genes, but those associated with growth factors and their receptors as well, including anti-VEGF-A secretion. Importantly for glioma studies, E804 did not induce *stat3* gene expression. Moreover, based on other published studies with E804 and other cancer cell types, this study supports future research with E804 with clinical applications in mind. This study also points to clear differences in responses to treatments between glioma cell lines, and suggests that future studies need to take into account differences in AHR activities between different glioma lines.

The ultimate goal of the research described herein is to replace current GBM post-operative practices of implanting carmustine-laden wafers in the cavity created by de-bulking the tumor mass. Carmustine is extremely toxic to not only glioma cells, but normal tissues as well, with severe negative effects of patients.

As an alternative, this study supports the use of E804-ladened wafers along with TMF to antagonize the AHR-associated responses of the compound. E804 may be anti-inflammatory, thus inhibit autocrine growth factors and cytokines and/or their receptors, block STAT3 signaling, and inhibit cyclin-dependent kinases. E804 is also an AHR ligand, and therefore it induces the expression of the battery of genes associated with AHR activation, including additional AHR expression, which is associated with glioma-derived kynurenine production, and thus pro-tumor properties. Simultaneous treatment with TMF may alleviate this particular property, and provide a non-toxic alternative to carmustine-laden wafers.

Acknowledgments

This work was funded, in part, by the Self-Regional Healthcare Human Genetics Research Program, Greenwood Genetics Center, Greenwood SC USA.

THE ANTI-INFLAMMATORY INDIRUBIN DERIVATIVE E804 [INDIRUBIN-3'-(2,3 DIHYDROXYPROPYL)-OXIMETHER)] DOES NOT ACTIVATE THE FULL UNFOLDED STRESS RESPONSE PATHWAY IN LN-18 AND T98G HUMAN GLIOMA CELL LINES.

Micaela R. Scobie

In review for publication in Chemico-Biological Interactions

Department of Biological Sciences

Clemson University, Clemson SC USA 29634

ABSTRACT

This study focused on the novel indirubin derivative E804 (indirubin-3'-(2,3 dihydroxypropyl)-oximether) and investigated its effects on endoplasmic reticulum stress in glioblastoma multiforme (GBM) cells *in vitro*. The unfolded protein response (UPR) pathway manages the cellular response to accumulated misfolded or unfolded proteins. I employed a gene array of 80+ genes to monitor the effect of E804 treatment at 24 h in LN-18 and T98G glioma cell lines, along with western blot analysis. The results suggest that E804 affects multiple arms of the UPR as indicated by fold changes in genes related to protein binding, protein degradation, UPR transcription factors, and apoptosis. Furthermore, these data demonstrate a reversal of heightened UPR stress in glioma cells, as shown by the down regulation of *hsp5, atf6, xbp1, atxn3,* and *perk*. Genes such as *hsp5* and *atxn3* have been implicated in tumor cell proliferation, and *atf6* and *xbp1* activate a stress response, indicating that E804 may provide a neuroprotective, yet anti-proliferative response in tumor cells. Given the sensitive location, brain cancer drugs should not induce widespread apoptosis that may affect healthy tissue. Desirably, effectors associated with apoptosis such as *chop, perk,* and GADD34 were down regulated by E804. Of note, down-regulation of *perk* has been associated with an improved response to chemotherapy in resistant tumors. Taken together, these results indicate that E804 is a strong modulator of the UPR in LN-18 and T98G cells and should be pursued further as a potential drug for neurological disorders such as GBM.

Key terms: Glioblastoma, E804, Indirubin, UPR, CHOP

1.0. INTRODUCTION

Some of the most difficult diseases to treat and manage are the primary brain and central nervous system cancers, of which roughly 30% are gliomas. Of these gliomas, glioblastoma multiforme (GBM) (WHO grade IV) is the most aggressive and lethal subset (Holland 2000). Found mainly in the cerebral hemispheres, GBM may arise from astrocytes, but other cell types may contribute as well, including neuronal and oligodendrocyte precursors (Zong, Verhaak, and Canoll 2012, Zong, Parada, and Baker 2015, Alcantara Llaguno and Parada 2016), which may determine the origin and nature of glioma stem cells (Jackson, Hassiotou, and Nowak 2014). Although glioblastoma cannot be cured surgically, the first management step is to surgically debulk as much of the tumor as possible.

Following surgery, GBM is usually treated with radiotherapy and chemotherapy, or immunotherapy with the goal of slowing tumor growth. Despite intense research efforts to date, no current treatments are completely curative (Young et al. 2015). Typical chemotherapy options include alkylating agents such as lomustine (chloroethyl cyclohexyl nitrosourea - CCNU) and temozolomide (TMZ), delivered orally, and carmustine (bischlorethyl nitrosourea -BCNU), delivered as an infused wafer directly to the brain post-operatively (Ramirez et al. 2013, Wei et al. 2014). Oral medications such as TMZ are difficult to deliver across the blood-brain barrier (Ramirez et al. 2013), and implantation of carmustine-infused biodegradable polymers has limited success with high risk of

brain edema and infection (Omuro and DeAngelis 2013). Moreover, these alkylating agents induce the unfolded protein response (UPR) and apoptosis indiscriminately (Hombach-Klonisch et al. 2018), and may be associated with severe systemic toxicity as well, including myelosuppression and pulmonary toxicity (Hombach-Klonisch et al. 2018). Thus, pharmacological alternatives to alkylating agents are needed.

Indirubin is the active ingredient in Danggui Longhui Wan, an ancient Chinese herbal remedy for neoplasia and inflammation derived from the plant *Polygonum tinctorium* (Hoessel, Leclerc, Endicott, Nobel, et al. 1999, Leclerc et al. 2001). Natural indirubin can be produced by *P. tinctorium* (Leclerc et al. 2001), bacteria (Bhushan, Samanta, and Jain 2000) , mollusks, and other biological sources (Meijer et al. 2003, Cooksey 2001). Indirubins synthetic derivatives are of interest in cancer research because of their ability to inhibit cyclin-dependent and glycogen synthase kinases (Leclerc et al. 2001, Cheng et al. 2017).

In addition to their effects on CDK activity, various indirubin derivatives also bind and activate the aryl hydrocarbon receptor (AHR) (Adachi et al. 2001, Springs and Rice 2006, Faber et al. 2018, Kawanishi et al. 2003, Scobie, Houke, and Rice 2019). The AHR is a member of the basic helix-loop-helix (bHLH-PAS) superfamily of proteins and functions as a ligand-activated transcription factor (Gu, Hogenesch, and Bradfield 2000) for multiple responsive gene products. Most notable of these genes include phase I and II drug-metabolizing enzymes

and transporters (Denison et al. 2002, Hu et al. 2007, Nebert et al. 2000, Köhle and Bock 2007). Other gene products include proteins associated with cell cycle arrest, such as *p21, p57*, and *p27* (Knockaert et al. 2004). Unlike many environmental AHR ligands, such as planar PCBs and TCDD, indirubins are metabolized very quickly (Guengerich et al. 2004) by phase I enzymes (CYP1A1, CY1B1) induced through AHR activation. It is now clear that the AHR plays a key role in a myriad of physiological roles; not only of drug metabolism, but also immune regulation, organogenesis, mucosal barrier function, and cell cycle arrest (Hubbard, Murray, and Perdew 2015). AHR-indirubin structure activity relationships (SARs) vary depending upon specific indirubin derivative structure and bioavailability (Blažević et al. 2015). Further elucidation of biological actions of indirubin derivatives is a promising avenue for GBM research.

One particular indirubin derivative, [indirubin-3'-(2,3 dihydroxypropyl)-oximether)] (E804) has also been shown to inhibit angiogenesis in human umbilical vein endothelial cells (HUVECs) *in vivo* (Shin and Kim 2012), has potent anti-inflammatory properties (Babcock, Anderson, and Rice 2013), inhibits STAT3 signaling (Nam et al. 2005a), and has shown promise in other systems as well (Kim et al. 2009, Moon et al. 2006, Nicolaou et al. 2012, Shin and Kim 2012). Moreover, I recently demonstrated that E804 has potent anti-inflammatory properties, suppresses STAT3 expression, and is a potent AHR ligand in glioma cell lines (Scobie, Houke, and Rice 2019). To my knowledge, it is not known if E804 induces apoptosis through the unfolded protein response

(UPR), and thus would have undesirable effects in non-tumor cells surrounding glioma cells *in situ*. One recent study demonstrated that select indirubin derivatives protect against the UPR in HT22 neuronal cells by down-regulating the apoptosis regulator CHOP, although E804 was not one of those examined (Kosuge et al. 2017).

The LN-18 and T98G cell lines were chosen for their sensitivity to indirubin compounds such as E804, due to differing basal expression of the aryl hydrocarbon receptor (AHR) (Gramatzki et al. 2009). To date, both cell lines have been used extensively in both brain cancer and ER stress research (Weatherbee, Kraus, and Ross 2016, Nguyen et al. 2019). Therefore, LN-18 and T98G cell lines are good models to study the potential neuro-protective effects of indirubins via alleviation of ER stress. LN-18 and T98G cells were initially collected from grade IV astrocytomas in Caucasian males ages 65 and 61, respectively (ATCC). Others have shown that LN-18 and T98G cells are sensitive to UPR pathway induction, especially via PERK signaling (Jia et al. 2010), and therefore provide a good in vitro system for further exploration.

Not only do these cell lines have an active protein stress response, they also express high levels of tumor suppressor genes that respond to genotoxic stress such as *p53* and *p21*. T98G cells typically have higher levels of p53 protein, as they are homozygous mutant at 237, while LN-18 cells are heterozygous mutant at 238. Both cell lines express high levels of p21 and do not express p16 *(Weller et al. 1998)*. T98G cells have higher protein levels of BCL-2

apoptotic family proteins, including BCL-2, MCL-1, BCL-X, and BAX. Additionally, the LN-18 cell line is generally more sensitive to drug-induced cytotoxicity than the T98G line (Weller et al. 1998).

Herein I show that E804 suppresses the expression of several key genes and proteins involved in the UPR, including CHOP, in two glioma cell lines differing in AHR activities. This study supports the use of E804 in future studies seeking advancement in the treatment of GBM.

2.0. MATERIALS AND METHODS

2.1. Chemicals: Indirubin-3'-(2,3 dihydroxypropyl)-oximether (E804) was obtained from Alexis Biochemical (CA,USA). Stock solution was prepared at 10^{-2} M by solubilizing in dimethyl sulfoxide (DMSO, Corning, NY, USA). DMSO carrier used at <0.1% v/v.

2.2. Cell culture: Human Glioblastoma Multiforme (GBM) cell lines, LN-18 (ATCC CRL-2610) and T98G (ATCC CRL-1690), were obtained from ATCC (VA, USA) and cultured using Dulbecco's Modified Eagle's Medium (DMEM, Cellgro, MA, USA) as the base medium. Medium was supplemented with 10% heat-inactivated fetal bovine serum supplemented with iron (Hyclone, USA), 20 mM HEPES, 10 mM l-glutamine, 100 U/ml penicillin, 100 µg/ml streptomycin,

110 µg/ml sodium pyruvate, 1% non-essential amino acids (100 × stock), 4.5 g/l glucose, and 1.5 g/l of $NaHCO_3$, each from Sigma (Sigma Aldrich, MO, USA). Cells were typically grown and maintained at 37 °C with 5% CO_2 in Corning 75 cm^2 culture flasks.

2.3. Focused commercial RT-qPCR arrays for Human Unfolded Protein Response Plus: LN-18 and T98G cells were seeded at 2 x 10^6 cells/mL in a 24-well plate and allowed to adhere for 24 h. Cells were then treated in triplicate with 10 µM E804 or 0.1% DMSO carrier control, in a total of 1 mL complete medium per well. Twenty-four hours post-exposure, cells from all three replicates were pooled and dissolved in 1 mL of RNAzol (Molecular Research, OH, USA) and mRNA was extracted using the RT2 First Strand Kit and according to manufacturer's instructions (Qiagen, Hilden, Germany). Complementary DNA was synthesized using RT^2 Easy First Strand Kit (Qiagen) and included removal of gDNA contamination using elimination mixture supplied by the manufacturer. A predesigned Unfolded Protein Response Plus Profile array of 96 genes was purchased from Qiagen Corporation (cat # PAHS-089Y) for use with RT² SYBR Green ROX qPCR mastermix from the same supplier, and provided instructions were followed. Real time-qPCR was performed on a StepOnePlus (Applied Biosystems) RT-qPCR machine. For data analysis, the ΔΔCt method was used; for each gene, fold-changes were calculated as difference in gene expression between untreated controls and treated cell cultures. Data were gathered and

interpreted using software provided by Qiagen. Details on methods have been previously published (Matsebatlela et al. 2015, Babcock, Anderson, and Rice 2013).

2.4. Western Blotting: LN-18 and T98G cells were seeded at 2 x 10^6 cells/mL in T-75 flasks and allowed to adhere for 24 h. Cells were then treated with 10 μM E804 or 0.1% DMSO carrier control for 24 h in a total volume of 10 ml. Supernatants were then removed, and cells lysed with 1 ml RIPA buffer (50 mM Tris HCl, pH 8, 150 mM NaCl, 1% NP-40, 0.5% sodium deoxycholate, and 0.1% SDS) containing Halt™ protease inhibitor cocktail (Thermo Fisher). Cell lysates were incubated on ice for 30 min, then centrifuged at 500 *g* for 2 min. The overlying supernatant was removed and centrifuged again for 20 min at 14,000 *g*, followed by quantification of protein content of overlying supernatants. Twenty-five μg of lysate protein from each sample were separated by SDS–PAGE on 4-20% gels (Biorad, Richmond CA USA), and transferred to a PVDF membrane (Immobilon-P, EMD Millipore, MA, USA) for 1 h at 100 V on ice. Membranes were blocked overnight at 4 °C in 10% bovine calf serum, then probed with primary antibody for 1 h, washed, and probed with secondary AP-conjugated antibody for 2 h at room temperature. Protein signals were detected using 5-bromo-4-chloro-3-indolyl-phosphate (BCIP) and Nitro Blue Tetrazolium (NBT) in alkaline phosphatase (AP) developer (Fisher). The rabbit polyclonal antibodies against ATF6a (ab203119; diluted 1:500) and XBP1 (ab37152; diluted 1:500)

were purchased from Abcam, GADD34 (10449-1-AP; diluted 1:333) from Protein Tech; and the mouse monoclonal antibody against CHOP (MA1-250; diluted 1:500) was purchased from Thermo Fisher. Beta-actin loading control antibody (AC-15, diluted 1:2500) was purchased from Sigma-Aldrich. Anti-rabbit and anti-mouse AP-labeled secondary antibodies were diluted 1:2000 (Thermo Fisher). The experiment was repeated three times. Band densities were imaged and quantified using ImageJ.

3.0. RESULTS

3.1. E804 induces UPR-related gene profiles in LN-18 and T98G glioma cells

Both LN-18 and T98G cell lines were responsive to the UPR stress-reduction properties of E804 (Table 4, Figure 6, Supplemental Table 1). Genes associated with binding of unfolded protein were affected by E804 treatment, especially in the T98G cell line. Specifically, *hspa1b* was up-regulated 96-fold in T98G cells, and *hspa2* was up-regulated 24- and 81-fold in LN-18 and T98G cells respectively. All other genes queried in this class were down-regulated by E804 in T98G cells, whereas LN-18 cells were primarily unaffected. Genes associated with protein degradation, such as *herpud1, htra2, mbtps2,* and *nploc4* were for the most part down-regulated by E804, especially in T98G cells. *Nploc4* was minorly up-regulated in LN-18 cells. The important transcription factor *atf6*,

responsible for signaling one arm of the apoptotic cascade in the UPR, was down regulated in both cell lines. Of note, transcription factors *atf4, creb3l3,* and *ire1* were all minorly up-regulated in both cell lines. Genes involved with apoptosis were affected by E804 treatment, including down regulation of *Atxn3, chop*, and *perk* in both cell lines, and by up to 25-fold in T98G cells. *Gadd34* was up-regulated by 4- and 24-fold in LN-18 and T98G cells, respectively.

Table 4. Select genes from commercial Human Unfolded Protein Response Plus™ array displaying genes associated with unfolded protein binding, ER associated degradation (ERAD), transcription, and apoptosis. Both cell lines treated with E804 at 10 μM for 24 h. Treatments were compared to 0.1% DMSO as carrier control. Samples were run in triplicate and pooled prior to mRNA extraction. Data represented as fold change compared to the control and normalized against house-keeping gene expression.

Gene Name	Entrez ID	Symbol	E804 Treatment	
			LN18	T98G
UNFOLDED PROTEIN BINDING				
Chaperonin containing TCP1 subunit 4	10575	CCT4	-1.57	-3.31
DnaJ heat shock protein family (Hsp40) member B9	4189	DNAJB9	1.48	-16.05
Endoplasmic reticulum oxidoreductase 1 beta	56605	ERO1B	1.65	-5.95
Heat shock protein family A (Hsp70) member 1B	3304	HSPA1B	-2.41	96.33
Heat shock protein family A (Hsp70) member 2	3306	HSPA2	24.00	81.70
Heat shock protein family A (Hsp70) member 5	3309	HSPA5	-1.65	-2.46
SIL1 nucleotide exchange factor	64374	SIL1	-1.41	-1.58
T-complex 1	6950	TCP1	1.05	-1.40
Torsin family 1 member A	1861	TOR1A	-1.26	-4.23
ER ASSOCIATED DEGRADATION (ERAD)				
Derlin 1	79139	DERL1	-1.46	3.24
ER degradation enhancing alpha-mannosidase like protein 1	9695	EDEM1	2.33	1.22
F-box protein 6	26270	FBXO6	-1.01	9.12
Homocysteine inducible ER protein with ubiquitin like domain 1	9709	HERPUD1	-1.72	-12.07
HtrA serine peptidase 2	27429	HTRA2	-4.34	-9.54
Membrane bound transcription factor peptidase, site 2	51360	MBTPS2	1.25	-10.75
NPL4 homolog, ubiquitin recognition factor	55666	NPLOC4	3.11	-2.29

TRANSCRIPTION FACTORS				
Activating transcription factor 4	468	ATF4	1.97	1.16
Activating transcription factor 6	22926	ATF6	-1.73	-2.22
cAMP responsive element binding protein 3 like 3	84699	CREB3L3	2.52	4.17
Endoplasmic reticulum to nucleus signaling 1	2081	IRE1	3.34	2.01
Endoplasmic reticulum to nucleus signaling 2	10595	IRE2	1.45	-1.45
SREBF chaperone	22937	SCAP	-1.53	1.95
Sterol regulatory element binding transcription factor 1	6720	SREBF1	4.44	-3.68
X-box binding protein 1	7494	XBP1	1.12	-6.93
APOPTOSIS				
Ataxin 3	4287	ATXN3	-2.20	-3.85
CCAAT enhancer binding protein beta	1051	CEBPB	-4.57	3.01
DNA damage inducible transcript 3	1649	CHOP	-8.47	-25.08
Protein phosphatase 1 regulatory subunit 15A	23645	GADD34	4.10	24.01
Eukaryotic translation initiation factor 2 alpha kinase 3	9451	PERK	-1.79	-3.20
Selenoprotein S	55829	VIMP	2.10	1.12

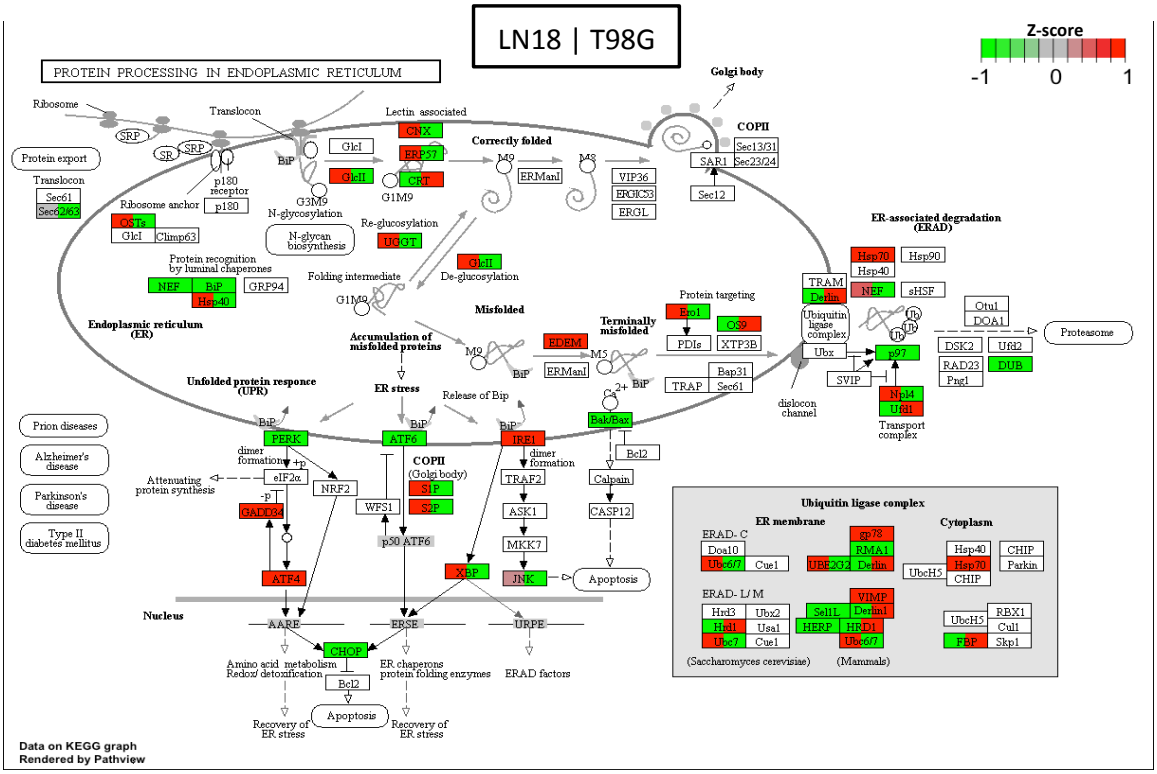

Figure 6. KEGG pathway of Protein Processing In Endoplasmic Reticulum, visually representing data presented in Table 1. Green boxes indicate fold down-regulation of E804-treated sample compared to the control, red boxes indicate fold up-regulation. Fold change v- scaled normalized to -1 through 1. Fold change of individual genes are split up into LN-18 cells on the left and T98G cells on the right within each box.

3.2. E804 affects GADD34 protein signaling in T98G glioma cells

Western blot analysis revealed no difference in protein expression of ATF6, sXBP1, uXBP1, or CHOP at 24 h post E804 treatment (Figure 7). GADD34 was decreased ($p < 0.0001$) by E804 in the T98G cell line. E804 appears to have an up-regulatory trend in the LN-18 cell line, as opposed to a down-regulatory trend in the T98G cell line. The active spliced XBP1 was expressed at basal levels in the LN-18 cell line, but not at all in the T98G cell line, and was unaffected by E804 treatment.

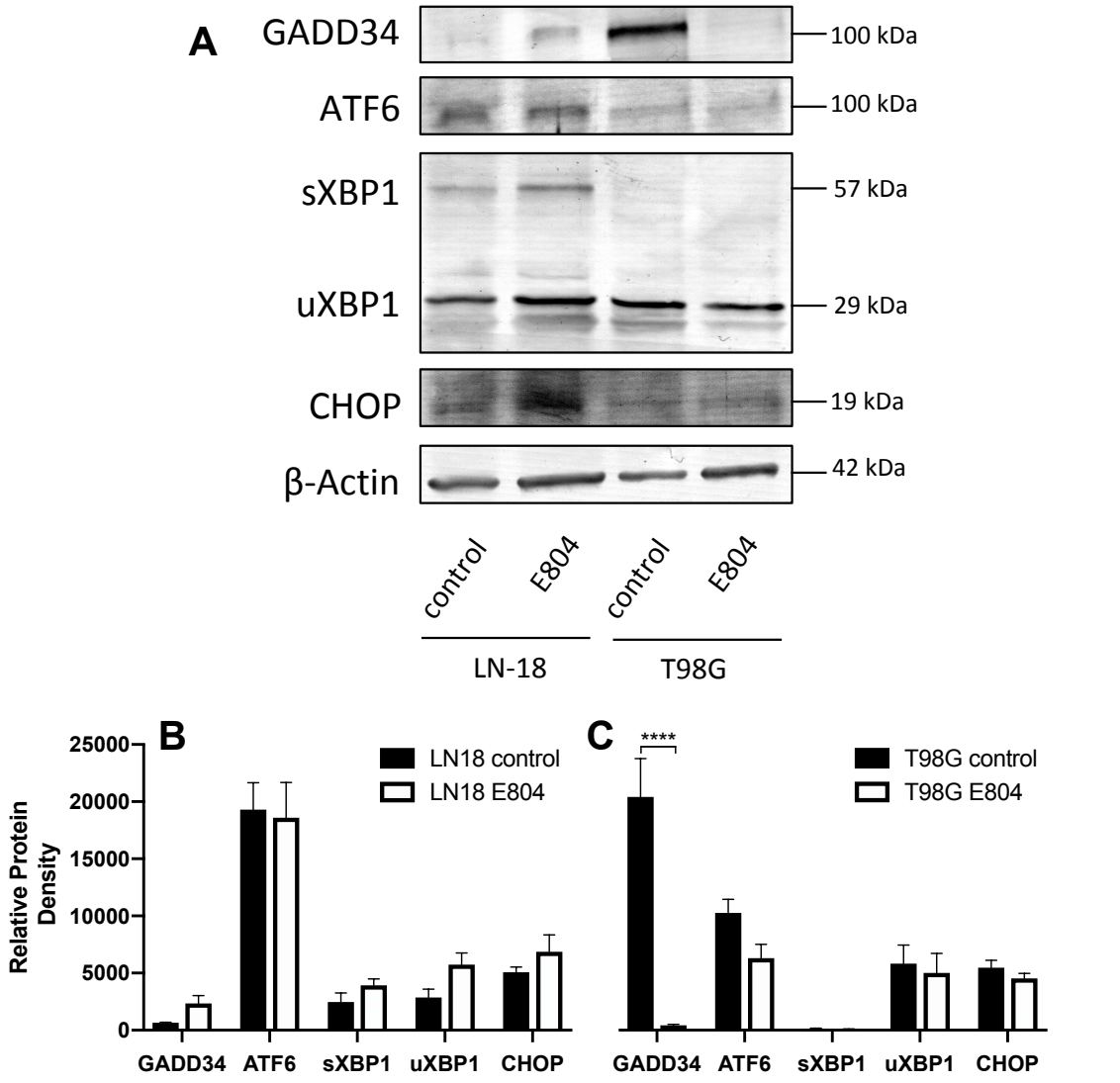

Figure 7. Protein levels of GADD34, ATF6, XBP1 (spliced and un-spliced), CHOP, and loading reference β-Actin, as measured by western blot (A) in both cells lines after treatment with E804 for 24 h. Relative protein density from western blot in LN-18 cell line (B) and T98G cell line (C).

4.0. DISCUSSION

Constitutive UPR activation has been reported in many cancers (Doultsinos et al. 2019). Although not completely understood, the IRE1 and PERK arms of the UPR appear to play a supporting role in tumorigenesis and progression. Due to mutation, hypoxic conditions, glucose deprivation, low pH, and rapid growth, glioma cells are exposed to many factors that heighten the risk of protein misfolding (Ma and Hendershot 2004). These stressors, combined with increased protein requirements, may lead to induction of the UPR. The adaptive healing and anti-apoptotic responses of the UPR are first induced in order to process the accumulation of misfolded proteins. If unsuccessful, later responses may lead to induction of apoptosis. However, tumors appear able to exploit these stress response pathways to benefit from initial pathway protective mechanisms, while avoiding later-stage apoptosis (Luo and Lee 2013). Because prolonged, chronic activation of the UPR pathways has been implicated in tumor progression, targeted down regulation of certain UPR-related genes is a likely therapeutic target for GBM and other cancers. The increase in UPR activity during glioma initiation and progression provides a fresh avenue of exploration for potential cancer therapeutics.

In this study I found that E804 induced changes in mRNA abundance in both cell lines (LN-18 and T98G), as determined using the commercially available qRT-PCR array. Among the groups of genes affected by treatment were the heat shock proteins (HSPs). HSPs are involved in an initial protective

response within the cell, as they identify and tag misfolded proteins for repair or removal (Sajjad, Samson, and Wyttenbach 2010). E804 induced up-regulation of *hspa2* in both cell lines, and *hspa1b* in T98G cells. Conversely, *hspa5*, known as the master regulator of the UPR, was down regulated, indicating a dichotomous response to E804. *Hspa5* has been implicated in an adaptive response to chronic stress in cancer. Of note, it has been reported that down-regulation of *hspa5* correlates to slowed glioma growth (Pyrko et al. 2007). Therefore, inhibition of *hspa5* is currently being investigated as a means to enhance autophagy via the UPR (Uckun et al. 2011, Cerezo and Rocchi 2017).

Another set of genes that may confer protective functions in surrounding tissue encodes the transcription factors associated with activating the UPR. The data herein indicates that E804 affects expression levels of *atf6, xbp1,* and *ire1*, among others. In addition to binding proteins such as *hspa5* above that may modulate autophagy, transcription factor IRE1 has been linked to autophagy, and is up-regulated in both glioma cell lines herein (Høyer-Hansen and Jäättelä 2007). ATF6 is one of three major transcriptional arms of the UPR and causes increased production of stress-response effectors such as XBP1 and pro-apoptotic factor CHOP (Epple et al. 2013, Yoshida et al. 2001). Down-regulation of *atf6* was observed in both glioma lines after treatment, which may indicate that E804 exeerts a dampening effect on the adaptation to ER stress that occurs in malignant tumors such as GBM, while also dampening one arm of the apoptotic signal. The down-regulation of both *atf6* and *xbp1* may indicate neuroprotective

effects via dampening of the UPR when these GBM cells are treated with E804 (Credle et al. 2015). These transcription factors are also known to activate other pathways such as STAT3 and thus E804-modulated activation of these genes could demonstrate crosstalk processes occurring (Chen and Zhang 2017).

Considering the physical proximity within which drugs are delivered to glioma tumors, it would be undesirable for E804, or similar small molecules, to initiate widespread apoptosis. The down-regulation of UPR, *atxn3, chop,* and *perk*, key regulators of the UPR, indicate that E804 delivers an anti-apoptotic signal to these glioma cells. Another important pro-apoptotic gene, *gadd34,* was upregulated in both cell lines, however protein expression of GADD34 was suppressed, may indicate that E804 inhibits pro-apoptotic profiles prior to 24 h. Until further studies are carried out, the significance of the pro-apoptotic gene expression profile over time in response to E804 remains unknown. Of note, PERK has been associated with higher-grade gliomas, and the silencing of *perk* has been found to ameliorate chemoresistance (Hou et al. 2015). Thus, the modest downregulation of *perk* by E804 may indicate a potential role as adjuvant therapy for E804 *in vivo*. While CHOP and PERK are pro-apoptotic, ATXN3 is responsible for cleaving ubiquitin from proteins marked for degradation. Other similar deubiquitylating enzymes have been implicated in cell proliferation during oncogenesis (Hussain, Zhang, and Galardy 2009), and thus inhibition of these enzymes, such as was seen by E804 herein, have clinical relevance.

Indirubin-induced *chop* down-regulation may be due to inhibition of glycogen synthase kinase 3 (GSK-3) (Meares et al. 2011). Additionally, GSK-3 is a major regulator of numerous and diverse pathways, and dysregulation of these pathways is implicated in many disease types, including cancer (Mancinelli et al. 2017). GSK-3 regulates the STAT3 pathway, which is also involved in glioma development (Ganguly et al. 2018) and has been found to be down-regulated by E804 treatment in my prior work (Scobie, Houke, and Rice 2019). A few studies have investigated the UPR in response to other indirubin derivatives (Joshi, Kulkarni, and Pal 2013, Meares et al. 2011, Kosuge et al. 2017), however to my knowledge this is the first study to examine the glioma UPR in response to E804 treatment. E804 is a known activator of the STAT3 cascade, an important inflammatory pathway in glioma autocrine signaling during tumorigenesis and promotion (McFarland et al. 2013). Of note, STAT3 can be activated in response to ER stress, a process partially dependent on the PERK arm of the UPR signaling cascade (Meares et al. 2014).

This study confirms that E804 regulates many genes involved in the unfolded protein response, including *perk, gadd34, chop, atf6,* and *xbp1*. Such regulation of the UPR in GBM cells has implications for treatment of neuroinflammatory conditions using this compound, and possibly in combination with others. Based on the extreme toxicity of current chemotherapeutic agents employed in glioma therapy, alternative and less toxic are needed, while also targeting glioma cells and not normal bystander cells of the central nervous

system. E804 and other indirubins are likely candidates that should be examined for their potential as treatment option for gliomas.

Acknowledgments:

This work was funded, in part, by the Self-Regional Healthcare Human Genetics Research Program, Greenwood Genetics Center, Greenwood SC USA.

SUPPLEMENTARY DATA

Supplementary Table 1. Select genes from commercial Human Unfolded Protein Response Plus™ array displaying genes associated with unfolded protein binding, ER associated degradation (ERAD), transcription, and apoptosis. Both cell lines treated with E804 at 10 μM for 24 h. Treatments were compared to 0.1% DMSO as carrier control. Samples were run in triplicate and pooled prior to mRNA extraction. Data represented as fold change compared to the control and normalized against house-keeping gene expression.

Gene Name	**Entrez ID**	**Symbol**	**E804 Treatment**	
			LN18	**T98G**
UNFOLDED PROTEIN BINDING				
calreticulin	811	CALR	-2.10	1.68
calnexin	821	CANX	1.40	-1.03
chaperonin containing TCP1 subunit 4	10575	CCT4	-1.57	-3.31
DnaJ heat shock protein family (Hsp40) member B9	4189	DNAJB9	1.48	-16.05
DnaJ heat shock protein family (Hsp40) member C10	54431	DNAJC10	1.09	-1.28
endoplasmic reticulum oxidoreductase 1 beta	56605	ERO1B	1.65	-5.95
heat shock protein family A (Hsp70) member 1B	3304	HSPA1B	-2.41	96.33
heat shock protein family A (Hsp70) member 2	3306	HSPA2	24.00	81.70
HtrA serine peptidase 2	27429	HTRA2	-4.34	-9.54
prefoldin subunit 5	5204	PFDN5	1.20	-1.09
peptidylprolyl isomerase A	5478	PPIA	1.05	-1.50
SREBF chaperone	22937	SCAP	-1.53	1.95
SEC63 homolog, protein translocation regulator	11231	SEC63	-1.07	-1.47
SIL1 nucleotide exchange factor	64374	SIL1	-1.41	-1.58

t-complex 1	6950	TCP1	1.05	-1.40
torsin family 1 member A	1861	TOR1A	-1.26	-4.23
UDP-glucose glycoprotein glucosyltransferase 1	56886	UGGT1	1.14	-1.12
ER PROTEIN FOLDING QUALITY CONTROL				
ER degradation enhancing alpha-mannosidase like protein 1	9695	EDEM1	2.33	1.22
glucosidase II alpha subunit	23193	GANAB	1.06	-2.26
glucosidase alpha, neutral C	2595	GANC	1.27	-13.20
protein kinase C substrate 80K-H	5589	PRKCSH	1.12	1.37
ribophorin I	6184	RPN1	1.14	-1.55
stress associated endoplasmic reticulum protein 1	27230	SERP1	-1.43	-6.06
endoplasmic reticulum protein 44	23071	ERP44	1.13	-1.87
UDP-glucose glycoprotein glucosyltransferase 1	56886	UGGT1	1.14	-1.12
REGULATION OF CHOLESTEROL METABOLISM				
insulin induced gene 2	51141	INSIG2	1.31	-3.62
membrane bound transcription factor peptidase, site 1	8720	MBTPS1	1.56	-1.54
membrane bound transcription factor peptidase, site 2	51360	MBTPS2	1.25	-10.75
SREBF chaperone	22937	SCAP	-1.53	1.95
sterol regulatory element binding transcription factor 1	6720	SREBF1	4.44	-3.68
REGULATION OF TRANSLATION				
eukaryotic translation initiation factor 2A	83939	EIF2A	1.15	-1.59
eukaryotic translation initiation factor 2 alpha kinase 3	9451	PERK	-1.79	-3.20
protein phosphatase 1 regulatory subunit 15A	23645	GADD34	4.10	24.01
stress associated endoplasmic reticulum protein 1	27230	SERP1	-1.43	-6.06
ER ASSOCIATED DEGRADATION (ERAD)				

autocrine motility factor receptor	267	AMFR	1.72	1.79
derlin 1	79139	DERL1	-1.46	3.24
ER degradation enhancing alpha-mannosidase like protein 1	9695	EDEM1	2.33	1.22
F-box protein 6	26270	FBXO6	-1.01	9.12
homocysteine inducible ER protein with ubiquitin like domain 1	9709	HERPUD 1	-1.72	-12.07
HtrA serine peptidase 2	27429	HTRA2	-4.34	-9.54
HtrA serine peptidase 4	203100	HTRA4	2.58	1.41
membrane bound transcription factor peptidase, site 1	8720	MBTPS1	1.56	-1.54
membrane bound transcription factor peptidase, site 2	51360	MBTPS2	1.25	-10.75
NPL4 homolog, ubiquitin recognition factor	55666	NPLOC4	3.11	-2.29
nucleobindin 1	4924	NUCB1	1.38	-1.18
OS9 endoplasmic reticulum lectin	10956	OS9	-1.24	1.34
SEL1L adaptor subunit of ERAD E3 ubiquitin ligase	6400	SEL1L	-1.41	-1.58
selenoprotein S	55829	VIMP	2.10	1.12
synoviolin 1	84447	SYVN1	-1.67	1.41
SEC62 homolog, preprotein translocation factor	7095	SEC62	1.04	-1.59
UBX domain protein 4	23190	UBXN4	1.43	-1.31
valosin containing protein	7415	VCP	-1.76	-1.79
UBIQUITINATION				
autocrine motility factor receptor	267	AMFR	1.72	1.79
homocysteine inducible ER protein with ubiquitin like domain 1	9709	HERPUD 1	-1.72	-12.07
ring finger protein 5	6048	RNF5	-1.67	-3.17
SEL1L adaptor subunit of ERAD E3 ubiquitin ligase	6400	SEL1L	-1.41	-1.58
SEC62 homolog, preprotein translocation factor	7095	SEC62	1.04	-1.59
ubiquitin conjugating enzyme E2 G2	7327	UBE2G2	1.51	-1.43
UBX domain protein 4	23190	UBXN4	1.43	-1.31

ubiquitin recognition factor In ER associated degradation 1	7353	UFD1L	-1.11	1.27
ubiquitin specific peptidase 14	9097	USP14	2.01	-1.32
valosin containing protein	7415	VCP	-1.76	-1.79
TRANSCRIPTION FACTORS				
activating transcription factor 4	468	ATF4	1.97	1.16
activating transcription factor 6	22926	ATF6	-1.73	-2.22
ataxin 3	4287	ATXN3	-2.20	-3.85
calreticulin	811	CALR	-2.10	1.68
CCAAT enhancer binding protein beta	1051	CEBPB	-4.57	3.01
cAMP responsive element binding protein 3	10488	CREB3	1.71	-1.47
cAMP responsive element binding protein 3 like 3	84699	CREB3L3	2.52	4.17
activating transcription factor 6 beta	1388	ATF6B	-1.44	1.39
DNA damage inducible transcript 3	1649	CHOP	-8.47	-25.08
endoplasmic reticulum to nucleus signaling 1	2081	IRE1	3.34	2.01
endoplasmic reticulum to nucleus signaling 2	10595	IRE2	1.45	-1.45
membrane bound transcription factor peptidase, site 1	8720	MBTPS1	1.56	-1.54
prefoldin subunit 5	5204	PFDN5	1.20	-1.09
SREBF chaperone	22937	SCAP	-1.53	1.95
sterol regulatory element binding transcription factor 1	6720	SREBF1	4.44	-3.68
X-box binding protein 1	7494	XBP1	1.12	-6.93
PROTEIN FOLDING				
calreticulin	811	CALR	-2.10	1.68
calnexin	821	CANX	1.40	-1.03
chaperonin containing TCP1 subunit 4	10575	CCT4	-1.57	-3.31
DnaJ heat shock protein family (Hsp40) member B9	4189	DNAJB9	1.48	-16.05
DnaJ heat shock protein family (Hsp40) member C10	54431	DNAJC10	1.09	-1.28

endoplasmic reticulum oxidoreductase 1 alpha	30001	ERO1A	1.31	-1.38
heat shock protein family A (Hsp70) member 4 like	22824	HSPA4L	-1.18	-19.76
prefoldin subunit 5	5204	PFDN5	1.20	-1.09
peptidylprolyl isomerase A	5478	PPIA	1.05	-1.50
SEC63 homolog, protein translocation regulator	11231	SEC63	-1.07	-1.47
SIL1 nucleotide exchange factor	64374	SIL1	-1.41	-1.58
t-complex 1	6950	TCP1	1.05	-1.40
torsin family 1 member A	1861	TOR1A	-1.26	-4.23
endoplasmic reticulum protein 44	23071	ERP44	1.13	-1.87
UDP-glucose glycoprotein glucosyltransferase 1	56886	UGGT1	1.14	-1.12
PROTEIN DISULFIDE ISOMERIZATION				
DNA damage inducible transcript 3	1649	CHOP	-8.47	-25.08
DnaJ heat shock protein family (Hsp40) member C10	54431	DNAJC10	1.09	-1.28
endoplasmic reticulum oxidoreductase 1 alpha	30001	ERO1A	1.31	-1.38
endoplasmic reticulum oxidoreductase 1 beta	56605	ERO1B	1.65	-5.95
protein disulfide isomerase family A member 3	2923	PDIA3	1.45	-1.53
selenoprotein S	55829	VIMP	2.10	1.12
sterol regulatory element binding transcription factor 1	6720	SREBF1	4.44	-3.68
endoplasmic reticulum protein 44	23071	ERP44	1.13	-1.87
HEAT SHOCK PROTEINS				
DnaJ heat shock protein family (Hsp40) member B9	4189	DNAJB9	1.48	-16.05
DnaJ heat shock protein family (Hsp40) member C10	54431	DNAJC10	1.09	-1.28
DnaJ heat shock protein family (Hsp40) member C3	5611	DNAJC3	1.75	-1.08
heat shock protein family A (Hsp70) member 4	3308	HSPA4	-1.64	-1.36
heat shock protein family A (Hsp70) member 5	3309	BIP	-1.65	-2.46
heat shock protein family H (Hsp110) member 1	10808	HSPH1	1.63	-2.71

SEC63 homolog, protein translocation regulator	11231	SEC63	-1.07	-1.47
APOPTOSIS				
mesencephalic astrocyte derived neurotrophic factor	7873	MANF	-1.70	-2.00
ataxin 3	4287	ATXN3	-2.20	-3.85
BCL2 associated X, apoptosis regulator	581	BAX	-1.07	-1.52
calreticulin	811	CALR	-2.10	1.68
CCAAT enhancer binding protein beta	1051	CEBPB	-4.57	3.01
DNA damage inducible transcript 3	1649	CHOP	-8.47	-25.08
eukaryotic translation initiation factor 2 alpha kinase 3	9451	PERK	-1.79	-3.20
endoplasmic reticulum to nucleus signaling 1	2081	IRE1	3.34	2.01
endoplasmic reticulum to nucleus signaling 2	10595	IRE2	1.45	-1.45
heat shock protein family A (Hsp70) member 1B	3304	HSPA1B	-2.41	96.33
HtrA serine peptidase 2	27429	HTRA2	-4.34	-9.54
mitogen-activated protein kinase 8	5599	MAPK8	-1.05	-1.99
mitogen-activated protein kinase 9	5601	MAPK9	1.45	-1.03
protein disulfide isomerase family A member 3	2923	PDIA3	1.45	-1.53
protein phosphatase 1 regulatory subunit 15A	23645	GADD34	4.10	24.01
selenoprotein S	55829	VIMP	2.10	1.12
valosin containing protein	7415	VCP	-1.76	-1.79
PATHWAY ACTIVATION SIGNATURE GENES				
adrenomedullin 2	79924	ADM2	2.49	1.00
asparagine synthetase (glutamine-hydrolyzing)	440	ASNS	5.23	2.66
brain expressed X-linked 2	84707	BEX2	1.23	1.71
DNA damage inducible transcript 3	1649	CHOP	-8.47	-25.08
DnaJ heat shock protein family (Hsp40) member B9	4189	DNAJB9	1.48	-16.05
GINS complex subunit 2	51659	GINS2	-1.35	1.62

homocysteine inducible ER protein with ubiquitin like domain 1	9709	HERPUD1	-1.72	-12.07
inhibin subunit beta E	83729	INHBE	1.00	1.00
potassium calcium-activated channel subfamily M regulatory beta subunit 3	27094	KCNMB3	-1.60	-4.42
minichromosome maintenance complex component 4	4173	MCM4	-1.27	-1.27
proliferating cell nuclear antigen	5111	PCNA	-4.48	-1.67
ribonucleotide reductase regulatory subunit M2	6241	RRM2	-2.69	-1.74
solute carrier family 17 member 2	10246	SLC17A2	1.95	1.00
tribbles pseudokinase 3	57761	TRIB3	2.36	3.76
thymidylate synthetase	7298	TYMS	-1.05	-1.09
ubiquitin like with PHD and ring finger domains 1	29128	UHRF1	-2.27	1.97

TRANSCRIPTOMIC RESPONSES IN MACROPHAGES EXPOSED TO CONDITIONED MEDIA FROM GBM CELL LINES PRE-TREATED WITH INDIRUBIN-3'-(2,3 DIHYDROXYPROPYL)-OXIMETHER AND 6, 2', 4'-TRIMETHOXYFLAVONE.

Micaela R. Scobie

Department of Biological Sciences

Clemson University, Clemson SC USA 29634

ABSTRACT

Standard treatments for the highly invasive and malignant brain cancer, Glioblastoma Multiforme (GBM), fall short of a cure and come with devastating side effects. Small molecules that can program or direct immune surveillance towards tumor prevention and/or removal are of intense interest. Glioma-associated macrophages (GAMs) can comprise 30% of GBM tumor bulk, and are known for their tumor promoting abilities and phenotypic plasticity. Studies have shown that GAMs can be polarized along a continuum between M1 and M2 phenotypes, dependent upon the cytokine signaling milieu in the tumor microenvironment, thus encouraging a tumor promoting or tumor preventing immune response. Previous work has implicated indirubin derivatives, such as indirubin-3'-(2,3 dihydroxypropyl)-oximether (E804), as potent modulators of inflammatory signaling. As a putative AHR ligand, E804 has been shown to regulate cytokines such as IL-1β, STAT3, VEGF, and IL-6 in GBM cells. Additionally, AHR antagonist 6, 2', 4'-trimethoxyflavone (TMF) may enhance beneficial immunomodulatory effects of E804 treatment, while inhibiting certain effects of AHR pathway activation. Herein, I explore an *in vitro* model of tumor microenvironment signaling via THP-1 monocyte-derived macrophages (MDMs) treated with GBM-conditioned media from LN-18 and T98G cells treated with E804, E804 + TMF, or control. Transcriptomic sequencing paired with pathway analysis revealed E804 and E804+TMF conditioned supernatants significantly affected macrophage gene expression in the Cell Cycle and TLR pathways, while

only E804 supernatants significantly down-regulated the macrophage Wnt pathway. Whether treatment is capable of inducing a shift in macrophage polarization remains to be elucidated. Based on this study, both E804 and particularly E804 + TMF, should be explored further as a potential therapy for instigating an anti-tumor immune response in GBM-resident macrophages.

Key terms: Glioblastoma Multiforme, GBM, E804, indirubin, TMF, macrophage polarization, Wnt, TLR, immunomodulation.

1.0. INTRODUCTION

With an incidence rate of 3 out of 100,000 in the US and a median life expectancy of 15 months (Thakkar et al. 2014), Glioblastoma Multiforme (GBM) remains without curative treatment. Classified as a grade IV astrocytoma, GBM is a highly invasive and malignant brain tumor (Louis et al. 2016). Standard treatment involves first a surgical resection of the tumor, followed by local placement of Gliadel wafers infused with DNA-alkylating agents such as temozolomide (TMZ) or carmustine. Radiotherapy is often employed concomitant with surgery and chemotherapy (Davis 2016). Even with treatment, GBM patient prognoses have not improved in over a decade. Continued efforts to understand the interplay between the immune system and tumor promotion promises greater understanding of drug resistance, along with identification of new treatment modalities.

The heterogeneous composition of gliomas is a key driver in therapeutic resistance and stunts therapeutic advancement (Motaln et al. 2015). Inducing a targeted anti-cancer immune response, or modifying existing immune processes, offers a logical approach to deal with a varied tumor microenvironment. Glioma-associate macrophages (GAMs) comprise up to 30% of the brain tumor mass (Charles et al. 2011), and are brain-intrinsic microglia, or recruited peripheral macrophages. Given their dynamic plasticity and programmability, immune cells continue to be a logical therapeutic target in treating inflammatory disease such as cancer (Matsebatlela et al. 2015). Indeed, GAMs can be co-opted by tumor

signaling to assist in tumor growth and metastasis. Dependent on secreted cytokines and growth factors in the glioma milieu, GAMs can be polarized towards the classically activated M1 phenotype, with tumor fighting characteristics, or towards the alternatively activated M2 phenotype, with tumor promoting characteristics (Yang and Zhang 2017). Higher M2 presence correlates with higher grade glioma, suggesting a tumor enhancing effect (Zhang et al. 2016). Because macrophage phenotype is dependent on external signaling molecules, encouraging macrophage polarization towards an M1 phenotype is of particular interest in cancer treatment. Interestingly, both M1 and M2 macrophages are capable of phagocytizing tumors given the right stimulus (Zhang et al. 2016). Understanding macrophage signaling in response to GBM-conditioned media is of particular interest.

Previous studies from the Rice lab have shown indirubin-3'-(2,3 dihydroxypropyl)-oximether (E804) is an aryl hydrocarbon receptor (AHR) agonist, and induces a broad spectrum of immunomodulatory affects in GBM cell lines (Scobie, Houke, and Rice 2019). In that study I found E804 to down-regulate *il1a, il1b, il12a, ptgs2, tlr4,* and others, and decrease protein secretion of IL-6 and VEGF. E804 has also been found to down-regulate STAT3 (Nam et al. 2005). Interleukin-1b, IL-6, VEGF, and STAT3 are all secreted at high levels by *in vitro* primary and continuous GBM cell lines, and reportedly help drive tumor development (Yeung et al. 2013). Targeting the AHR for cancer treatment has long been of interest, however it is debated whether AHR activity should be

inhibited or amplified (Jin et al. 2019, Reed et al. 2017). Although the complete role of the AHR in tumor prevention versus development remains unclear, high AHR expression in gliomas is associated with poor prognosis (Takenaka et al. 2019) and activation may drive gliomagenesis (Gabriely et al. 2017). 6, 2', 4'-trimethoxyflavone (TMF) was used herein as a pharmacological inhibitor of the AHR, shown previously to effectively inhibit AHR activation when used with E804 in LN-18 and T98G cell lines (Scobie, Houke, and Rice 2019). Therefore, a treatment regimen of TMF as an AHR antagonist plus E804 was explored in order to maintain the immunomodulatory benefits of E804 while blocking deleterious affects of AHR activation in glioma cells.

My goal in this study was to model the effects that E804- or E804+TMF-treated glioblastoma cells have on glioma-associated macrophages using THP-1 macrophages as an *in vitro* model. To that aim, I queried gene expression via RNA-sequencing in THP-1 macrophages following treatment with conditioned media of either the glioma LN-18 or T98G cell lines that had been pre-treated with AHR agonist E804, or combination treatment of E804 plus AHR antagonist TMF. Here I show that factors secreted by treated glioma cells down-regulate important pathways in macrophages such as Wnt and TLR signaling, as well as altering expression of genes associated with cholesterol and steroid metabolism.

2.0. MATERIALS AND METHODS

2.1. Chemicals: Indirubin-3'-(2,3 dihydroxypropyl)-oximether (E804) was purchased from Alexis Biochemical (CA, USA) and 6, 2′, 4′-trimethoxyflavone (TMF) was purchased from Sigma-Aldrich (MO, USA). Stock solutions at 10^{-2} M were prepared by solubilizing compounds in dimethyl sulfoxide (DMSO, Corning, NY, USA). Chemical structures for E804 and TMF are shown in Figure 8.

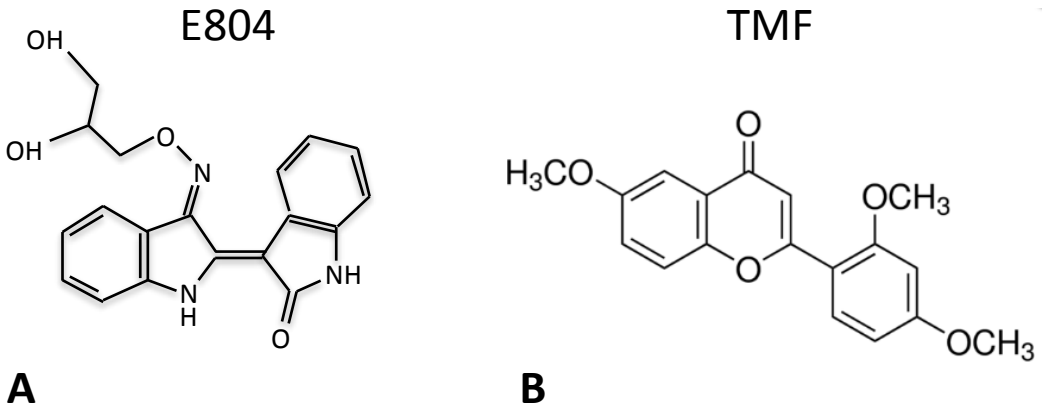

Figure 8. Chemical structures for a) indirubin-3'-(2,3 dihydroxypropyl)-oximether (E804) and b) 6, 2', 4'-trimethoxyflavone (TMF).

2.2. Cell culture: Human Glioblastoma Multiforme cell lines, LN-18 (CRL-2610) and T98G (CRL-1690), and human THP-1 monocytes (TIB-202) were obtained from ATCC (VA, USA) and cultured using Dulbecco's Modified Eagle's Medium (DMEM, Cellgro, MA, USA) as the base medium. Medium was supplemented with 10% heat-inactivated fetal calf serum (FCS) with iron (Atlas, CO, USA), 20 mM HEPES, 10 mM l-glutamine, 100 U/ml penicillin, 100 µg/ml streptomycin,

110 µg/ml sodium pyruvate, 1% non-essential amino acids (100x stock), 4.5 g/l glucose, and 1.5 g/l of $NaHCO_3$, each from Sigma-Aldrich. Cells were typically grown and maintained at 37 °C with 5% CO_2 in Corning 75 cm^2 culture flasks.

2.3. ***Treatments*****:** LN-18 and T98G cell lines were pre-treated with either TMF or carrier control for 24 h, before removing old media and replacing with appropriate treatment of E804, E804 plus TMF, or carrier control. THP-1 monocytes were differentiated using 16 nm PMA for 48 h, followed by a 24 h resting period in media only. THP-1-differentiated macrophages were then treated with 1:2 diluted sterile supernatant from above treated GBM cell lines for 24 h. All media was removed, cells were washed with cold PBS, dissolved in 1 mL TRIzol (Invitrogen, MA, USA), and frozen on dry ice prior to mRNA extraction.

2.4. ***Sample preparation and mRNA sequencing:*** After a 24 h freezing period, mRNA was extracted and purified by poly-a-tail enrichment. Strand-specific libraries were prepared by kit NEBNext® Ultra™ II Directional RNA Library Prep Kit for Illumina® (NEB E7760). Qualified libraries were then sequenced on an Illumina HiSeq 4000 Platform using a paired-end 150 run (2×150 bases). Sequencing depth approximately 12 GB/sample.

2.5. Data analysis: Data quality control performed using FastQC, and trimmed for paired end data with Trimmomatic v-0.36. Reads were aligned to human

reference genome GRCh38.p12 using GSNAP (Ensembl release 95 annotation), and mapped counts were summarized using Subread featureCounts (frag length 50 – 600 bp). Raw counts were analyzed with edgeR to estimate the common negative binomial dispersion by conditional maximum likelihood (CML). Treatment effect was measured by calculating the log2 counts per million (CPM) of each gene and then using glm.ft to fit the generalized linear model. Unless otherwise noted, differential gene expression was considered statistically significant if both the *P*-value and the false discovery rate (FDR) were <0.05, with a log fold change (logFC) > |1|.

3.0. RESULTS

3.1. E804- and E804+TMF-treated GBM supernatants affect gene regulation in successfully differentiated THP-1 macrophages.

Untreated THP-1 monocytes versus THP-1 monocytes treated with PMA show highly disparate gene profiles based on a heatmap of logCPMs (Fig. 16A). Additionally, differentiated THP-1 cells exhibit up-regulation of key genetic markers associated with macrophages, showing successful monocyte-to-macrophage differentiation (Fig. 16B). In order to investigate the polarization profiles of THP-1 macrophages treated with glioma culture media of GBM cells priorly treated with E804 or E804+TMF, I sequenced the mRNA transcriptome of the macrophages in biological triplicate. Macrophages that were cultured with E804- or E804+TMF-treated glioma supernatants were compared to macrophages that were cultured with carrier-treated glioma supernatants. Principle component analysis (PCA) revealed a high variance in gene expression between untreated, undifferentiated THP-1 monocytes, and untreated, differentiated THP-1 macrophages (Fig. 17). The PCA plot also revealed that control-treated LN-18 and control-treated T98G cells induced a common change in gene expression in macrophages, while E804- or E804+TMF-treated LN-18 and T98G cells induced a different set of common changes in in macrophage gene expression.

A

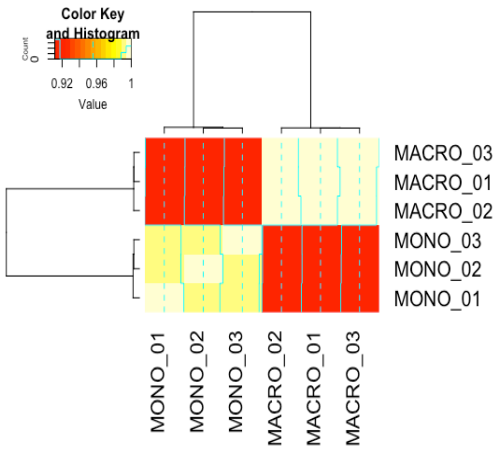

B

Gene	Symbol	logFC	P value
Matrix metalloproteinase 9	*mmp9*	7.13	< 0.0001
Alpha 2 macroglobulin	*a2m*	6.63	< 0.0001
Apolipoprotein-E	*apoe*	5.92	< 0.0001
Macrophage scavenger receptor	*msr1*	4.93	< 0.0001
FC gamma receptor III	*fcgr3a*	4.87	< 0.0001
Integrin alpha M (CD11b)	*itgam*	2.79	< 0.0001
Integrin beta 2 (CD18)	*itgb2*	2.50	< 0.0001
Toll-like receptor 4	*tlr4*	2.00	< 0.0001
Chitinase 3 Like 1	*chi3l1*	1.38	< 0.0001
Transcription Factor EC	*tfec*	1.33	< 0.0001

Figure 9. A, Heatmap of correlation matrix from log counts per million (logCPM) for untreated THP-1 monocytes (n=3) and untreated PMA-differentiated THP-1 macrophages (n=3). B, Macrophage over monocyte differential gene expression (DGE) data of genetic markers associated with macrophages, showing successful monocyte-to-macrophage differentiation.

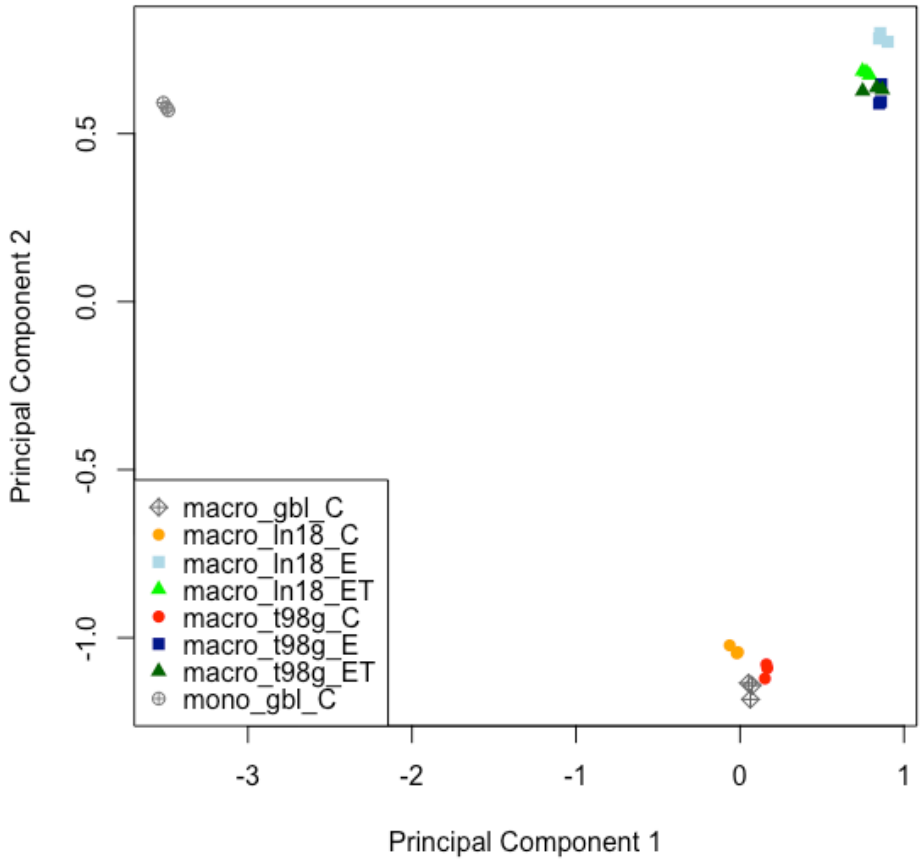

Figure 10. Two-dimensional Principle Component Analysis (PCA) plot of transcriptome of macrophages cultured with unconditioned media (grey diamonds), macrophages cultured with control-treated LN-18 supernatants (orange circles), macrophages cultured with E804-treated LN-18 supernatants (light blue squares), macrophages cultured with E804 plust TMF-treated LN-18 supernatants (bright green triangles), macrophages cultured with control-treated T98G supernatants (red circles), macrophages cultured with E804-treated T98G supernatants (navy blue squares), macrophages cultured with E804 plus TMF-treated T98G supernatants (dark green triangles), and undifferentiated monocytes cultured with unconditioned media, showing variance in gene expression across all samples. All treatments n=3.

3.2. E804- and E804+TMF-treated GBM supernatants exert more effect on macrophage gene regulation than does GBM cell line type.

A heatmap of logCPM values from the 500 most variable genes (unsupervised hierarchical clustering, scaled by row) revealed drastic clustering of treatment groups away from gene clustering of control groups (Fig. 18). Furthermore, clustering revealed the effect of supernatant treatment was more dependent on E804 or E804+TMF treatment groups over that of GBM cell lines. Thus, the addition of TMF influences macrophage gene expression to a greater extent than GBM cell line.

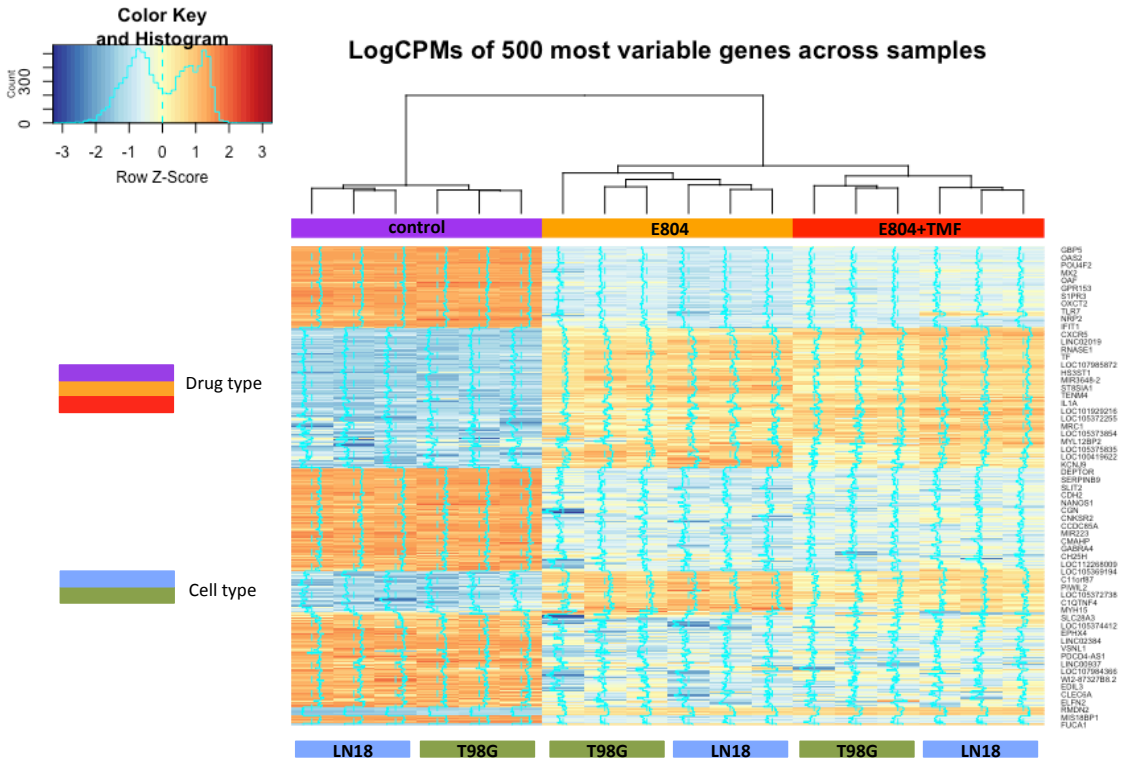

Figure 11. Heatmap of the top 500 most highly variable genes in macrophages after treatment, based on log counts per million (logCPM). Scaling by row revealed clustering of macrophages cultured with GBM cells (LN-18, light blue; T98G, green) treated with control media (purple), versus macrophages cultured with GBM cells treated with either E804 (orange) or E804+TMF (red) .

3.3. Macrophages experience strong up- and down-regulation of genes following treatment with conditioned medium.

To delineate extreme gene expression differences in macrophages cultured with GBM-treated supernatants versus macrophages cultured with GBM controls, I selected genes with a $|\log_2$ fold change (logFC)$| \geq 4$ and p-value < 0.001 (Fig. 12). Treated macrophages (all treatments over respective controls) experienced down-regulation of genes involved in hydrolase activity, cytokine activity, and protein binding (*FUCA1, IL1A, CYP1A1)*. Separately, only macrophages treated with E804-GBM supernatants (Fig. 12A, 12C) experienced up-regulation of a gene involved in promoting IFN-producing dendritic cells *(SPIB)*, and down-regulation of genes involved in growth factor activity and enzyme inhibition *(ANGPTL4, LEFTY1, RNA45SN2)*. Macrophages treated with E804+TMF-GBM supernatants (Fig. 12B, 12D) experienced up-regulation of genes involved in chemokine signaling and binding *(CCR7, CXCL10, CXCL13, IFI44L, KLHL38)* and down-regulation of genes involved in enzyme and microtubule activity (*ADAMTS12, DNAH10, NPTX1, SEMA6B, SV2B).*

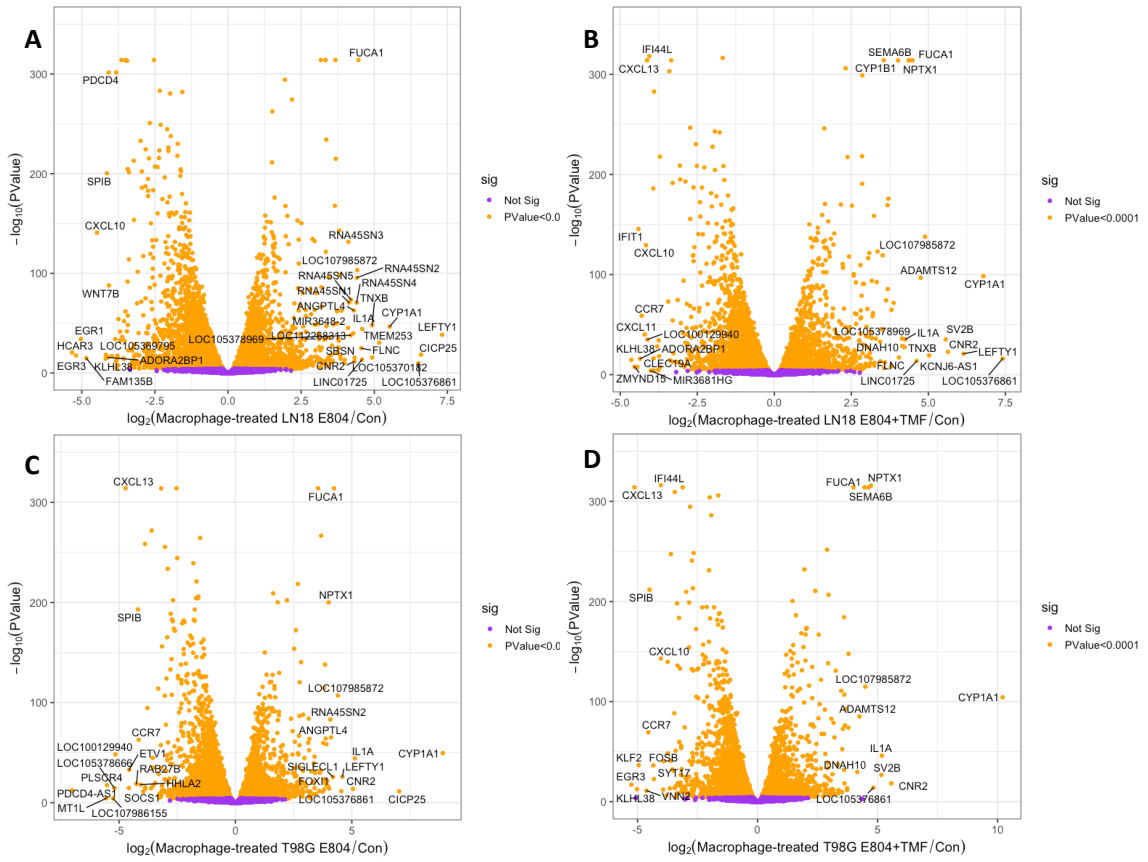

Figure 12. Volcano plots of transcriptional differences in macrophages between culturing with E804- or E804+TMF-treated GBM supernatants, versus culturing with control-treated GBM supernatants. Individual differences are plotted as log2 fold change vs. –log10P value. All points are P < 0.01, and all points P < 0.0001 are colored orange. All points with logFC > |4| are labeled.

3.4. Macrophages show mixed M1/M2 polarization following treatment with conditioned medium.

In order to determine whether or not supernatant treatment was polarizing the macrophages towards an M1 or M2 genotype, I focused exclusively on genes that have been reported in the literature as M1 or M2 gene markers (Fig. 13). M1 genes queried included *CCL2, CCR7, CD80, CXCL19, CXCL11, GPR18, IL1B, IL6 KCCN2,* and *MARCO.* M2 genes queried included *CXCL12, CCR2, EGR2, IL10, MRC1,* and *MYC.* Expression profiles of M1 and M2 associated genes were mixed up- and down-regulated, in all treatment groups.

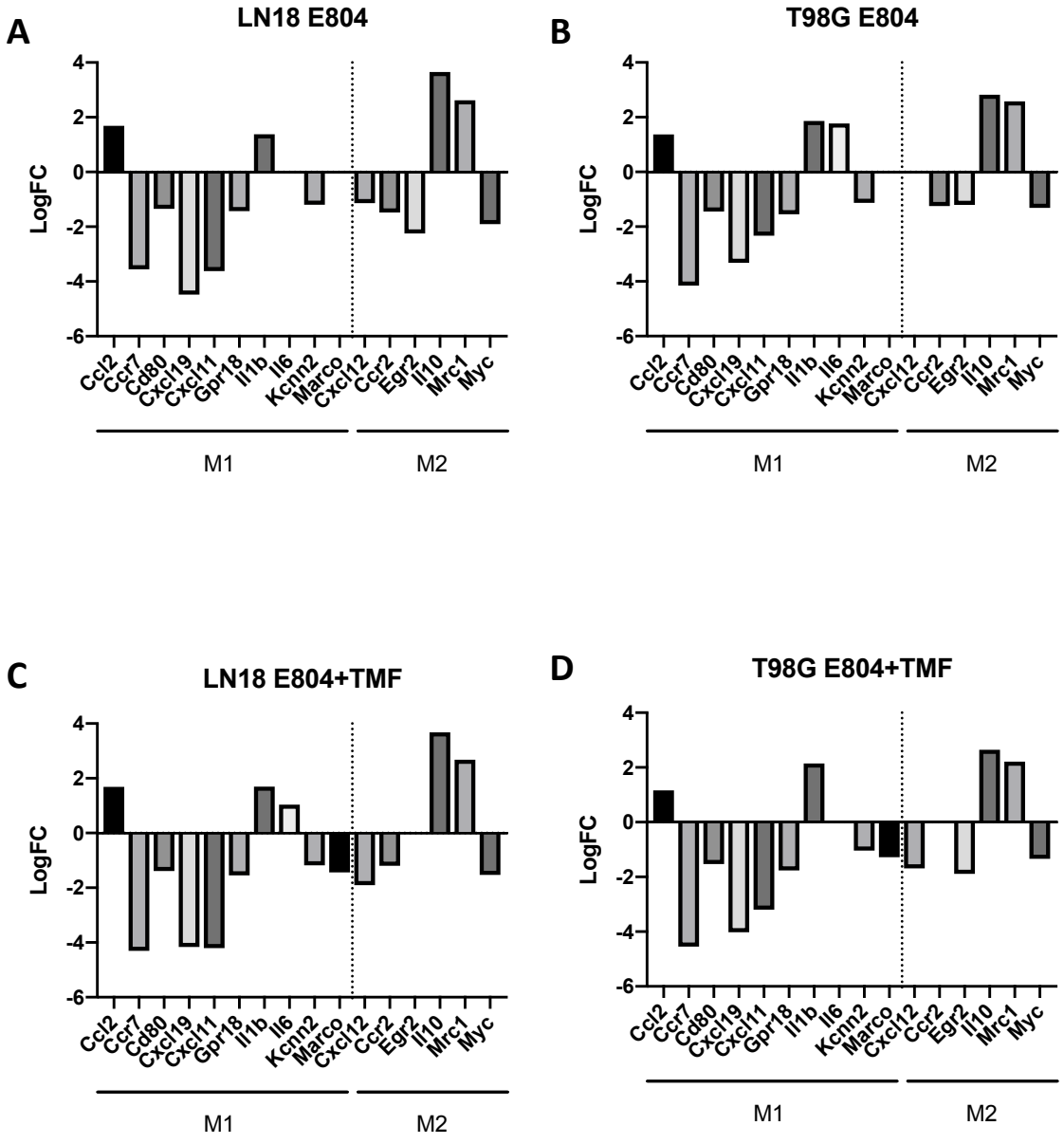

Figure 13. Log fold change (LogFC) for genes implicated in M1 or M2 macrophage polarization. a) Macrophages cultured with E804-treated LN-18 supernatants, b) macrophages cultured with E804-treated T98G supernatants, c) macrophages cultured with E804 plus TMF-treated LN-18 supernatants, d) macrophages cultured with E804 plus TMF-treated T98G supernatants (n=3).

3.5. Significantly up- and down-regulated genes analyzed separately for GO term enrichment, show differences in treatment effect on macrophage gene regulation.

In order to determine biological pathway function, the top GO terms for biological processes were generated using R package enrichGO including genes with p-value <0.01 and |logFC| > 1 (Fig. 14). GO term lists were generated for up-regulated and down-regulated genes separately. GO terms presented are those that were found represented in both LN-18-E804 and T98G-E804 treatments, or both LN-18-E804+TMF and T98G-E804+TMF treatments. All enriched GO terms for up-regulated genes are presented, and up to the top 5 GO terms for down-regulated genes are presented. Up-regulated terms (Fig. 14A, 14B) common among all treatment groups included Organic hydroxy compound metabolic process, Hormone metabolic process, and Leukocyte migration. The up-regulated term unique to GBM-E804+TMF treatment was Positive regulation of vasculature development. Down-regulated terms (Fig. 14C, 14D) common among all treatment groups included Leukocyte differentiation, Regulation of leukocyte activation, Positive regulation of cytokine production, T cell activation and Positive regulation of cell adhesion. Down-regulated terms unique to GBM-E804 treatment were Skeletal system development and Regulation of protein binding; while terms unique to GBM-E804+TMF treatment included Leukocyte migration, Regulation of multi-organism process, Negative regulation of cytokine production, Adaptive immune response based on somatic recombination of

immune receptors built from immunoglobulin superfamily domains, and Homeostasis of number of cells.

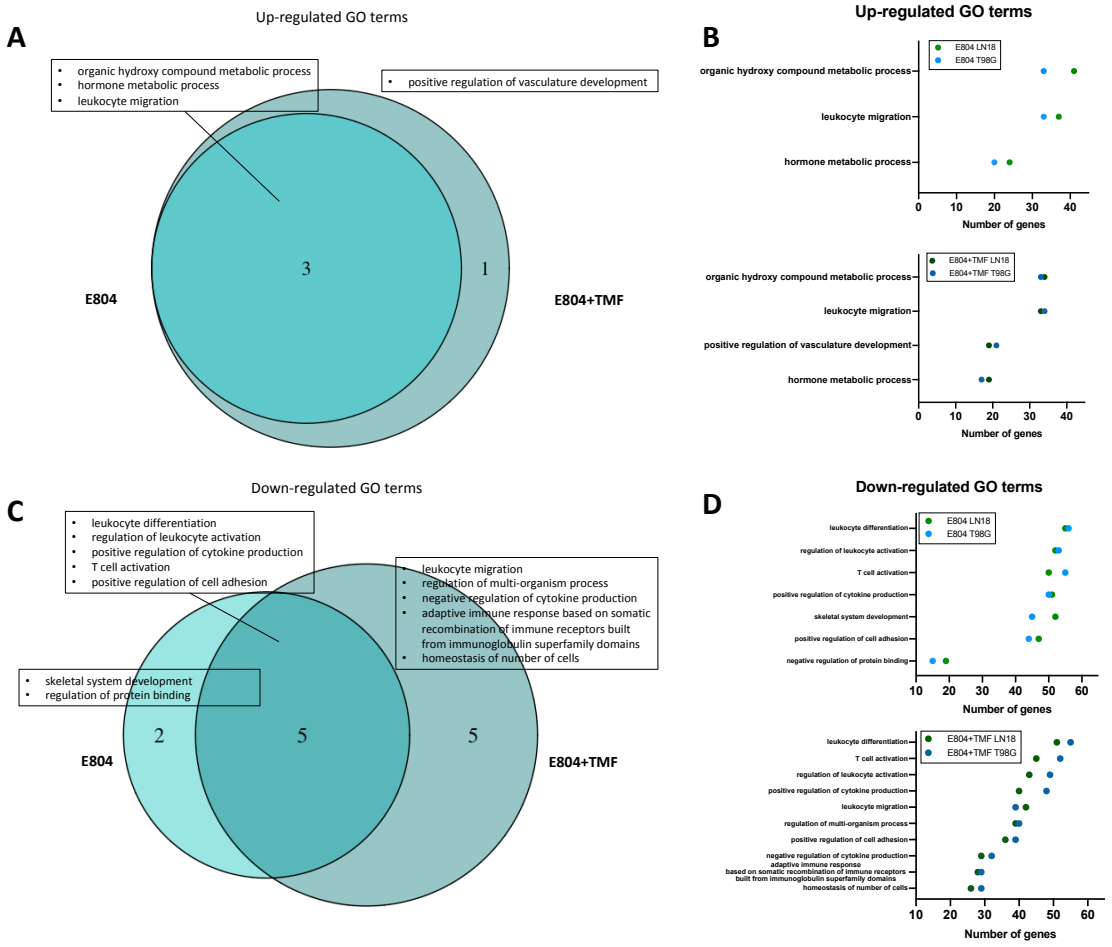

Figure 14. GO terms involved in biological processes that are significantly enriched ($P < 0.01$). Venn diagrams show overlap in GO terms enriched in a) up-regulated and c) down-regulated gene lists between macrophages cultured with E804-treated GBM supernatants and macrophages cultured with E804 plus TMF-treated GBM supernatants. Same GO terms as displayed in Venn diagrams, b) for up-regulated and d) down-regulated gene lists, with number of genes involved in each GO term plotted on the x-axis, and shows distribution between LN-18 and T98G supernatant cultures.

3.6. Barcode enrichment plots of key GO terms show distribution of gene regulation within gene set.

Barcode plots display gene set enrichment for key GO terms (Fig. 15 – 20). Terms affected by both E804 and E804+TMF supernatant treatments include hormone metabolic process (up-regulated, Fig. 15), leukocyte differentiation (down-regulated, Fig. 16), and T cell activation (down-regulated, Fig. 17). Terms affected by E804 supernatant treatment include skeletal system development (down-regulated, Fig. 18). Terms affected by E804+TMF supernatant treatment include positive regulation of vasculature development (up-regulated, Fig. 19), leukocyte migration (down), and homeostasis of number of cells (down-regulated, Fig. 20). Genes that were significantly differentially expressed, and present in a GO term, are listed (Tables 5 – 10).

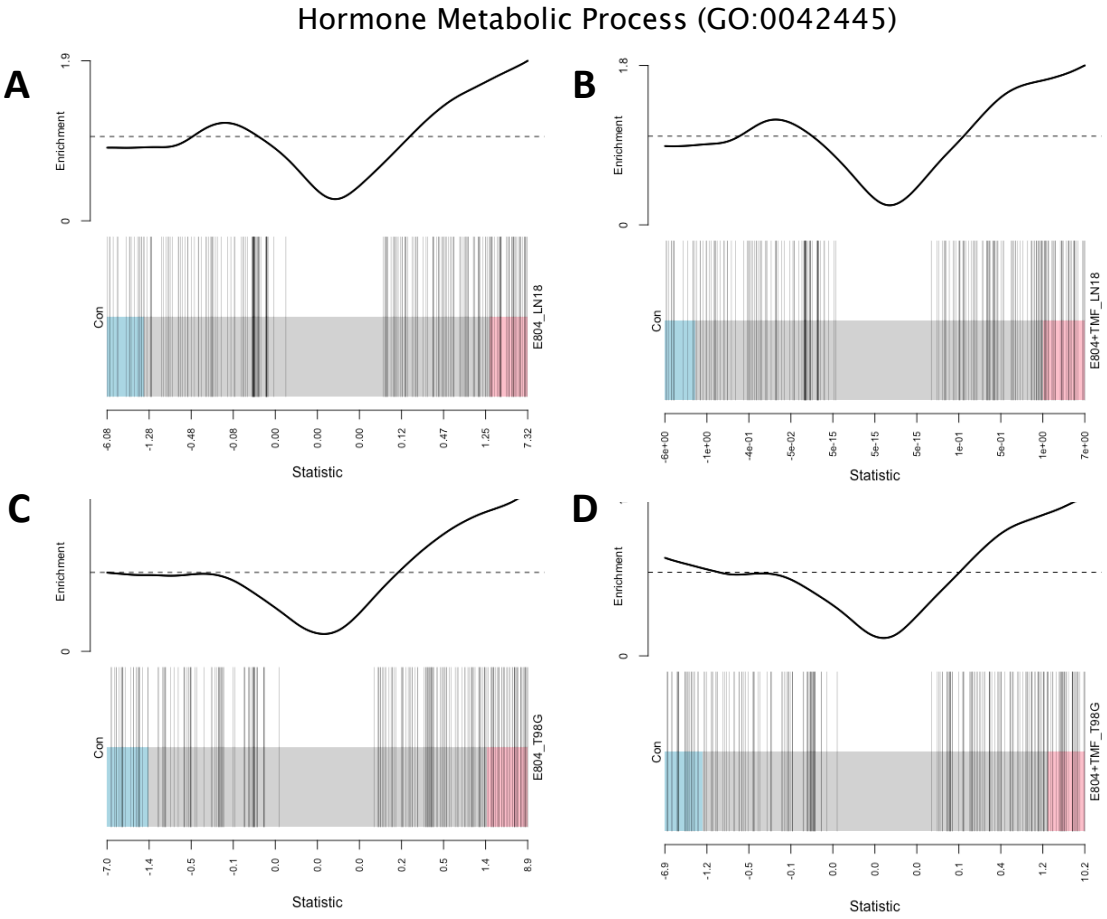

Figure 15. Barcode plots for GO:0042445 term "hormone metabolic process" show over-representation in treatments versus controls. Enrichment distribution between up- and down-regulated genes for macrophages cultured with a) E804-treated LN18 supernatant, b) E804 plus TMF-treated LN18 supernatant, c) E804-treated T98G supernatant, and d) E804 plus TMF-treated T98G supernatant. $P < 0.01$, n=3.

Table 5. Gene lists from over represented GO term Hormone Metabolic Process (GO:0042445), as displayed in barcode plot in fig. 15, for macrophages cultured with E804-treated LN18 supernatant, E804-treated T98G supernatant, E804 plus TMF-treated LN18 supernatant, and E804 plus TMF-treated T98G supernatant (n=3).

Hormone Metabolic Process (GO:0042445)

	Macrophages cultured with LN18 E804 sup	
Symbol	**Log FC**	**P-value**
EGR1	-5.03	< 0.0001
DHRS9	-3.39	< 0.0001
HSD11B1	-2.82	< 0.0001
ALDH1A3	-2.61	< 0.0001
PLB1	-1.94	< 0.0001
PDGFRA	-1.89	< 0.0001
ECE1	-1.76	< 0.0001
CYP26B1	-1.70	< 0.0001
RPE65	-1.58	< 0.0001
STAR	-1.43	< 0.0001
CYP46A1	-1.34	< 0.0001
TCF7L2	-1.22	< 0.0001
GAL	-1.20	< 0.0001
STC2	1.00	< 0.0001
ADM	1.03	< 0.0001
DDO	1.06	< 0.0001
DGKQ	1.15	< 0.0001
HSD17B7	1.24	< 0.0001
IL1B	1.38	< 0.0001
HSD17B14	1.48	< 0.0001
RDH12	1.50	< 0.0001
POR	1.55	< 0.0001
RDH5	1.60	< 0.0001
ALDH8A1	1.60	< 0.0001
ALDH1A2	1.85	< 0.0001
PAX8	2.16	< 0.0001
AKR1C2	2.20	< 0.0001
TIPARP	2.51	< 0.0001
TG	2.55	< 0.0001
SRD5A2	2.90	< 0.0001
DIO2	3.11	< 0.0001
CRABP2	3.21	< 0.0001
CYP1B1	3.67	< 0.0001
CYP1A1	5.53	< 0.0001

	Macrophages cultured with T98G E804 sup	
Symbol	**Log FC**	**P-value**
DHRS9	-3.15	< 0.0001
CYP26B1	-2.94	< 0.0001
HSD11B1	-2.61	< 0.0001
ALDH1A3	-2.45	< 0.0001
EGR1	-2.27	< 0.0001
PDGFRA	-2.19	< 0.0001
PLB1	-1.79	< 0.0001
RPE65	-1.41	< 0.0001
ECE1	-1.38	< 0.0001
TCF7L2	-1.04	< 0.0001
ALDH1A2	1.16	< 0.0001
POR	1.24	< 0.0001
CYP19A1	1.36	< 0.0001
ALDH8A1	1.36	< 0.0001
HSD17B14	1.44	< 0.0001
RDH5	1.75	< 0.0001
STC2	1.82	< 0.0001
IL1B	1.86	< 0.0001
TG	1.97	< 0.0001
PAX8	2.07	< 0.0001
DIO2	2.10	< 0.0001
SRD5A2	2.22	< 0.0001
TIPARP	2.52	< 0.0001
CRABP2	2.59	< 0.0001
AKR1C2	2.69	< 0.0001
CYP11A1	3.21	< 0.0001
CYP1B1	3.55	< 0.0001
CYP1A1	8.91	< 0.0001

	Macrophages cultured with LN18 E804+TMF sup	
Symbol	**Log FC**	**P-value**
DHRS9	-3.30	< 0.0001
HSD11B1	-3.07	< 0.0001
ALDH1A3	-2.50	< 0.0001
PLB1	-1.55	< 0.0001
ECE1	-1.55	< 0.0001
PDGFRA	-1.46	< 0.0001
GAL	-1.37	< 0.0001
STAR	-1.22	< 0.0001
ALDH8A1	1.05	< 0.0001
RBP1	1.14	< 0.0001
STC2	1.15	< 0.0001
ALDH1A2	1.20	< 0.0001
RDH12	1.22	< 0.0001
HSD17B14	1.23	< 0.0001
DGKQ	1.34	< 0.0001
RBP4	1.40	< 0.0001
HSD11B2	1.53	< 0.0001
POR	1.59	< 0.0001
IL1B	1.70	< 0.0001
RDH5	1.72	< 0.0001
SRD5A2	1.73	< 0.0001
PAX8	2.07	< 0.0001
TG	2.11	< 0.0001
AKR1C2	2.11	< 0.0001
CRABP2	2.13	< 0.0001
DIO2	2.52	< 0.0001
TIPARP	2.85	< 0.0001
CYP1B1	4.02	< 0.0001
CYP1A1	6.78	< 0.0001

	Macrophages cultured with T98G E804+TMF sup	
Symbol	**Log FC**	**P-value**
EGR1	-3.32	< 0.0001
HSD11B1	-2.85	< 0.0001
DHRS9	-2.68	< 0.0001
ALDH1A3	-2.23	< 0.0001
PDGFRA	-1.69	< 0.0001
ECE1	-1.63	< 0.0001
PLB1	-1.34	< 0.0001
SPP1	-1.22	< 0.0001
TCF7L2	-1.06	< 0.0001
PCSK6	-1.00	< 0.0001
PPARGC1A	1.02	< 0.0001
RBP4	1.13	< 0.0001
DIO2	1.20	< 0.0001
RDH5	1.21	< 0.0001
CYP19A1	1.40	< 0.0001
POR	1.41	< 0.0001
TG	1.45	< 0.0001
HSD17B14	1.57	< 0.0001
CRABP2	1.72	< 0.0001
STC2	1.80	< 0.0001
SRD5A2	1.95	< 0.0001
IL1B	2.15	< 0.0001
AKR1C2	2.18	< 0.0001
PAX8	2.25	< 0.0001
TIPARP	2.96	< 0.0001
CYP1B1	4.00	< 0.0001
CYP1A1	10.21	< 0.0001

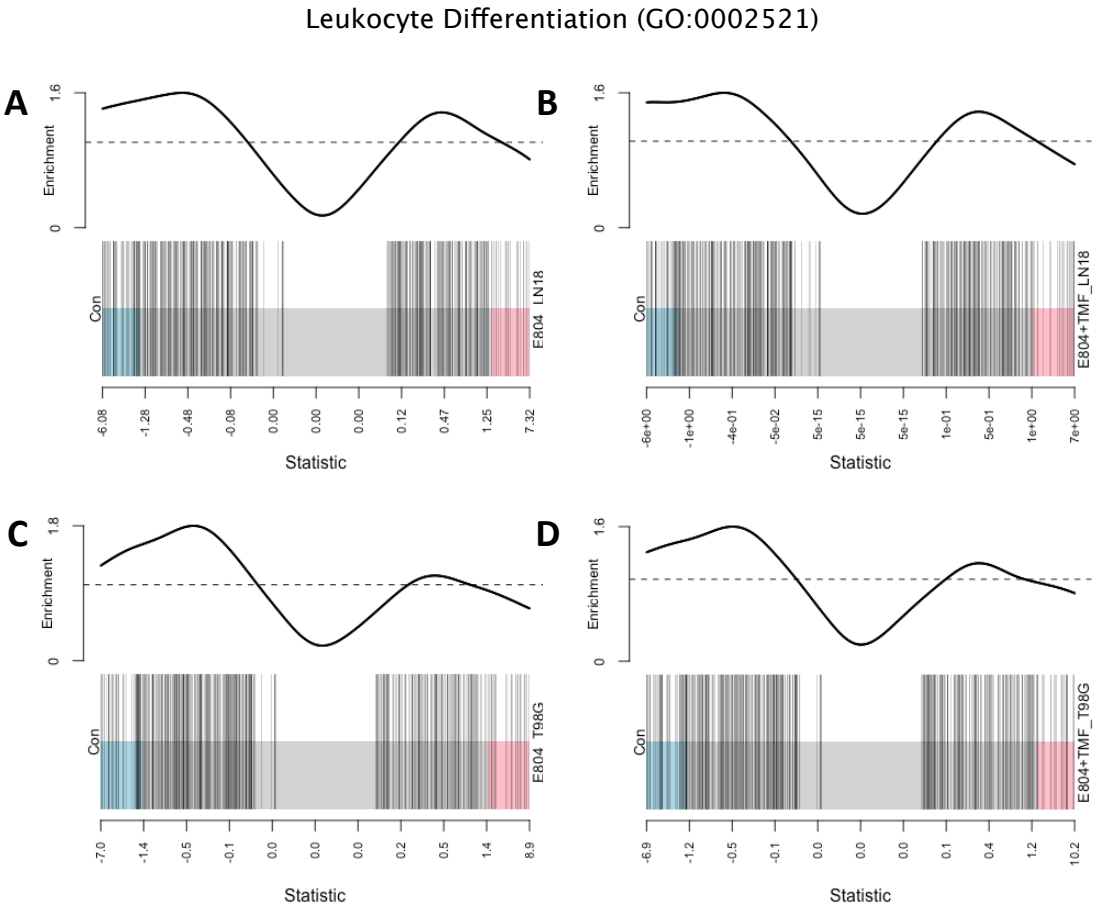

Figure 16. Barcode plots for GO:0002521 term “leukocyte differentiation” show under-representation in treatments versus controls. Enrichment distribution between up- and down-regulated genes for macrophages cultured with a) E804-treated LN18 supernatant, b) E804 plus TMF-treated LN18 supernatant, c) E804-treated T98G supernatant, and d) E804 plus TMF-treated T98G supernatant. $P < 0.01$, n=3.

Table 6. Gene lists from under represented GO term Leukocyte Differentiation (GO:0002521), as displayed in barcode plot in fig. 16, for macrophages cultured with E804-treated LN18 supernatant, E804-treated T98G supernatant, E804 plus TMF-treated LN18 supernatant, and E804 plus TMF-treated T98G supernatant (n=3).

Leukocyte Differentiation (GO:0002521)

	Macrophages cultured with LN18 E804 sup	
Symbol	**Log FC**	**P-value**
EGR3	-5.20	< 0.0001
EGR1	-5.03	< 0.0001
SOCS1	-3.79	< 0.0001
CCR7	-3.56	< 0.0001
PLA2G2D	-3.41	< 0.0001
ZBTB16	-3.37	< 0.0001
VCAM1	-3.22	< 0.0001
DLL4	-2.99	< 0.0001
MIR223	-2.80	< 0.0001
CLEC4E	-2.74	< 0.0001
CLEC4D	-2.55	< 0.0001
AXL	-2.53	< 0.0001
VNN1	-2.52	< 0.0001
POU4F2	-2.50	< 0.0001
DCSTAMP	-2.37	< 0.0001
BCL2	-2.30	< 0.0001
CBFA2T3	-2.16	< 0.0001
CD83	-2.05	< 0.0001
MIR17HG	-1.94	< 0.0001
MYC	-1.90	< 0.0001
FZD7	-1.83	< 0.0001
IL18R1	-1.72	< 0.0001
FOS	-1.72	< 0.0001
TLR2	-1.72	< 0.0001
CR2	-1.71	< 0.0001
CCL19	-1.70	< 0.0001
CYP26B1	-1.70	< 0.0001
RSAD2	-1.66	< 0.0001
POU2F2	-1.62	< 0.0001
MT1G	-1.61	< 0.0001
IKZF3	-1.59	< 0.0001
BCL6	-1.57	< 0.0001
IL31RA	-1.57	< 0.0001
IRF7	-1.53	< 0.0001
NRARP	-1.49	< 0.0001
CCR2	-1.48	< 0.0001
CD1D	-1.48	< 0.0001
TNFRSF18	-1.44	< 0.0001
CDK6	-1.43	< 0.0001
GPR18	-1.43	< 0.0001
CD80	-1.35	< 0.0001
SFRP1	-1.34	< 0.0001
IL18	-1.30	< 0.0001
LEF1	-1.28	< 0.0001
PPARGC1B	-1.27	< 0.0001
MEF2C	-1.27	< 0.0001
FOXP1	-1.22	< 0.0001
RASGRP1	-1.22	< 0.0001
KLF6	-1.22	< 0.0001
NRROS	-1.14	< 0.0001
SLC9B2	-1.09	< 0.0001
BATF3	-1.09	< 0.0001
PIK3R6	-1.09	< 0.0001
MYB	-1.05	< 0.0001
ADA	-1.03	< 0.0001
EOMES	-1.03	< 0.0001
MSH2	-1.01	< 0.0001
TUSC2	1.01	< 0.0001
GPR183	1.03	< 0.0001
RARA	1.09	< 0.0001
RUNX2	1.11	< 0.0001
TCF7	1.14	< 0.0001
LIG4	1.15	< 0.0001
VSIR	1.15	< 0.0001
BAD	1.21	< 0.0001
KIT	1.28	< 0.0001
CEBPE	1.28	< 0.0001
CEACAM1	1.44	< 0.0001
ROR2	1.78	< 0.0001
PRR7	1.80	< 0.0001
TLR9	1.89	< 0.0001
IL10	3.65	< 0.0001

	Macrophages cultured with T98G E804 sup	
Symbol	**Log FC**	**P-value**
SOCS1	-4.58	< 0.0001
CCR7	-4.16	< 0.0001
PLA2G2D	-3.05	< 0.0001
CLEC4E	-2.94	< 0.0001
CYP26B1	-2.94	< 0.0001
EGR3	-2.81	< 0.0001
DLL4	-2.78	< 0.0001
DCSTAMP	-2.60	< 0.0001
VNN1	-2.50	< 0.0001
VCAM1	-2.47	< 0.0001
EGR1	-2.27	< 0.0001
CR2	-2.26	< 0.0001
POU4F2	-2.22	< 0.0001
KLF6	-2.07	< 0.0001
AXL	-2.02	< 0.0001
ZBTB16	-2.01	0.0030
PIK3R6	-1.88	< 0.0001
BCL2	-1.87	< 0.0001
CCL19	-1.72	< 0.0001
CBFA2T3	-1.72	< 0.0001
SLC46A2	-1.71	< 0.0001
LILRB1	-1.66	< 0.0001
IL18R1	-1.64	< 0.0001
FZD7	-1.63	< 0.0001
BCL6	-1.63	< 0.0001
TLR2	-1.61	< 0.0001
POU2F2	-1.60	< 0.0001
IRF7	-1.59	< 0.0001
TNFRSF18	-1.59	< 0.0001
GPR18	-1.54	< 0.0001
MIR223	-1.54	< 0.0001
CLEC4D	-1.50	< 0.0001
CD83	-1.47	< 0.0001
FOS	-1.45	< 0.0001
RSAD2	-1.45	< 0.0001
CD80	-1.45	< 0.0001
MEF2C	-1.39	< 0.0001
IL18	-1.36	< 0.0001
SFRP1	-1.33	< 0.0001
MYC	-1.31	< 0.0001
CDK6	-1.27	< 0.0001
LEF1	-1.26	< 0.0001
CCR2	-1.25	< 0.0001
TESC	-1.25	< 0.0001
MIR17HG	-1.25	< 0.0001
NRARP	-1.22	< 0.0001
RASGRP1	-1.15	< 0.0001
CD1D	-1.14	< 0.0001
ADA	-1.13	< 0.0001
TNFSF4	-1.06	< 0.0001
FOXP1	-1.05	< 0.0001
IKZF3	-1.05	< 0.0001
IL31RA	-1.05	< 0.0001
NRROS	-1.04	< 0.0001
PPARGC1B	-1.04	< 0.0001
TNFRSF11A	-1.04	< 0.0001
SATB1	-1.03	< 0.0001
VEGFA	1.02	< 0.0001
GLO1	1.02	< 0.0001
VSIR	1.04	< 0.0001
TCF7	1.08	< 0.0001
BMP4	1.16	< 0.0001
PIR	1.18	< 0.0001
TLR9	1.28	< 0.0001
PRR7	1.33	< 0.0001
ROR2	1.64	< 0.0001
IL6	1.77	< 0.0001
KIT	1.87	< 0.0001
IL10	2.82	< 0.0001

	Macrophages cultured with LN18 E804+TMF sup	
Symbol	**Log FC**	**P-value**
CCR7	-4.30	< 0.0001
PLA2G2D	-3.27	< 0.0001
VCAM1	-3.05	< 0.0001
CLEC4E	-2.84	< 0.0001
TNFRSF18	-2.79	< 0.0001
DCSTAMP	-2.46	< 0.0001
ZBTB16	-2.44	0.0002
DLL4	-2.41	< 0.0001
POU4F2	-2.35	< 0.0001
SOCS1	-2.34	< 0.0001
AXL	-2.28	< 0.0001
VNN1	-2.08	< 0.0001
MIR223	-1.93	< 0.0001
CLEC4D	-1.88	0.0001
BCL2	-1.87	< 0.0001
CD83	-1.78	< 0.0001
CCL19	-1.72	< 0.0001
BCL6	-1.69	< 0.0001
MT1G	-1.66	< 0.0001
POU2F2	-1.65	< 0.0001
IRF7	-1.60	< 0.0001
RSAD2	-1.60	< 0.0001
GPR18	-1.55	< 0.0001
MYC	-1.53	< 0.0001
IKZF3	-1.51	< 0.0001
TLR2	-1.50	< 0.0001
LEF1	-1.48	< 0.0001
AICDA	-1.48	0.0001
FZD7	-1.41	< 0.0001
CD80	-1.39	< 0.0001
PIK3R6	-1.37	< 0.0001
CDK6	-1.33	< 0.0001
NRARP	-1.33	< 0.0001
KLF6	-1.33	< 0.0001
MEF2C	-1.32	< 0.0001
FOXP1	-1.31	< 0.0001
MIR17HG	-1.30	< 0.0001
IL18	-1.25	< 0.0001
CR2	-1.24	0.0029
CCR2	-1.20	< 0.0001
IL18R1	-1.19	< 0.0001
HMGB1	-1.17	< 0.0001
ADA	-1.15	< 0.0001
NRROS	-1.11	< 0.0001
TYRO3	-1.10	< 0.0001
CBFA2T3	-1.06	< 0.0001
PRTN3	-1.03	< 0.0001
HDAC9	-1.01	< 0.0001
IL6	1.04	0.0030
FZD9	1.14	< 0.0001
FAM20C	1.16	< 0.0001
TCF7	1.19	< 0.0001
VEGFA	1.20	< 0.0001
RUNX2	1.20	< 0.0001
GPR183	1.23	< 0.0001
PRR7	1.37	< 0.0001
BMP4	1.39	< 0.0001
TLR9	1.43	< 0.0001
SH3PXD2A	1.49	< 0.0001
CEACAM1	1.73	0.0019
ROR2	2.42	< 0.0001
IL10	3.68	< 0.0001
KIT	3.87	< 0.0001

	Macrophages cultured with T98G E804+TMF sup	
Symbol	**Log FC**	**P-value**
EGR3	-5.25	< 0.0001
CCR7	-4.55	< 0.0001
EGR1	-3.32	< 0.0001
CLEC4E	-3.18	< 0.0001
TNFRSF18	-2.61	< 0.0001
VCAM1	-2.51	< 0.0001
FOS	-2.50	< 0.0001
POU4F2	-2.26	< 0.0001
VNN1	-2.25	< 0.0001
KLF6	-2.23	< 0.0001
DLL4	-2.21	< 0.0001
PLA2G2D	-2.08	< 0.0001
AXL	-2.03	< 0.0001
POU2F2	-1.99	< 0.0001
SOCS1	-1.98	< 0.0001
BCL2	-1.98	< 0.0001
DCSTAMP	-1.93	< 0.0001
IRF7	-1.89	< 0.0001
GPR18	-1.77	< 0.0001
TRIB1	-1.76	< 0.0001
IKZF3	-1.72	< 0.0001
BCL6	-1.69	< 0.0001
CCL19	-1.69	< 0.0001
CD83	-1.62	< 0.0001
LILRB1	-1.60	< 0.0001
MIR223	-1.54	< 0.0001
CD80	-1.53	< 0.0001
RSAD2	-1.53	< 0.0001
PIK3R6	-1.52	< 0.0001
TLR2	-1.49	< 0.0001
GAS6	-1.44	< 0.0001
MEF2C	-1.43	< 0.0001
FZD7	-1.43	< 0.0001
IL18R1	-1.41	< 0.0001
CDK6	-1.36	< 0.0001
LILRB2	-1.35	< 0.0001
CR2	-1.34	0.0006
MYC	-1.34	< 0.0001
SLC46A2	-1.34	0.0010
LEF1	-1.33	< 0.0001
ZBTB16	-1.33	0.0258
NRROS	-1.33	< 0.0001
IL18	-1.33	< 0.0001
DLL1	-1.29	< 0.0001
CBFA2T3	-1.29	< 0.0001
NRARP	-1.24	< 0.0001
ADA	-1.22	< 0.0001
FOXP1	-1.17	< 0.0001
TYRO3	-1.16	< 0.0001
MIR17HG	-1.14	< 0.0001
TESC	-1.10	< 0.0001
PLCL2	-1.06	< 0.0001
CLEC4D	-1.04	0.0152
PPARGC1B	-1.02	< 0.0001
FAM20C	1.01	< 0.0001
CEBPE	1.03	< 0.0001
RHOH	1.05	< 0.0001
TLR9	1.06	0.0003
GPR183	1.08	< 0.0001
PIR	1.09	< 0.0001
VEGFA	1.17	< 0.0001
GLO1	1.20	< 0.0001
RUNX2	1.25	< 0.0001
SH3PXD2A	1.30	< 0.0001
GPR55	1.44	< 0.0001
CEACAM1	1.49	0.0035
BMP4	1.76	< 0.0001
ROR2	2.28	< 0.0001
IL10	2.64	< 0.0001
KIT	3.78	< 0.0001

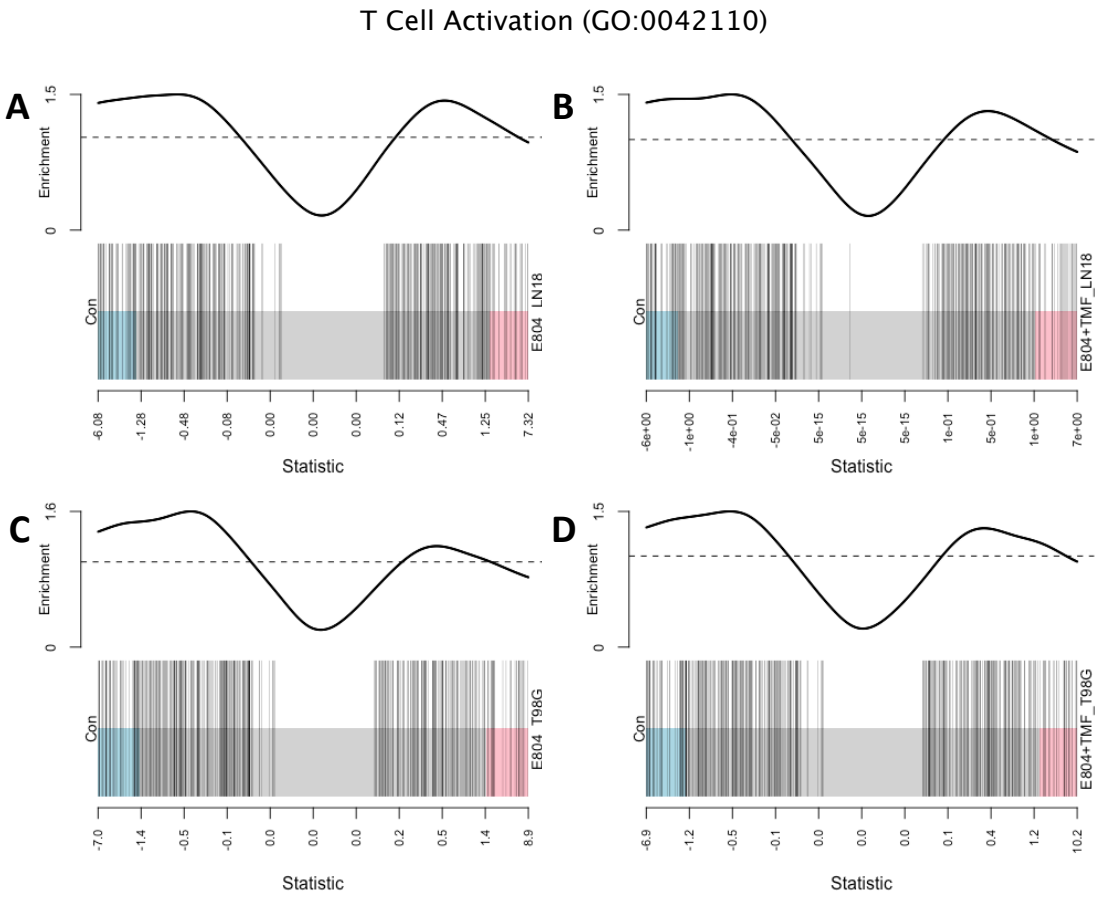

Figure 17. Barcode plots for GO:0042110 term “T-cell activation” show under-representation in treatments versus controls. Enrichment distribution between up- and down-regulated genes for macrophages cultured with a) E804-treated LN18 supernatant, b) E804 plus TMF-treated LN18 supernatant, c) E804-treated T98G supernatant, and d) E804 plus TMF-treated T98G supernatant. $P < 0.01$, n=3.

Table 7. Gene lists from under represented GO term T Cell Activation (GO:0042110), as displayed in barcode plot in fig. 17, for macrophages cultured with E804-treated LN18 supernatant, E804-treated T98G supernatant, E804 plus TMF-treated LN18 supernatant, and E804 plus TMF-treated T98G supernatant (n=3).

T Cell Activation (GO:0042110)

	Macrophages cultured with LN18 E804 sup	
Symbol	**Log FC**	**P-value**
EGR3	-5.20	< 0.0001
EGR1	-5.03	< 0.0001
SOCS1	-3.79	< 0.0001
CCR7	-3.56	< 0.0001
RIPOR2	-3.51	< 0.0001
CAV1	-3.43	< 0.0001
PLA2G2D	-3.41	< 0.0001
ZBTB16	-3.37	< 0.0001
VCAM1	-3.22	< 0.0001
DLL4	-2.99	< 0.0001
CD24	-2.84	< 0.0001
HHLA2	-2.84	< 0.0001
CLEC4E	-2.74	< 0.0001
TNFRSF4	-2.61	< 0.0001
P2RX7	-2.56	< 0.0001
CLEC4D	-2.55	< 0.0001
VNN1	-2.52	< 0.0001
BCL2	-2.30	< 0.0001
CD83	-2.05	< 0.0001
FGL2	-2.03	< 0.0001
GJA1	-1.95	< 0.0001
PRLR	-1.84	< 0.0001
FZD7	-1.83	< 0.0001
IDO1	-1.80	< 0.0001
IL18R1	-1.72	< 0.0001
CCL19	-1.70	< 0.0001
CYP26B1	-1.70	< 0.0001
RSAD2	-1.66	< 0.0001
BCL6	-1.57	< 0.0001
CD44	-1.56	< 0.0001
PRKCQ	-1.54	< 0.0001
PIK3CG	-1.53	< 0.0001
NRARP	-1.49	< 0.0001
CCR2	-1.48	< 0.0001
CD1D	-1.48	< 0.0001
TNFRSF18	-1.44	< 0.0001
CDK6	-1.43	< 0.0001
GPR18	-1.43	< 0.0001
CD80	-1.35	< 0.0001
CD274	-1.31	< 0.0001
IL18	-1.30	< 0.0001
LEF1	-1.28	< 0.0001
VSIG4	-1.25	< 0.0001
FOXP1	-1.22	< 0.0001
RASGRP1	-1.22	< 0.0001
FYN	-1.19	< 0.0001
PIK3R6	-1.09	< 0.0001
CDH26	-1.08	0.0002
MYB	-1.05	< 0.0001
BTN3A1	-1.04	< 0.0001
ADA	-1.03	< 0.0001
EOMES	-1.03	< 0.0001
NCK2	-1.02	< 0.0001
CD300A	1.03	< 0.0001
MAPK8IP1	1.03	0.0001
GPR183	1.03	< 0.0001
RARA	1.09	< 0.0001
RUNX2	1.11	< 0.0001
TNFRSF13C	1.11	0.0028
TCF7	1.14	< 0.0001
LIG4	1.15	< 0.0001
VSIR	1.15	< 0.0001
TNFSF14	1.16	< 0.0001
JAML	1.17	< 0.0001
BAD	1.21	< 0.0001
SPTA1	1.21	< 0.0001
PRNP	1.23	< 0.0001
SRC	1.27	< 0.0001
KIT	1.28	< 0.0001
MAP3K8	1.29	< 0.0001
EFNB2	1.32	< 0.0001
NLRC3	1.33	0.0008
IL1B	1.38	< 0.0001
CEACAM1	1.44	0.0104
CCL2	1.69	< 0.0001
FGL1	1.76	< 0.0001
PRR7	1.80	< 0.0001
CD7	2.52	< 0.0001
IGF1	2.96	< 0.0001
IL10	3.65	< 0.0001

	Macrophages cultured with T98G E804 sup	
Symbol	**Log FC**	**P-value**
SOCS1	-4.58	< 0.0001
CCR7	-4.16	< 0.0001
HHLA2	-4.07	< 0.0001
RIPOR2	-3.78	< 0.0001
CD24	-3.30	< 0.0001
PLA2G2D	-3.05	< 0.0001
CLEC4E	-2.94	< 0.0001
CYP26B1	-2.94	< 0.0001
CAV1	-2.93	< 0.0001
EGR3	-2.81	< 0.0001
DLL4	-2.78	< 0.0001
P2RX7	-2.74	< 0.0001
VNN1	-2.50	< 0.0001
VCAM1	-2.47	< 0.0001
GJA1	-2.31	< 0.0001
EGR1	-2.27	< 0.0001
ZBTB16	-2.01	0.0030
PIK3R6	-1.88	< 0.0001
PRLR	-1.87	< 0.0001
BCL2	-1.87	< 0.0001
FGL2	-1.75	< 0.0001
CCL19	-1.72	< 0.0001
SLC46A2	-1.71	0.0001
TNFRSF4	-1.67	< 0.0001
LILRB1	-1.66	< 0.0001
IL18R1	-1.64	< 0.0001
FZD7	-1.63	< 0.0001
BCL6	-1.63	< 0.0001
TNFRSF18	-1.59	< 0.0001
GPR18	-1.54	< 0.0001
PDE5A	-1.54	< 0.0001
CD44	-1.52	< 0.0001
CLEC4D	-1.50	0.0010
CD83	-1.47	< 0.0001
RSAD2	-1.45	< 0.0001
CD80	-1.45	< 0.0001
PIK3CG	-1.44	< 0.0001
IDO1	-1.42	< 0.0001
VSIG4	-1.40	< 0.0001
IL18	-1.36	< 0.0001
FYN	-1.33	< 0.0001
CDK6	-1.27	< 0.0001
LEF1	-1.26	< 0.0001
CCR2	-1.25	< 0.0001
NRARP	-1.22	< 0.0001
RASGRP1	-1.15	< 0.0001
CD1D	-1.14	< 0.0001
ADA	-1.13	< 0.0001
BTN3A1	-1.09	< 0.0001
PDCD1LG2	-1.08	< 0.0001
TNFSF4	-1.06	< 0.0001
FOXP1	-1.05	< 0.0001
SATB1	-1.03	< 0.0001
SLC11A1	-1.01	< 0.0001
PRNP	1.02	< 0.0001
VSIR	1.04	< 0.0001
TCF7	1.08	< 0.0001
BMP4	1.16	< 0.0001
FKBP1B	1.16	< 0.0001
SRC	1.24	< 0.0001
TNFRSF13C	1.31	0.0005
PRR7	1.33	< 0.0001
TNFSF14	1.35	< 0.0001
CCL2	1.37	< 0.0001
FGL1	1.53	< 0.0001
SLA2	1.64	0.0002
CD7	1.66	< 0.0001
EFNB2	1.75	< 0.0001
IL6	1.77	< 0.0001
IL1B	1.86	< 0.0001
KIT	1.87	< 0.0001
IGF1	2.76	< 0.0001
IL10	2.82	< 0.0001

	Macrophages cultured with LN18 E804+TMF sup	
Symbol	**Log FC**	**P-value**
CCR7	-4.30	< 0.0001
HHLA2	-3.74	< 0.0001
CAV1	-3.71	< 0.0001
PLA2G2D	-3.27	< 0.0001
VCAM1	-3.05	< 0.0001
RIPOR2	-3.03	< 0.0001
CLEC4E	-2.84	< 0.0001
TNFRSF18	-2.79	< 0.0001
CD24	-2.69	< 0.0001
P2RX7	-2.59	< 0.0001
TNFRSF4	-2.47	< 0.0001
ZBTB16	-2.44	0.0002
GJA1	-2.43	< 0.0001
DLL4	-2.41	< 0.0001
SOCS1	-2.34	< 0.0001
VNN1	-2.08	< 0.0001
CLEC4D	-1.88	0.0001
BCL2	-1.87	< 0.0001
CD83	-1.78	< 0.0001
FGL2	-1.78	< 0.0001
CCL19	-1.72	< 0.0001
PRLR	-1.69	< 0.0001
BCL6	-1.69	< 0.0001
CD44	-1.67	< 0.0001
RSAD2	-1.60	< 0.0001
GPR18	-1.55	< 0.0001
CD274	-1.53	< 0.0001
VSIG4	-1.53	< 0.0001
LEF1	-1.48	< 0.0001
IDO1	-1.46	< 0.0001
FZD7	-1.41	< 0.0001
CD80	-1.39	< 0.0001
PIK3R6	-1.37	< 0.0001
CDK6	-1.33	< 0.0001
NRARP	-1.33	< 0.0001
FOXP1	-1.31	< 0.0001
FYN	-1.30	< 0.0001
IL18	-1.25	< 0.0001
PIK3CG	-1.24	< 0.0001
CCR2	-1.20	< 0.0001
IL18R1	-1.19	< 0.0001
HMGB1	-1.17	< 0.0001
ADA	-1.15	< 0.0001
SRC	1.02	< 0.0001
CCDC88B	1.03	< 0.0001
IL6	1.04	0.0030
CD300A	1.05	< 0.0001
TCF7	1.19	< 0.0001
RUNX2	1.20	< 0.0001
GPR183	1.23	< 0.0001
SPTA1	1.32	< 0.0001
PRR7	1.37	< 0.0001
BMP4	1.39	< 0.0001
TNFSF14	1.65	< 0.0001
CCL2	1.69	< 0.0001
IL1B	1.70	< 0.0001
CEACAM1	1.73	0.0019
FGL1	1.96	< 0.0001
EFNB2	2.15	< 0.0001
JAML	2.26	< 0.0001
IGF1	3.24	< 0.0001
CD7	3.49	< 0.0001
IL10	3.68	< 0.0001
KIT	3.87	< 0.0001

	Macrophages cultured with T98G E804+TMF sup	
Symbol	**Log FC**	**P-value**
EGR3	-5.25	< 0.0001
CCR7	-4.55	< 0.0001
RIPOR2	-3.46	< 0.0001
CAV1	-3.35	< 0.0001
EGR1	-3.32	< 0.0001
GJA1	-3.22	< 0.0001
HHLA2	-3.20	< 0.0001
CLEC4E	-3.18	< 0.0001
P2RX7	-2.85	< 0.0001
CD24	-2.85	< 0.0001
TNFRSF4	-2.66	< 0.0001
TNFRSF18	-2.61	< 0.0001
VCAM1	-2.51	< 0.0001
VNN1	-2.25	< 0.0001
DLL4	-2.21	< 0.0001
PLA2G2D	-2.08	< 0.0001
SOCS1	-1.98	< 0.0001
BCL2	-1.98	< 0.0001
GPR18	-1.77	< 0.0001
BCL6	-1.69	< 0.0001
CCL19	-1.69	< 0.0001
PRLR	-1.65	< 0.0001
CD44	-1.64	< 0.0001
CD83	-1.62	< 0.0001
LILRB1	-1.60	< 0.0001
VSIG4	-1.57	< 0.0001
CD80	-1.53	< 0.0001
RSAD2	-1.53	< 0.0001
PIK3R6	-1.52	< 0.0001
FGL2	-1.51	< 0.0001
LAX1	-1.49	0.0049
FZD7	-1.43	< 0.0001
IL18R1	-1.41	< 0.0001
CD274	-1.41	< 0.0001
CDK6	-1.36	< 0.0001
LILRB2	-1.35	0.0001
IDO1	-1.35	< 0.0001
SLC46A2	-1.34	0.0010
LEF1	-1.33	< 0.0001
ZBTB16	-1.33	0.0258
IL18	-1.33	< 0.0001
CDH26	-1.33	< 0.0001
FYN	-1.25	< 0.0001
PDCD1LG2	-1.25	< 0.0001
NRARP	-1.24	< 0.0001
ADA	-1.22	< 0.0001
FOXP1	-1.17	< 0.0001
SLC11A1	-1.13	< 0.0001
CLEC4D	-1.04	0.0152
NCK2	-1.02	< 0.0001
PIK3CG	-1.01	< 0.0001
BTN3A1	-1.00	< 0.0001
PDE5A	-1.00	0.0002
SRC	1.00	< 0.0001
RHOH	1.05	< 0.0001
GPR183	1.08	< 0.0001
CCL2	1.16	< 0.0001
RUNX2	1.25	< 0.0001
SPTA1	1.25	< 0.0001
CEACAM1	1.49	0.0035
FGL1	1.65	< 0.0001
TNFSF14	1.67	< 0.0001
JAML	1.73	< 0.0001
BMP4	1.76	< 0.0001
IL1B	2.15	< 0.0001
CD7	2.23	< 0.0001
EFNB2	2.24	< 0.0001
IL10	2.64	< 0.0001
IGF1	2.95	< 0.0001
KIT	3.78	< 0.0001

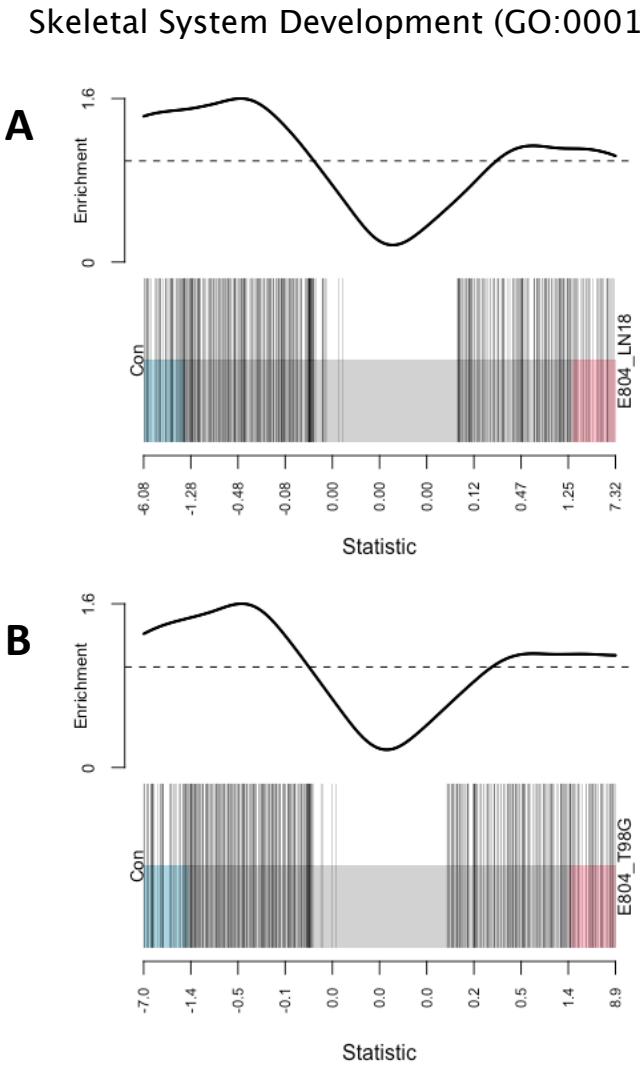

Figure 18. Barcode plots for GO:0001501 term “skeletal system development” show under-representation in treatments versus controls. Enrichment distribution between up- and down-regulated genes for macrophages cultured with a) E804-treated LN18 supernatant, and b) E804-treated T98G supernatant. $P < 0.01$, n=3.

Table 8. Gene lists from under represented GO term Skeletal System Development (GO:0001501), as displayed in barcode plot in fig. 18, for macrophages cultured with E804-treated LN18 supernatant, E804-treated T98G supernatant, E804 plus TMF-treated LN18 supernatant, and E804 plus TMF-treated T98G supernatant (n=3).

Skeletal System Development (GO:0001501)

	Macrophages cultured with LN18 E804 sup	
Symbol	**Log FC**	**P-value**
WNT7B	-4.07	< 0.0001
ZBTB16	-3.37	< 0.0001
TP63	-3.24	< 0.0001
P2RX7	-2.56	< 0.0001
TNFRSF11B	-2.12	< 0.0001
UNCX	-2.07	< 0.0001
BMP8B	-1.98	< 0.0001
GJA1	-1.95	< 0.0001
PDGFRA	-1.89	< 0.0001
WDR48	-1.87	< 0.0001
PBX1	-1.86	< 0.0001
DMRT2	-1.79	< 0.0001
GHRL	-1.72	< 0.0001
CYP26B1	-1.70	< 0.0001
ACVR2A	-1.64	< 0.0001
ARID5B	-1.58	< 0.0001
CD44	-1.56	< 0.0001
TEAD4	-1.54	< 0.0001
CSGALNACT1	-1.53	< 0.0001
TBX3	-1.53	< 0.0001
TWIST1	-1.48	< 0.0001
MEF2D	-1.46	< 0.0001
FGF2	-1.45	< 0.0001
PAX5	-1.45	< 0.0001
DLX1	-1.45	< 0.0001
GDF11	-1.42	< 0.0001
BBX	-1.41	< 0.0001
EXT1	-1.37	< 0.0001
SIX1	-1.36	< 0.0001
SFRP1	-1.34	< 0.0001
SCIN	-1.33	< 0.0001
ALX4	-1.32	< 0.0001
TRIM45	-1.30	< 0.0001
MBTD1	-1.27	< 0.0001
FOXN3	-1.27	< 0.0001
PPARGC1B	-1.27	< 0.0001
MEF2C	-1.27	< 0.0001
EYA1	-1.25	0.0060
AMER1	-1.25	< 0.0001
TGFB2	-1.23	< 0.0001
ZNF385A	-1.23	< 0.0001
FOXP1	-1.22	< 0.0001
TYMS	-1.19	< 0.0001
PITX2	-1.16	0.0081
FGFR3	-1.10	0.0060
SLC9B2	-1.09	< 0.0001
PITX1	-1.07	0.0002
NAB2	-1.06	< 0.0001
CHSY1	-1.05	< 0.0001
RYR1	-1.05	0.0002
NSD2	-1.03	< 0.0001
USP1	-1.02	< 0.0001
MAF	1.00	< 0.0001
SLC39A1	1.03	< 0.0001
CTSK	1.04	< 0.0001
RARA	1.09	< 0.0001
RUNX2	1.11	< 0.0001
HOXB7	1.12	0.0005
SNAI2	1.17	0.0006
TGFBI	1.22	< 0.0001
KIT	1.28	< 0.0001
TBX15	1.30	< 0.0001
SNORC	1.30	< 0.0001
RARG	1.33	< 0.0001
FMN1	1.44	< 0.0001
POR	1.55	< 0.0001
INSIG1	1.61	< 0.0001
PAPPA2	1.70	< 0.0001
ROR2	1.78	< 0.0001
CMKLR1	2.17	< 0.0001
TIPARP	2.51	< 0.0001
IGF1	2.96	< 0.0001
ADAMTS12	3.73	< 0.0001

	Macrophages cultured with T98G E804 sup	
Symbol	**Log FC**	**P-value**
TP63	-3.45	< 0.0001
CYP26B1	-2.94	< 0.0001
P2RX7	-2.74	< 0.0001
WNT7B	-2.70	< 0.0001
GJA1	-2.31	< 0.0001
PDGFRA	-2.19	< 0.0001
ARID5B	-2.04	< 0.0001
ZBTB16	-2.01	0.0030
BBX	-1.75	< 0.0001
BMP8B	-1.69	< 0.0001
ALX4	-1.67	< 0.0001
LILRB1	-1.66	< 0.0001
WDR48	-1.54	< 0.0001
EYA1	-1.52	0.0017
CD44	-1.52	< 0.0001
GHRL	-1.51	< 0.0001
SCIN	-1.51	< 0.0001
PITX2	-1.50	0.0004
TNFRSF11B	-1.43	< 0.0001
ACVR2A	-1.42	< 0.0001
MEF2C	-1.39	< 0.0001
GDF11	-1.38	< 0.0001
FGFR3	-1.33	0.0009
SFRP1	-1.33	< 0.0001
FGF2	-1.32	< 0.0001
EXT1	-1.32	< 0.0001
MEF2D	-1.31	< 0.0001
TWIST1	-1.28	< 0.0001
CSGALNACT1	-1.22	< 0.0001
TBX3	-1.19	< 0.0001
HOXA5	-1.18	< 0.0001
COL19A1	-1.17	< 0.0001
PITX1	-1.17	< 0.0001
RYR1	-1.16	< 0.0001
UNCX	-1.14	0.0013
DMRT2	-1.13	< 0.0001
FOXN3	-1.11	< 0.0001
ZNF385A	-1.10	< 0.0001
CHSY1	-1.07	< 0.0001
FOXP1	-1.05	< 0.0001
PPARGC1B	-1.04	< 0.0001
SIX1	-1.02	< 0.0001
TGFB3	-1.00	0.0012
CTSK	1.07	< 0.0001
FMN1	1.14	< 0.0001
COL1A1	1.15	0.0048
BMP4	1.16	< 0.0001
NPR2	1.18	0.0002
RARG	1.22	< 0.0001
SNORC	1.24	< 0.0001
POR	1.24	< 0.0001
PAPPA2	1.38	< 0.0001
INSIG1	1.45	< 0.0001
SNAI2	1.49	< 0.0001
CDKN1C	1.58	0.0088
ROR2	1.64	< 0.0001
KIT	1.87	< 0.0001
CMKLR1	2.05	< 0.0001
TIPARP	2.52	< 0.0001
IGF1	2.76	< 0.0001
ADAMTS12	3.40	< 0.0001

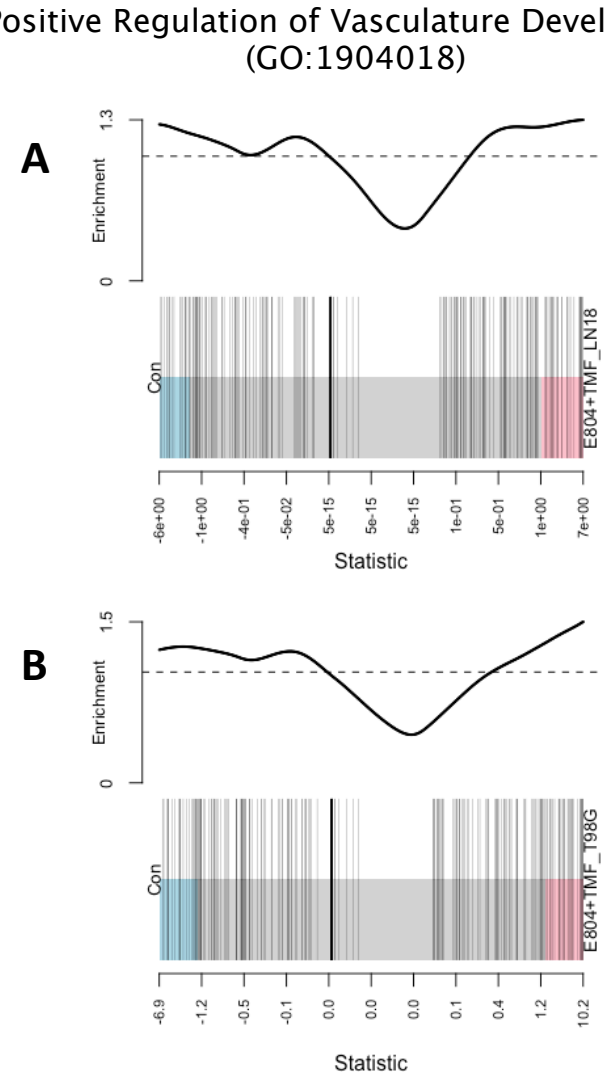

Figure 19. Barcode plots for GO:1904018 term "positive regulation of vasculature development" show over-representation in treatments versus controls. Enrichment distribution between up- and down-regulated genes for macrophages cultured with a) E804 plus TMF-treated LN18 supernatant, and b) E804 plus TMF-treated T98G supernatant. $P < 0.01$, n=3.

Table 9. Gene lists from over represented GO term Positive Regulation of Vasculature Development (GO:1904018), as displayed in barcode plot in fig. 19, for macrophages cultured with E804-treated LN18 supernatant, E804-treated T98G supernatant, E804 plus TMF-treated LN18 supernatant, and E804 plus TMF-treated T98G supernatant (n=3).

Positive Regulation of Vasculature Development (GO:1904018)

	Macrophages cultured with LN18 E804+TMF sup	
Symbol	**Log FC**	**P-value**
TERT	-3.30	< 0.0001
ADAM12	-2.70	< 0.0001
CX3CR1	-2.16	< 0.0001
GHRL	-1.62	< 0.0001
HGF	-1.47	< 0.0001
PIK3R6	-1.37	< 0.0001
DDAH1	-1.30	< 0.0001
TWIST1	-1.29	< 0.0001
PLK2	-1.24	< 0.0001
BTG1	-1.20	< 0.0001
C5AR1	-1.17	< 0.0001
JUP	-1.15	< 0.0001
FGF2	-1.14	< 0.0001
ANXA3	-1.13	< 0.0001
RAPGEF2	-1.05	< 0.0001
CELA1	-1.03	0.0068
HDAC9	-1.01	< 0.0001
LRG1	1.02	< 0.0001
HK2	1.16	< 0.0001
VEGFA	1.20	< 0.0001
PTGS2	1.22	< 0.0001
PIK3C2A	1.24	< 0.0001
PDGFD	1.27	< 0.0001
IL1B	1.70	< 0.0001
CEACAM1	1.73	0.0019
F3	1.89	< 0.0001
EFNB2	2.15	< 0.0001
GATA6	2.19	< 0.0001
CCL24	2.52	< 0.0001
ANGPTL4	3.43	< 0.0001
THBS1	3.55	< 0.0001
IL10	3.68	< 0.0001
KIT	3.87	< 0.0001
CYP1B1	4.02	< 0.0001
IL1A	4.25	< 0.0001

	Macrophages cultured with T98G E804+TMF sup	
Symbol	**Log FC**	**P-value**
EGR1	-3.32	< 0.0001
ADAM12	-2.62	< 0.0001
CX3CR1	-2.54	< 0.0001
TERT	-2.31	< 0.0001
HGF	-1.60	< 0.0001
PIK3R6	-1.52	< 0.0001
TWIST1	-1.51	< 0.0001
CELA1	-1.46	< 0.0001
DDAH1	-1.40	< 0.0001
GHRL	-1.40	< 0.0001
C5AR1	-1.35	< 0.0001
TBXA2R	-1.31	< 0.0001
DLL1	-1.29	< 0.0001
ANXA3	-1.26	< 0.0001
JUP	-1.25	< 0.0001
BTG1	-1.25	< 0.0001
PLK2	-1.15	< 0.0001
RAPGEF3	-1.04	0.0108
VEGFA	1.17	< 0.0001
CXCL8	1.19	< 0.0001
FLT1	1.21	< 0.0001
LRG1	1.22	< 0.0001
CCR3	1.22	0.0003
HK2	1.31	< 0.0001
BMPER	1.41	< 0.0001
CEACAM1	1.49	0.0035
PDGFD	1.53	< 0.0001
GATA6	1.62	< 0.0001
F3	2.10	< 0.0001
IL1B	2.15	< 0.0001
EFNB2	2.24	< 0.0001
IL10	2.64	< 0.0001
CCL24	2.69	< 0.0001
THBS1	2.90	< 0.0001
ANGPTL4	3.34	< 0.0001
KIT	3.78	< 0.0001
CYP1B1	4.00	< 0.0001
IL1A	5.18	< 0.0001

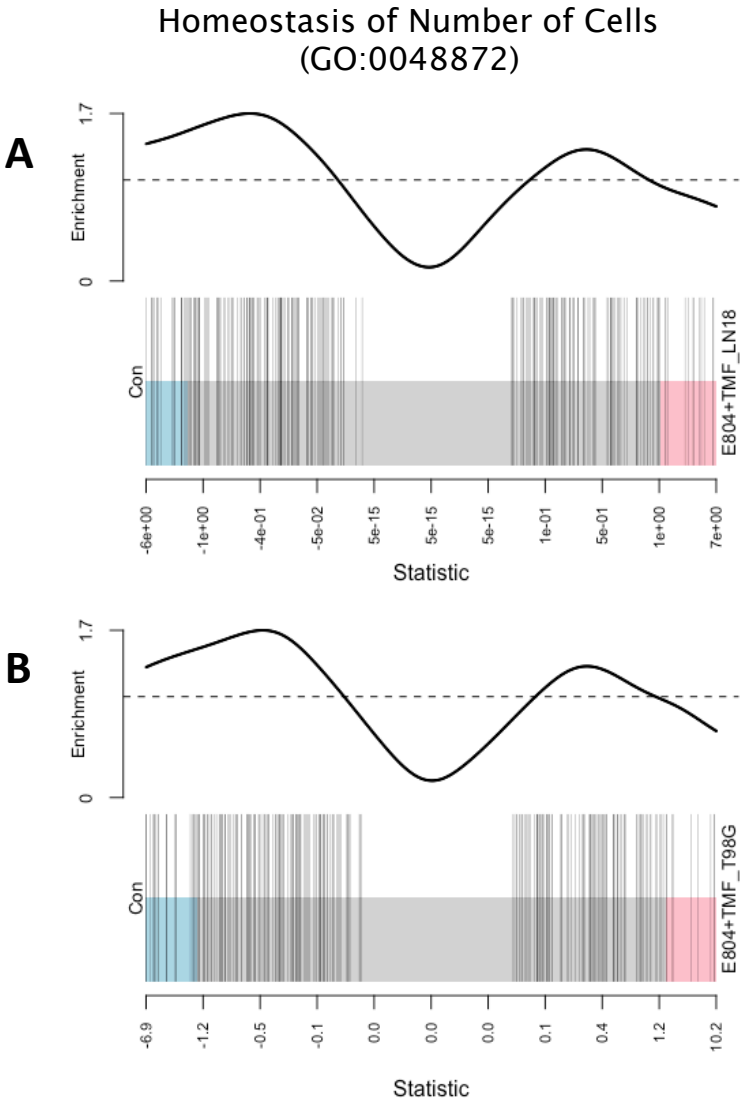

Figure 20. Barcode plots for GO:0048872 term “homeostasis of number of cells” show under-representation in treatments versus controls. Enrichment distribution between up- and down-regulated genes for macrophages cultured with a) E804 plus TMF-treated LN18 supernatant, and b) E804 plus TMF-treated T98G supernatant. $P < 0.01$, n=3.

Table 10. Gene lists from under represented GO term Homeostasis of Number of Cells (GO:0048872), as displayed in barcode plot in fig. 20, for macrophages cultured with E804-treated LN18 supernatant, E804-treated T98G supernatant, E804 plus TMF-treated LN18 supernatant, and E804 plus TMF-treated T98G supernatant (n=3).

Homeostasis of Number of Cells (GO:0048872)

	Macrophages cultured with LN18 E804+TMF sup			Macrophages cultured with T98G E804+TMF sup	
Symbol	**Log FC**	**P-value**	**Symbol**	**Log FC**	**P-value**
CCR7	-4.30	< 0.0001	*KLF2*	-4.95	< 0.0001
ADGRF5	-3.18	< 0.0001	*CCR7*	-4.55	< 0.0001
P2RX7	-2.59	< 0.0001	*P2RX7*	-2.85	< 0.0001
AXL	-2.28	< 0.0001	*ADGRF5*	-2.67	< 0.0001
RHEX	-1.96	< 0.0001	*AXL*	-2.03	< 0.0001
CDH2	-1.88	< 0.0001	*BCL2*	-1.98	< 0.0001
BCL2	-1.87	< 0.0001	*RHEX*	-1.97	< 0.0001
ACVR2A	-1.72	< 0.0001	*CDH2*	-1.74	< 0.0001
TGFBR3	-1.69	< 0.0001	*BCL6*	-1.69	< 0.0001
ISG15	-1.69	< 0.0001	*ACVR2A*	-1.57	< 0.0001
BCL6	-1.69	< 0.0001	*SH2B2*	-1.50	< 0.0001
HMGB2	-1.61	< 0.0001	*SMO*	-1.49	< 0.0001
WDR48	-1.43	< 0.0001	*MEF2C*	-1.43	< 0.0001
SH2B2	-1.37	< 0.0001	*CDK6*	-1.36	< 0.0001
CDK6	-1.33	< 0.0001	*ISG15*	-1.35	< 0.0001
MEF2C	-1.32	< 0.0001	*ADA*	-1.22	< 0.0001
MIR17HG	-1.30	< 0.0001	*HMGB2*	-1.19	< 0.0001
SMO	-1.17	< 0.0001	*WDR48*	-1.17	< 0.0001
ADA	-1.15	< 0.0001	*MIR17HG*	-1.14	< 0.0001
ILDR2	-1.07	< 0.0001	*ILDR2*	-1.13	< 0.0001
EZH2	-1.07	< 0.0001	*TGFBR3*	-1.10	< 0.0001
KLF2	-1.07	0.0004	*EZH2*	-1.05	< 0.0001
VEGFA	1.20	< 0.0001	*GPR183*	1.08	< 0.0001
GPR183	1.23	< 0.0001	*VEGFA*	1.17	< 0.0001
SPTA1	1.32	< 0.0001	*SPTA1*	1.25	< 0.0001
BMP4	1.39	< 0.0001	*TNFSF14*	1.67	< 0.0001
TNFSF14	1.65	< 0.0001	*BMP4*	1.76	< 0.0001
DYRK3	1.68	< 0.0001	*DYRK3*	2.08	< 0.0001
KIT	3.87	< 0.0001	*KIT*	3.78	< 0.0001

3.7. KEGG analysis reveals significant down-regulation of TLR, Cell Cycle, and Wnt pathways.

KEGG pathway analysis revealed that DEGs were significantly enriched across all treatments in the toll-like receptor (TLR) signaling pathway (Fig. 21), as well as the cell cycle pathway (Fig. 22). Cell cycle pathway enrichment was more down-regulated by LN-18-E804 or LN-18-E804+TMF supernatants, as compared to T98G supernatants. Conversely, the Wnt pathway was only down-regulated by E804 supernatant treatment (Fig. 23). Additionally, two key ligands for the Wnt pathway, Wnt7b and Wnt10a, were also down-regulated by all treatments (Fig. 24). Further analysis of DEGs that were silenced by E804+TMF supernatant treatment, but down-regulated by E804 supernatant treatment, revealed that 7 of these genes are involved in the Wnt pathway (Fig. 25, Table 11). When TMF was introduced, for the E804+TMF supernatant treatment, the Wnt pathway was no longer significantly down-regulated.

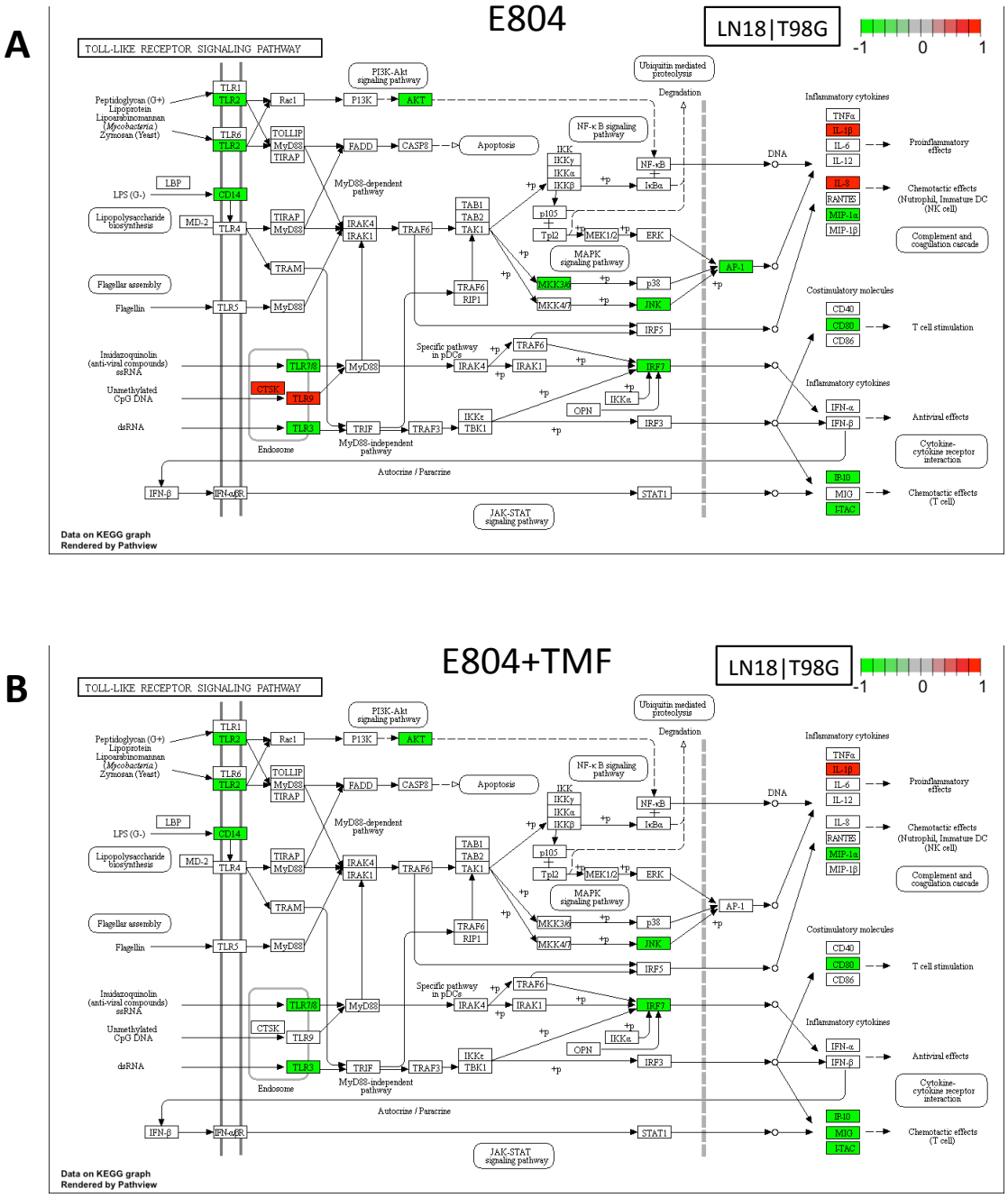

Figure 21. KEGG view of the Toll-Like Receptor (TLR) Signaling Pathway, showing multiple-sample data. DGE of macrophages cultured with a) E804-treated or b) E804+TMF-treated LN-18 (left side of box) or T98G supernatants (right side of box), compared to controls. Green represents down-regulated z-score, red represents up-regulated z-score.

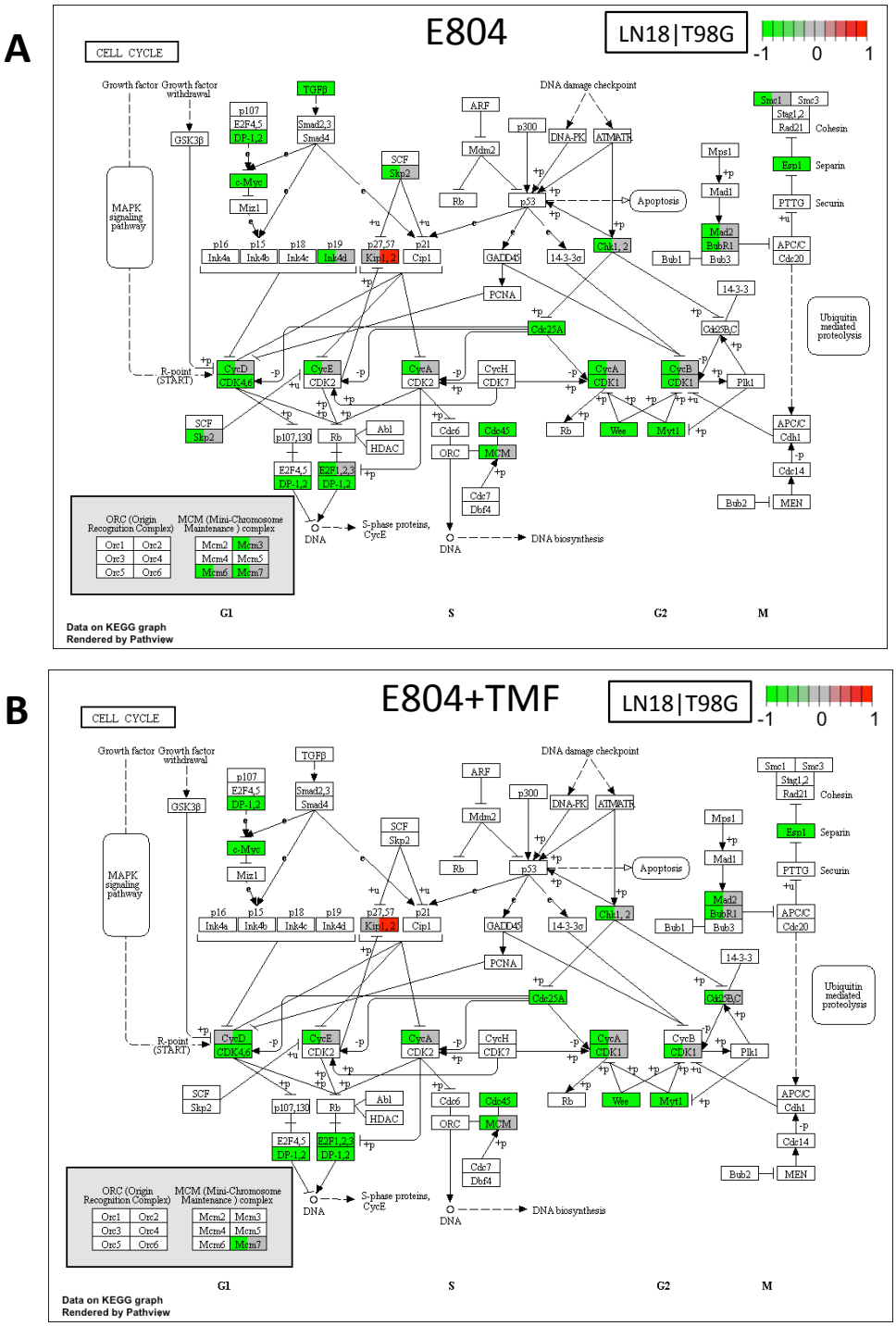

Figure 22. KEGG view of the Cell Cycle Pathway, showing multiple-sample data. DGE of macrophages cultured with a) E804-treated or b) E804+TMF-treated LN-18 (left side of box) or T98G supernatants (right side of box), compared to controls. Green represents down-regulated z-score, red represents up-regulated z-score.

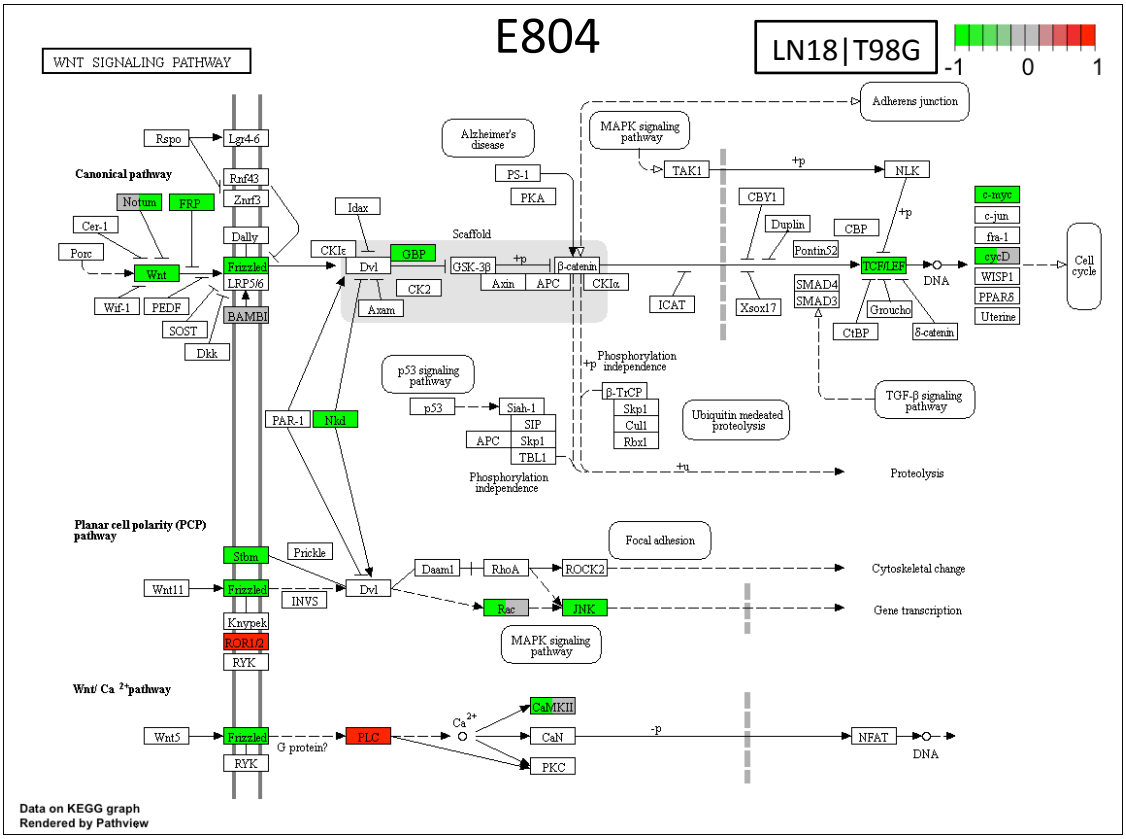

Figure 23. KEGG view of the Wnt Signaling Pathway, showing multiple-sample data. DGE of macrophages cultured with E804-treated LN-18 (left side of box) or T98G supernatants (right side of box), compared to controls. Green represents down-regulated z-score, red represents up-regulated z-score.

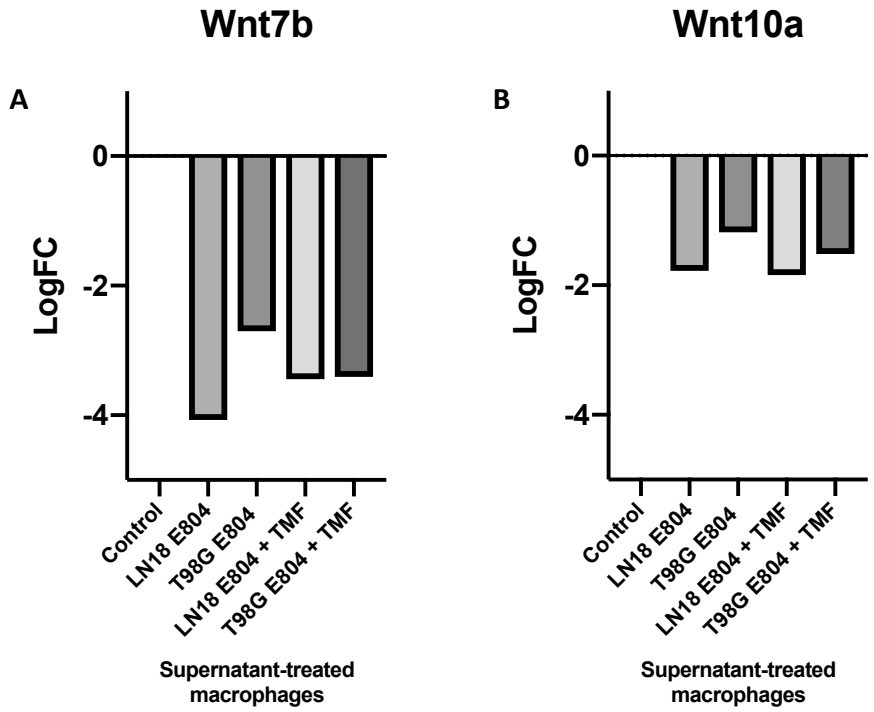

Figure 24. Log fold change (LogFC) for Wnt pathway ligands a) Wnt7b and b) Wnt10a in macrophages following culture with supernatants from E804-treated LN-18 or T98G cells, and E804+TMF-treated LN-18 or T98G cells.

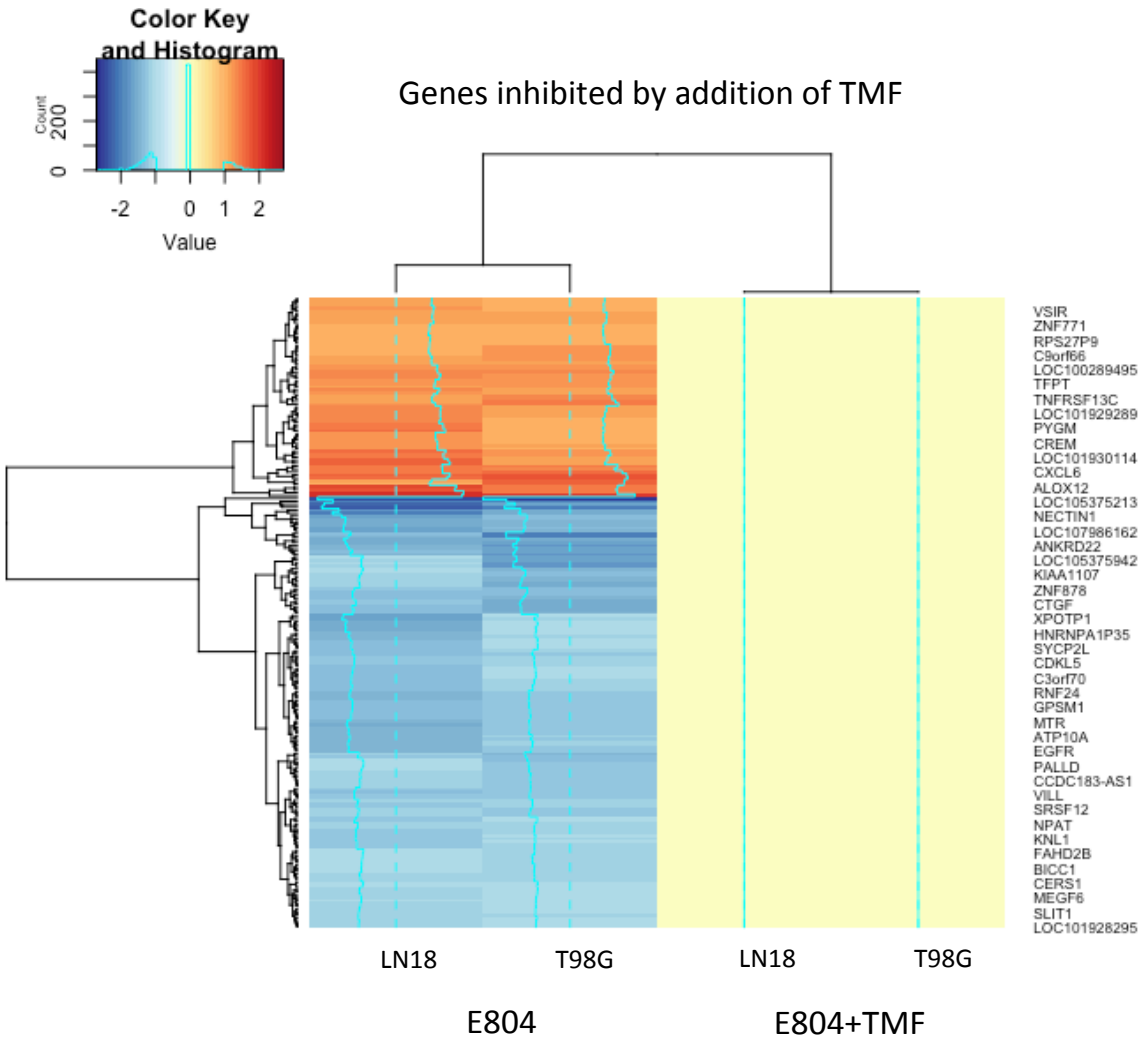

Figure 25. Heatmap of DGE in cultured macrophages inhibited by addition of TMF to treated GBM-supernatants. Blue represents down-regulated genes, red represents up-regulated genes, and yellow represents zero DGE. No scaling.

Table 11. Differential gene expression (DGE) of macrophages cultured with E804 or E804+TMF-treated GBM supernatants. Genes shown are involved in the Wnt pathway, and are down-regulated by E804-treated supernatants, but not differential expressed after E804+TMF-treated supernatants.

			Gene expression of supernatant-treated Macrophages			
Gene Name	**Symbol**	**Entrez ID**	**LN18-E804**	**T98G-E804**	**LN18-E804+TMF**	**T98G-E804+TMF**
Bicaudal-C 1	BICC1	80114	-1.08	-1.11	0.00	0.00
Epidermal growth factor receptor	EGFR	1956	-1.48	-1.20	0.00	0.00
Frizzled class receptor 4	FZD4	8322	-1.25	-1.11	0.00	0.00
Glypican 5	GPC5	2262	-1.31	-1.52	0.00	0.00
NKD inhibitor of WNT signaling pathway 2	NKD2	85409	-1.09	-1.27	0.00	0.00
Protocadherin 11 Y-Linked	PCDH11Y	83259	-1.17	-1.26	0.00	0.00
Secreted frizzled related protein 1	SFRP1	6422	-1.34	-1.33	0.00	0.00

4.0. DISCUSSION

My study demonstrates that supernatants from glioma cells (conditioned media) treated with E804 alone, or E804 plus TMF, modulate the expression of genes in macrophages associated with several key pathways. From mRNA sequencing in conjunction with GO term and pathway analysis, I observed modulation of key terms involved with macrophage-GBM function, such as down-regulation of the Cell Cycle, Toll Like Receptor (TLR), and Wnt pathways, and modulation of genes involved in steroid hormone metabolism and vasculature development. Other studies have reported the importance of GBM-secreted factors on macrophage function and polarization, such as extracellular vesicles (van der Vos et al. 2015), periostin (Zhou et al. 2015), and macrophage migration inhibitory factor (Otvos et al. 2016).

I did not observe a conclusive polarization towards M1 or M2 macrophage based on literature-backed gene expression profiles. Neither GBM cell type nor AHR antagonism conclusively changed the ratio of M1 to M2 genes. However, both E804 and E804+TMF supernatants induced down-regulation of genes involved in GO terms Leukocyte Differentiation and T Cell Activation, along with the Cell Cycle KEGG pathway. Thus, the GBM treated supernatants were able to dampen a lymphocyte activation response in THP-1 macrophages compared to controls. E804 has already been shown to inhibit CDKs in the cell cycle (Leclerc et al. 2001, Hoessel, Leclerc, Endicott, Noble, et al. 1999) and suppress inflammatory profiles in GBM cells (Scobie, Houke, and Rice 2019), therefore

supernatant induced inhibition of key genes involved in the cell cycle such as TGF-β may be due to altered states of differentiation in those macrophages. Moreover, the disparate reaction of macrophages to supernatants from the different GBM cell lines may be in part due to differences in AHR activity in the two cell lines (Gramatzki et al. 2009), and validates the need for personalized testing in cancer therapy.

Additionally, the Toll-Like Receptor (TLR) pathway was down-regulated by E804 and E804+TMF supernatants. While *nfkb* was unaffected, many upstream pathway components were down-regulated such as *tlr2, tlr3, tlr7/8, akt,* and *jnk*, as well as downstream effectors such as *mip1a, cd80, ip10,* and *itac*. The down-regulation of these genes could have a significant effect on subsequent immune cell recruitment and activation. Of note, E804-conditioned supernatant up-regulated pro-inflammatory genes *il1b* and *il8*, both of which are linked to pro-tumor activity, but also linked to M1 polarization (Chittezhath et al. 2014). Addition of AHR antagonist inhibited up-regulation of *il8,* supporting concomitant use of E804 plus TMF. TLR2 signaling has been implicated in STAT3-driven gastric tumorigenesis (Tye et al. 2012), as well as macrophage-assisted immune evasion in GBM via down-regulation of MHC II proteins (Qian et al. 2018). Additionally, M2 bone marrow derived macrophage polarization by hepatoma-conditioned media was driven by TLR2 (Chang et al. 2013). Thus, TLR2 is a relevant target in glioma therapy, and is down-regulated by E804 and E804+TMF-treated GBM conditioned media.

Conditioned supernatants via E804-treated GBM cells had a significant inhibitory effect on the Wnt pathway in THP-1 macrophages. The Wnt pathway is a powerful regulator of embryonic development and cell differentiation, and has been implicated in the promotion of many cancer types such as colorectal cancer, hepatocellular carcinoma, and GBM (Bienz and Clevers 2000, Capurro et al. 2005, Duan et al. 2015, Kim et al. 2012). High levels of *wnt* in GBM cells aids in microglial recruitment, as well as tumor growth and invasion (Matias et al. 2017), however the role of the Wnt pathway in macrophages is less known. I speculate that ligands present in E804-treated GBM supernatants are likely to have caused pathway down-regulation in macrophages cultured with the supernatant. Future studies should investigate candidate ligands such as PEDF (Ma et al. 2010), sclerostin (SOST), dickkopf (Dkk)1, or secreted frizzled-related protein (sFRP) (Bodine et al. 2009, Mason and Williams 2010).

In addition to Wnt pathway down-regulation, key tumor-regulating Wnt ligands *wnt7b* and *wnt10a* (Kirikoshi and Katoh 2002, Kirikoshi et al. 2001) were down-regulated in THP-1 macrophages in response to treatment. Interestingly, macrophage-derived Wnt7b signaling has been found to promote tumor progression via increased angiogenesis and metastasis (Ojalvo et al. 2010). Additionally, in breast-to-brain cancer metastasis microglial cells have been shown to produce high levels of related Wnt ligand Wnt5a, which may aid in cancer migration (Pukrop et al. 2010). Therefore, inhibition of macrophage-derived Wnt ligands is a viable therapeutic target. These data indicate candidate

genes, such as *wnt7b* and *wnt10a,* for future research investigating the effects of E804 and E804 + TMF on the tumor microenvironment.

Furthermore, evidence for AHR and Wnt pathway crosstalk has been found in choriocarcinoma cells (Wu et al. 2018), liver progenitor cells (Procházková et al. 2011), prostate cancer cells (Chesire et al. 2004), and an *in vivo* mouse model for intestinal cancer (Kawajiri et al. 2009). AHR activation via dietary ligands in intestinal models has been shown to negatively regulate members of the Wnt pathway and thus restrict intestinal stem cell proliferation, indicating a tumor-preventative effect (Metidji et al. 2018). Because indirubins are metabolized rapidly, in a similar fashion to dietary-derived AHR ligands (Adachi et al. 2004), Wnt pathway modulation via indirubin treatment should be investigated further. Moreover, down-regulation of the Wnt pathway was no longer significant after addition of AHR-antagonist TMF, implying that this pathway is indeed tied to AHR signaling in this model. While E804 plus TMF treatment did not significantly alter Wnt pathway signaling, individual gene members were still affected. It is possible that a treatment regimen of E804 plus TMF could avoid negative affects of AHR pathway stimulation, while still targeting enough of the macrophage Wnt pathway to aid in decreased GBM tumor growth, invasion, and macrophages activation.

I found the GO term “positive regulation of vasculature development” to be enriched in genes up-regulated by E804 plus TMF supernatants. Tumor vascularization has long been viewed as a major culprit in tumor growth and

metastasis, yet vascular endothelial growth factor (VEGF)/VEGF receptor inhibition has failed to increase GBM patient survival (Peterson et al. 2016). Indeed, Bevacizumab, the standard of care anti-VEGF antibody, has been found to enhance tumor cell invasion via promotion of hypoxic conditions (Keunen et al. 2011). Dysregulation of angiogenesis has deleterious consequences in GBM and other cancers, thus treatments aimed at normalizing vasculature shows greater promise than inhibition of VEGF alone. The modulation of many genes involved in vascularization highlights yet another reason to investigate E804 plus TMF treatment in GBM cells and GAMs.

One key observation from this study is the effect(s) of conditioned media from treated glioma cells on key components of steroid metabolism in the THP-1 macrophage model. Expression of the gene *cyp7b1* was suppressed in both cell lines by both E804- and E804+TMF, and *cyp26b1* and *cyp46a1* were reduced by E804 and not E804 + TMF. These genes and their protein products are involved in cholesterol and cholesterol-based steroid metabolism (Niwa et al. 2015), and the significance of these finding is unclear at the moment. Lipid metabolism by macrophages is the subject of intense research because of their role in cardiovascular diseases, and especially atherosclerosis (Remmerie and Scott 2018). The role(s) of altered cholesterol and steroid metabolism in macrophages under the influence of the glioma micro-environment is unclear. The observation that *cyp19a1* (aromatase) expression is increased by supernatants from glioma cells treated with TMF suggests that the AHR has a role in the conversion of

testosterone to estradiol. The same may be implied in the case of macrophage *cyp11a1* due to treatment of LN-18 cells with TMF. This enzyme, known as side-chain-cleavage, is a mitochondrial enzyme that converts cholesterol to pregnenolone (Hanukoglu 1992). Also related to the AHR, high expression of *cyp1a1* and *cyp1b1* in macrophages treated with either E804 or E804+TMF suggests the presence of a strong AHR ligand in conditioned media. It is possible that traces of E804 are in those supernatants, but this is unlikely because indirubins are metabolized very quickly to non-AHR active intermediates (Spink et al. 2003). More than likely, there are other ligands secreted by glioma cells leading to the induction of these two genes, and the many speculated candidates include kynurenines and their metabolites, as well as steroid intermediates. Overall, it is clear that future studies should focus on macrophage-glioma cross-talk in terms of steroid and lipid metabolism.

Because the focus of this study was on gene regulation in macrophages only, I have yet to elucidate the functional role these gene changes have on co-cultured GBM cells. Future work in this lab aims to investigate genetic and phenotypic changes in GBM cells cultured with the supernatants of the treated macrophages herein. It is also relevant to note that published literature examining macrophage polarization looks at gene changes between 24 to 72 h. While 24 h is a commonly accepted time-point, due to the known plasticity of macrophages, it is possible that certain genetic markers for M1/M2 polarization occurred outside this window. Nonetheless, at 24 h clear changes in gene

regulation were observed, particularly in the Wnt pathway and TLR signaling. It remains to be investigated how these alterations in macrophage activation affect physiological changes in the tumor microenvironment. These findings suggest that both E804 and E804+TMF -treated GBM supernatants down-regulate gene profiles in THP-1 macrophages that are linked to tumor progression. Taken together with previous results from this lab (Scobie, Houke, and Rice 2019), I conclude that E804+TMF treatment represents an opportunity to modulate macrophage immune signaling within the GBM environment, and should be investigated further. Certainly, as the importance of the Wnt pathway in glioma-GAM interaction continues to be elucidated, the potential clinical relevance of E804+TMF treatment should not be underestimated.

Acknowledgments

I would like to acknowledge Clemson University for allotment of compute time on the Palmetto cluster. Additionally, Rooksana Noorai and the Clemson University Genomics and Bioinformatics Facility for their assistance in data sequence alignment and counting, made possible by the National Institute of General Medical Sciences Grant (P20GM109094). Library preparation and sequencing were performed by Novogene Co, Ltd. This work was funded, in part, by the Self-Regional Healthcare Human Genetics Research Program, Greenwood Genetics Center, Greenwood, SC USA.

CONCLUSION

This body of research aims to describe a new small molecule that could replace, or adjuvant, current chemotherapeutics such as temozolomide or carmustine. These drugs are DNA-alkylating agents that are infused into wafers and placed in the brain during surgical resection (Fukai et al. 2016). DNA-alkylating agents, sometimes environmental carcinogens themselves, work by transferring an alkyl group to base pair guanine, causing strand breakage and subsequent widespread apoptosis (Kaina et al. 2007). Carmustine is extremely toxic: not only to target GBM cells, but also to surrounding healthy brain tissue. As an alternative, this study supports the use of E804-ladened wafers along with TMF to antagonize the AHR-associated responses of the compound.

This study indicates that E804 possesses anti-inflammatory properties, with ability to inhibit GBM autocrine signaling such as IL-6 and VEGF, along with prior studies showing inhibition of STAT3 and CDKs. Herein, E804 was also shown to influence expression of key genes such as *ifng, ptsg2, il12b, tnfa, il10, il13, pd1, pdl1,* and *hla*. Additionally, I have shown that E804 regulates UPR stress response genes such as *perk, gadd34, chop, atf6,* and *xbp1.* UPR regulation is a therapeutic target for neuro-inflammatory diseases such as GBM, and E804 is a likely candidate. Importantly, E804 did not strongly induce a pro-apoptotic gene profile, indicating it could be used as an immune regulator without causing widespread apoptosis to surrounding healthy brain tissue. E804 is an

AHR ligand, and therefore it induces the expression of genes associated with AHR activation. AHR activation has been associated with glioma-derived kynurenine production and further up-regulation of AHR itself. Thus, chronic activation of the AHR may help drive pro-tumor capabilities. Simultaneous treatment with AHR antagonist TMF may alleviate this particular property, and provide a non-toxic alternative to carmustine-laden wafers.

E804 not only modulates inflammatory and stress response profiles in GBM, but also induces release of GBM-derived ligands that effect gene profiles in tumor-associated macrophages. The significant down-regulation of tumor-related signaling such as the Wnt, TLR, and Cell Cycle pathways, indicates a clear role for E804 in future GBM studies. Addition of TMF yielded similar results as those obtained by E804 treatment alone, thus E804 plus TMF treatment should continue to be investigated. Key questions remain to be investigated before E804 or E804 plus TMF can progress to therapeutic potential. These include 1) match current genetic data with physiological and functional changes in THP-1 macrophages following culture with E804 and E804 plus TMF-treated GBM cells; 2) perform crosstalk study investigating backend signaling originating from macrophages to GBM cells, post original GBM treatment and macrophage culture with supernatants; and 3) determine therapeutic potential of E804 plus TMF for protection against GBM-induced animal lethality.

REFERENCES

Abou-Ghazal, Mohamed, David S. Yang, Wei Qiao, Chantal Reina-Ortiz, Jun Wei, Ling-Yuan Kong, Gregory N. Fuller, Nobuyoshi Hiraoka, Waldemar Priebe, Raymond Sawaya, and Amy B. Heimberger. 2008. "The Incidence, Correlation with Tumor-Infiltrating Inflammation, and Prognosis of Phosphorylated STAT3 Expression in Human Gliomas." *Clinical Cancer Research* 14 (24):8228-8235. doi: 10.1158/1078-0432.Ccr-08-1329.

Adachi, Jun, Yoshitomo Mori, Saburo Matsui, and Tomonari Matsuda. 2004. "Comparison of Gene Expression Patterns between 2,3,7,8-Tetrachlorodibenzo-p-dioxin and a Natural Arylhydrocarbon Receptor Ligand, Indirubin." *Toxicological Sciences* 80 (1):161-169. doi: 10.1093/toxsci/kfh129.

Adachi, Jun, Yoshitomo Mori, Saburo Matsui, Hidetaka Takigami, Junko Fujino, Hiroko Kitagawa, Charles A. Miller, Takaaki Kato, Kenichi Saeki, and Tomonari Matsuda. 2001. "Indirubin and Indigo Are Potent Aryl Hydrocarbon Receptor Ligands Present in Human Urine." *Journal of Biological Chemistry* 276 (34):31475-31478. doi: 10.1074/jbc.C100238200.

Alcantara Llaguno, Sheila R., and Luis F. Parada. 2016. "Cell of origin of glioma: biological and clinical implications." *British Journal of Cancer* 115 (12):1445-1450. doi: 10.1038/bjc.2016.354.

Alifieris, Constantinos, and Dimitrios T. Trafalis. 2015. "Glioblastoma multiforme: Pathogenesis and treatment." *Pharmacology & Therapeutics* 152:63-82. doi: https://doi.org/10.1016/j.pharmthera.2015.05.005.

Almiron Bonnin, D. A., M. C. Havrda, M. C. Lee, H. Liu, Z. Zhang, L. N. Nguyen, L. X. Harrington, S. Hassanpour, C. Cheng, and M. A. Israel. 2017. "Secretion-mediated STAT3 activation promotes self-renewal of glioma stem-like cells during hypoxia." *Oncogene* 37:1107. doi: 10.1038/onc.2017.404

https://www.nature.com/articles/onc2017404 - supplementary-information.

American Brain Tumor Association, ABTA. 2014. "Types of Tumors: Glioblastoma (GBM)." http://www.abta.org/brain-tumor-information/types-of-tumors/glioblastoma.html?referrer=https://www.google.com/.

Babcock, Abigail S., Amy L. Anderson, and Charles D. Rice. 2013. "Indirubin-3′ -(2,3 dihydroxypropyl)-oximether (E804) is a potent modulator of LPS-stimulated macrophage functions." *Toxicology and Applied Pharmacology* 266 (1):157-166. doi: http://dx.doi.org/10.1016/j.taap.2012.10.011.

Bhat, Krishna P L., Veerakumar Balasubramaniyan, Brian Vaillant, Ravesanker Ezhilarasan, Karlijn Hummelink, Faith Hollingsworth, Khalida Wani, Lindsey Heathcock, Johanna D James, Lindsey D Goodman, Siobhan Conroy, Lihong Long, Nina Lelic, Suzhen Wang, Joy Gumin, Divya Raj, Yoshinori Kodama, Aditya Raghunathan, Adriana Olar, Kaushal Joshi, Christopher E Pelloski,

Amy Heimberger, Se Hoon Kim, Daniel P Cahill, Ganesh Rao, Wilfred F A. Den Dunnen, Hendrikus W G. M. Boddeke, Heidi S Phillips, Ichiro Nakano, Frederick F Lang, Howard Colman, Erik P Sulman, and Kenneth Aldape. 2013. "Mesenchymal Differentiation Mediated by NF-κB Promotes Radiation Resistance in Glioblastoma." *Cancer Cell* 24 (3):331-346. doi: http://dx.doi.org/10.1016/j.ccr.2013.08.001.

Bhushan, B., S.K. Samanta, and R.K. Jain. 2000. "Indigo production by naphthalene-degrading bacteria." *Letters in Applied Microbiology* 31 (1):5-9. doi: 10.1046/j.1472-765x.2000.00754.x.

Bienz, M., and H. Clevers. 2000. "Linking colorectal cancer to Wnt signaling." *Cell* 103 (2):311-20. doi: 10.1016/s0092-8674(00)00122-7.

Bigner, Darell D. 2011. PVSRIPO for Recurrent Glioblastoma (GBM). edited by National Cancer Institute (NCI).

Bigner, Darell D. 2017. Phase 1b Study PVSRIPO for Recurrent Malignant Glioma in Children. edited by Solving Kids' Cancer.

Blažević, Tina, Elke H. Heiss, Atanas G. Atanasov, Johannes M. Breuss, Verena M. Dirsch, and Pavel Uhrin. 2015. "Indirubin and Indirubin Derivatives for Counteracting Proliferative Diseases." *Evidence-based Complementary and Alternative Medicine : eCAM* 2015:654098. doi: 10.1155/2015/654098.

Bodine, Peter V. N., Barbara Stauffer, Helga Ponce-de-Leon, Ramesh A. Bhat, Annamarie Mangine, Laura M. Seestaller-Wehr, Robert A. Moran, Julia Billiard, Shoichi Fukayama, Barry S. Komm, Keith Pitts, Girija Krishnamurthy, Ariamala Gopalsamy, Mengxiao Shi, Jeffrey C. Kern, Thomas J. Commons, Richard P. Woodworth, Matthew A. Wilson, Gregory S. Welmaker, Eugene J. Trybulski, and William J. Moore. 2009. "A small molecule inhibitor of the Wnt antagonist secreted frizzled-related protein-1 stimulates bone formation." *Bone* 44 (6):1063-1068. doi: https://doi.org/10.1016/j.bone.2009.02.013.

Bygd, Hannah C., Kiva D. Forsmark, and Kaitlin M. Bratlie. 2014. "The significance of macrophage phenotype in cancer and biomaterials." *Clinical and Translational Medicine* 3:62. doi: 10.1186/s40169-014-0041-2.

Capurro, Mariana I., Yun-Yan Xiang, Corrinne Lobe, and Jorge Filmus. 2005. "Glypican-3 Promotes the Growth of Hepatocellular Carcinoma by Stimulating Canonical Wnt Signaling." *Cancer Research* 65 (14):6245-6254. doi: 10.1158/0008-5472.Can-04-4244.

Casili, Giovanna, Maria Caffo, Michela Campolo, Valeria Barresi, Gerardo Caruso, Salvatore M. Cardali, Marika Lanza, Raffaella Mallamace, Alessia Filippone, Alfredo Conti, Antonino Germanò, Salvatore Cuzzocrea, and Emanuela Esposito. 2018. "TLR-4/Wnt modulation as new therapeutic strategy in the treatment of glioblastomas." *Oncotarget* 9 (101):37564-37580. doi: 10.18632/oncotarget.26500.

Cavallo, Jo. 2015. "Will the PVS-RIPO Poliovirus Be a Game Changer in the Treatment of Recurrent Glioblastoma? A Conversation With Darell D. Bigner, MD, PhD." accessed 08/25/17. http://www.ascopost.com/issues/may-25-2015/will-

the-pvs-ripo-poliovirus-be-a-game-changer-in-the-treatment-of-recurrent-glioblastoma/.
Cerezo, Michaël, and Stéphane Rocchi. 2017. "New anti-cancer molecules targeting HSPA5/BIP to induce endoplasmic reticulum stress, autophagy and apoptosis." *Autophagy* 13 (1):216-217. doi: 10.1080/15548627.2016.1246107.
Chakraborty, S., S. Ghosh, B. Banerjee, A. Santra, J. Bhat, A. Adhikary, S. Chatterjee, A. K. Misra, and P. C. Sen. 2016. "Mephebrindole, a synthetic indole analog coordinates the crosstalk between p38MAPK and eIF2alpha/ATF4/CHOP signalling pathways for induction of apoptosis in human breast carcinoma cells." *Apoptosis* 21 (10):1106-24. doi: 10.1007/s10495-016-1268-8.
Chamberlain, Marc C. 2011. "Bevacizumab for the Treatment of Recurrent Glioblastoma." *Clinical Medicine Insights. Oncology* 5:117-129. doi: 10.4137/CMO.S7232.
Chan, Yuk-Kit, Hoi-Hin Kwok, Lai-Sheung Chan, Kelvin Sze-Yin Leung, Jue Shi, Nai-Ki Mak, Ricky Ngok-Shun Wong, and Patrick Ying-Kit Yue. 2012. "An indirubin derivative, E804, exhibits potent angiosuppressive activity." *Biochem Pharmacol* 83 (5):598-607. doi: 10.1016/j.bcp.2011.12.003.
Chang, C. P., Y. C. Su, C. W. Hu, and H. Y. Lei. 2013. "TLR2-dependent selective autophagy regulates NF-κB lysosomal degradation in hepatoma-derived M2 macrophage differentiation." *Cell Death & Differentiation* 20 (3):515-523. doi: 10.1038/cdd.2012.146.
Chang, Nakho, Sun Hee Ahn, Doo-Sik Kong, Hye Won Lee, and Do-Hyun Nam. 2017. "The role of STAT3 in glioblastoma progression through dual influences on tumor cells and the immune microenvironment." *Molecular and Cellular Endocrinology* 451:53-65. doi: https://doi.org/10.1016/j.mce.2017.01.004.
Chanput, W., J. Mes, R. A. Vreeburg, H. F. Savelkoul, and H. J. Wichers. 2010. "Transcription profiles of LPS-stimulated THP-1 monocytes and macrophages: a tool to study inflammation modulating effects of food-derived compounds." *Food Funct* 1 (3):254-61. doi: 10.1039/c0fo00113a.
Charles, N. A., E. C. Holland, R. Gilbertson, R. Glass, and H. Kettenmann. 2011. "The brain tumor microenvironment." *Glia* 59 (8):1169-80. doi: 10.1002/glia.21136.
Chaudhari, N., P. Talwar, A. Parimisetty, C. Lefebvre d'Hellencourt, and P. Ravanan. 2014. "A molecular web: endoplasmic reticulum stress, inflammation, and oxidative stress." *Front Cell Neurosci* 8:213. doi: 10.3389/fncel.2014.00213.
Chen, Cheng, and Xuejun Zhang. 2017. "IRE1α-XBP1 pathway promotes melanoma progression by regulating IL-6/STAT3 signaling." *Journal of Translational Medicine* 15 (1):42. doi: 10.1186/s12967-017-1147-2.
Cheng, X., and K. H. Merz. 2016. "The Role of Indirubins in Inflammation and Associated Tumorigenesis." *Adv Exp Med Biol* 929:269-290. doi: 10.1007/978-3-319-41342-6_12.

Cheng, Xinlai, Karl-Heinz Merz, Sandra Vatter, Jochen Zeller, Stephan Muehlbeyer, Andrea Thommet, Jochen Christ, Stefan Wölfl, and Gerhard Eisenbrand. 2017. "Identification of a Water-Soluble Indirubin Derivative as Potent Inhibitor of Insulin-like Growth Factor 1 Receptor through Structural Modification of the Parent Natural Molecule." *Journal of Medicinal Chemistry* 60 (12):4949-4962. doi: 10.1021/acs.jmedchem.7b00324.

Chesire, D. R., T. A. Dunn, C. M. Ewing, J. Luo, and W. B. Isaacs. 2004. "Identification of aryl hydrocarbon receptor as a putative Wnt/beta-catenin pathway target gene in prostate cancer cells." *Cancer Res* 64 (7):2523-33.

Chittezhath, Manesh, Manprit Kaur Dhillon, Jyue Yuan Lim, Damya Laoui, Irina N Shalova, Yi Ling Teo, Jinmiao Chen, Revathy Kamaraj, Lata Raman, Josephine Lum, Thomas Paulraj Thamboo, Edmund Chiong, Francesca Zolezzi, Henry Yang, Jo A Van Ginderachter, Michael Poidinger, Alvin S C. Wong, and Subhra K Biswas. 2014. "Molecular Profiling Reveals a Tumor-Promoting Phenotype of Monocytes and Macrophages in Human Cancer Progression." *Immunity* 41 (5):815-829. doi: https://doi.org/10.1016/j.immuni.2014.09.014.

Cooksey, Christopher J. 2001. "Tyrian Purple: 6,6'-Dibromoindigo and Related Compounds." *Molecules* 6 (9):736-769.

Credle, Joel J., Patrick A. Forcelli, Michael Delannoy, Adam W. Oaks, Eva Permaul, Deborah L. Berry, Valeriy Duka, Jonathan Wills, and Anita Sidhu. 2015. "α-Synuclein-mediated inhibition of ATF6 processing into COPII vesicles disrupts UPR signaling in Parkinson's disease." *Neurobiology of Disease* 76:112-125. doi: https://doi.org/10.1016/j.nbd.2015.02.005.

Davis, Mary Elizabeth. 2016. "Glioblastoma: Overview of Disease and Treatment." *Clinical journal of oncology nursing* 20 (5 Suppl):S2-S8. doi: 10.1188/16.CJON.S1.2-8.

Denison, Michael S., Alessandro Pandini, Scott R. Nagy, Enoch P. Baldwin, and Laura Bonati. 2002. "Ligand binding and activation of the Ah receptor." *Chemico-Biological Interactions* 141 (1–2):3-24. doi: 10.1016/s0009-2797(02)00063-7.

Doultsinos, Dimitrios, Mari McMahon, Konstantinos Voutetakis, Joanna Obacz, Raphael Pineau, Florence Jouan, Pierre-Jean Le Reste, Akram Obiedat, Juhi Samal, John B. Patterson, Qingping Zheng, Afshin Samali, Abhay Pandit, Boaz Tirosh, Aristotelis Chatziioannou, Eric Chevet, and Tony Avril. 2019. "Control of glioblastoma differentiated-to-stem cell reprogramming by IREIα/XBPls signaling." *bioRxiv*:594630. doi: 10.1101/594630.

Duan, Ran, Lei Han, Qixue Wang, Jianwei Wei, Luyue Chen, Jianning Zhang, Chunsheng Kang, and Lei Wang. 2015. "HOXA13 is a potential GBM diagnostic marker and promotes glioma invasion by activating the Wnt and TGF-β pathways." *Oncotarget* 6 (29):27778-27793. doi: 10.18632/oncotarget.4813.

Duebgen, Matthias, Jordi Martinez-Quintanilla, Kaoru Tamura, Shawn Hingtgen, Navid Redjal, Hiroaki Wakimoto, and Khalid Shah. 2014. "Stem Cells Loaded With Multimechanistic Oncolytic Herpes Simplex Virus Variants for Brain Tumor Therapy." *JNCI: Journal of the National Cancer Institute* 106 (6):dju090-dju090. doi: 10.1093/jnci/dju090.

Dunn, G. P., M. L. Rinne, J. Wykosky, G. Genovese, S. N. Quayle, I. F. Dunn, P. K. Agarwalla, M. G. Chheda, B. Campos, A. Wang, C. Brennan, K. L. Ligon, F. Furnari, W. K. Cavenee, R. A. Depinho, L. Chin, and W. C. Hahn. 2012. "Emerging insights into the molecular and cellular basis of glioblastoma." *Genes Dev* 26 (8):756-84. doi: 10.1101/gad.187922.112.

Epple, Laura M., Rebecca D. Dodd, Andrea L. Merz, Anjelika M. Dechkovskaia, Matthew Herring, Benjamin A. Winston, Alex M. Lencioni, Rae L. Russell, Helen Madsen, Meheret Nega, Nathaniel L. Dusto, Jason White, Darell D. Bigner, Christopher V. Nicchitta, Natalie J. Serkova, and Michael W. Graner. 2013. "Induction of the Unfolded Protein Response Drives Enhanced Metabolism and Chemoresistance in Glioma Cells." *PLOS ONE* 8 (8):e73267. doi: 10.1371/journal.pone.0073267.

Faber, Samantha C., Anatoly A. Soshilov, Sara Giani Tagliabue, Laura Bonati, and Michael S. Denison. 2018. "Comparative In Vitro and In Silico Analysis of the Selectivity of Indirubin as a Human Ah Receptor Agonist." *International journal of molecular sciences* 19 (9):2692. doi: 10.3390/ijms19092692.

Feng, Xi, Frank Szulzewsky, Alexan Yerevanian, Zhihong Chen, David Heinzmann, Rikke Darling Rasmussen, Virginia Alvarez-Garcia, Yeonghwan Kim, Bingcheng Wang, Ilaria Tamagno, Hao Zhou, Xiaoxia Li, Helmut Kettenmann, Richard M. Ransohoff, and Dolores Hambardzumyan. 2015. "Loss of CX3CR1 increases accumulation of inflammatory monocytes and promotes gliomagenesis." *Oncotarget* 6 (17):15077-15094.

Feng, Y., J. Ren, Y. Gui, W. Wei, B. Shu, Q. Lu, X. Xue, X. Sun, W. He, J. Yang, and C. Dai. 2018. "Wnt/beta-Catenin-Promoted Macrophage Alternative Activation Contributes to Kidney Fibrosis." *J Am Soc Nephrol* 29 (1):182-193. doi: 10.1681/asn.2017040391.

Fukai, Junya, Hiroki Nishibayashi, Yuji Uematsu, Yonehiro Kanemura, Koji Fujita, and Naoyuki Nakao. 2016. "Rapid regression of glioblastoma following carmustine wafer implantation: A case report." *Molecular and clinical oncology* 5 (1):153-157. doi: 10.3892/mco.2016.894.

Gabriely, Galina, and Francisco J. Quintana. 2019. "Role of AHR in the control of GBM-associated myeloid cells." *Seminars in Cancer Biology*. doi: https://doi.org/10.1016/j.semcancer.2019.05.014.

Gabriely, Galina, Michael A. Wheeler, Maisa C. Takenaka, and Francisco J. Quintana. 2017. "Role of AHR and HIF-1α in Glioblastoma Metabolism." *Trends in Endocrinology & Metabolism* 28 (6):428-436. doi: https://doi.org/10.1016/j.tem.2017.02.009.

Ganguly, D., M. Fan, C. H. Yang, B. Zbytek, D. Finkelstein, M. F. Roussel, and L. M. Pfeffer. 2018. "The critical role that STAT3 plays in glioma-initiating cells: STAT3 addiction in glioma." *Oncotarget* 9 (31):22095-22112. doi: 10.18632/oncotarget.25188.

Genin, Marie, Francois Clement, Antoine Fattaccioli, Martine Raes, and Carine Michiels. 2015. "M1 and M2 macrophages derived from THP-1 cells differentially modulate the response of cancer cells to etoposide." *BMC Cancer* 15 (1):577. doi: 10.1186/s12885-015-1546-9.

Goetz, Christian, Elena Dobrikova, Mayya Shveygert, Mikhail Dobrikov, and Matthias Gromeier. 2011. "Oncolytic poliovirus against malignant glioma." *Future virology* 6 (9):1045-1058. doi: 10.2217/fvl.11.76.

Goodenberger, McKinsey L., and Robert B. Jenkins. 2012. "Genetics of adult glioma." *Cancer Genetics* 205 (12):613-621. doi: https://doi.org/10.1016/j.cancergen.2012.10.009.

Gramatzki, D., G. Pantazis, J. Schittenhelm, G. Tabatabai, C. Kohle, W. Wick, M. Schwarz, M. Weller, and I. Tritschler. 2009. "Aryl hydrocarbon receptor inhibition downregulates the TGF-[beta]/Smad pathway in human glioblastoma cells." *Oncogene* 28 (28):2593-2605.

Gu, Yi-Zhong, John B. Hogenesch, and Christopher A. Bradfield. 2000. "The PAS Superfamily: Sensors of Environmental and Developmental Signals." *Annual Review of Pharmacology and Toxicology* 40 (1):519-561. doi: doi:10.1146/annurev.pharmtox.40.1.519.

Guastella, Anthony R., Sharon K. Michelhaugh, Neil V. Klinger, Hassan A. Fadel, Sam Kiousis, Rouba Ali-Fehmi, William J. Kupsky, Csaba Juhász, and Sandeep Mittal. 2018. "Investigation of the aryl hydrocarbon receptor and the intrinsic tumoral component of the kynurenine pathway of tryptophan metabolism in primary brain tumors." *Journal of Neuro-Oncology* 139 (2):239-249. doi: 10.1007/s11060-018-2869-6.

Guengerich, P. F., Martha V. Martin, W. Andrew McCormick, Linh P. Nguyen, Edward Glover, and Christopher A. Bradfield. 2004. "Aryl hydrocarbon receptor response to indigoids in vitro and in vivo." *Archives of Biochemistry and Biophysics* 423 (2):309-316. doi: http://dx.doi.org/10.1016/j.abb.2004.01.002.

Hambardzumyan, Dolores, David H. Gutmann, and Helmut Kettenmann. 2016. "The role of microglia and macrophages in glioma maintenance and progression." *Nat Neurosci* 19 (1):20-27. doi: 10.1038/nn.4185.

Hamilton, Jackson D., Marion Rapp, Timo Marcel Schneiderhan, Michael Sabel, Anne Hayman, Axel Scherer, Patric Kröpil, Wilfried Budach, Usha Kretschmar, Peter Arne Gerber, Sujit Prabhu, Lawrence E. Ginsberg, Edwin Bölke, and Christiane Matuschek. 2014. "Glioblastoma Multiforme Metastasis Outside the CNS: Three Case Reports and Possible Mechanisms of Escape." *Journal of Clinical Oncology* 32 (22):e80-e84. doi: 10.1200/JCO.2013.48.7546.

Hanukoglu, Israel. 1992. "Steroidogenic enzymes: Structure, function, and role in regulation of steroid hormone biosynthesis." *The Journal of Steroid Biochemistry and Molecular Biology* 43 (8):779-804. doi: https://doi.org/10.1016/0960-0760(92)90307-5.

Hendrayani, Siti-Fauziah, Bothaina Al-Harbi, Mysoon M. Al-Ansari, Gabriela Silva, and Abdelilah Aboussekhra. 2016. "The inflammatory/cancer-related IL-6/STAT3/NF-κB positive feedback loop includes AUF1 and maintains the active state of breast myofibroblasts." *Oncotarget* 7 (27):41974-41985. doi: 10.18632/oncotarget.9633.

Hetz, Claudio, Eric Chevet, and Scott A. Oakes. 2015. "Proteostasis control by the unfolded protein response." *Nature Cell Biology* 17:829. doi: 10.1038/ncb3184.

Hoessel, Ralph, Sophie Leclerc, Jane A. Endicott, Martin E. M. Nobel, Alison Lawrie, Paul Tunnah, Maryse Leost, Eve Damiens, Dominique Marie, Doris Marko, Ellen Niederberger, Weici Tang, Gerhard Eisenbrand, and Laurent Meijer. 1999. "Indirubin, the active constituent of a Chinese antileukaemia medicine, inhibits cyclin-dependent kinases." *Nat Cell Biol* 1 (1):60-67. doi: http://www.nature.com/ncb/journal/v1/n1/suppinfo/ncb0599_60_S1.html.

Holland, Eric C. 2000. "Glioblastoma multiforme: The terminator." *Proceedings of the National Academy of Sciences* 97 (12):6242-6244. doi: 10.1073/pnas.97.12.6242.

Hombach-Klonisch, Sabine, Maryam Mehrpour, Shahla Shojaei, Craig Harlos, Marshall Pitz, Ahmed Hamai, Krzysztof Siemianowicz, Wirginia Likus, Emilia Wiechec, Brian D. Toyota, Reyhane Hoshyar, Amir Seyfoori, Zahra Sepehri, Sudharsana R. Ande, Forough Khadem, Mohsen Akbari, Adrienne M. Gorman, Afshin Samali, Thomas Klonisch, and Saeid Ghavami. 2018. "Glioblastoma and chemoresistance to alkylating agents: Involvement of apoptosis, autophagy, and unfolded protein response." *Pharmacology & Therapeutics* 184:13-41. doi: https://doi.org/10.1016/j.pharmthera.2017.10.017.

Hou, Xu, Yaohua Liu, Huailei Liu, Xin Chen, Min Liu, Hui Che, Fei Guo, Chunlei Wang, Daming Zhang, Jianing Wu, Xiaofeng Chen, Chen Shen, Chenguang Li, Fei Peng, Yunke Bi, Zhuowen Yang, Guang Yang, Jing Ai, Xin Gao, and Shiguang Zhao. 2015. "PERK silence inhibits glioma cell growth under low glucose stress by blockage of p-AKT and subsequent HK2's mitochondria translocation." *Scientific Reports* 5:9065. doi: 10.1038/srep09065

https://www.nature.com/articles/srep09065 - supplementary-information.

Høyer-Hansen, M., and M. Jäättelä. 2007. "Connecting endoplasmic reticulum stress to autophagy by unfolded protein response and calcium." *Cell Death And Differentiation* 14:1576. doi: 10.1038/sj.cdd.4402200.

Hu, Wenyue, Claudio Sorrentino, Michael S. Denison, Kyle Kolaja, and Mark R. Fielden. 2007. "Induction of Cyp1a1 Is a Nonspecific Biomarker of Aryl Hydrocarbon Receptor Activation: Results of Large Scale Screening of

Pharmaceuticals and Toxicants in Vivo and in Vitro." *Molecular Pharmacology* 71 (6):1475.
Huang, Yuhui, Shom Goel, Dan G. Duda, Dai Fukumura, and Rakesh K. Jain. 2013. "Vascular Normalization as an Emerging Strategy to Enhance Cancer Immunotherapy." *Cancer Research* 73 (10):2943-2948. doi: 10.1158/0008-5472.Can-12-4354.
Hubbard, Troy D., Iain A. Murray, Robert G. Nichols, Kaitlyn Cassel, Michael Podolsky, Guray Kuzu, Yuan Tian, Phillip Smith, Mary J. Kennett, Andrew D. Patterson, and Gary H. Perdew. 2017. "Dietary Broccoli Impacts Microbial Community Structure and Attenuates Chemically Induced Colitis in Mice in an Ah receptor dependent manner." *Journal of functional foods* 37:685-698. doi: 10.1016/j.jff.2017.08.038.
Hubbard, Troy D., Iain A. Murray, and Gary H. Perdew. 2015. "Indole and Tryptophan Metabolism: Endogenous and Dietary Routes to Ah Receptor Activation." *Drug Metabolism and Disposition* 43 (10):1522.
Hussain, Sajjad, Ying Zhang, and Paul Galardy. 2009. "DUBs and cancer: The role of deubiquitinating enzymes as oncogenes, non-oncogenes and tumor suppressors." *Cell Cycle* 8 (11):1688-1697. doi: 10.4161/cc.8.11.8739.
Jackson, Melanie, Foteini Hassiotou, and Anna Nowak. 2014. "Glioblastoma stem-like cells: at the root of tumor recurrence and a therapeutic target." *Carcinogenesis* 36 (2):177-185. doi: 10.1093/carcin/bgu243.
Jia, Wentao, Roger M. Loria, Margaret A. Park, Adly Yacoub, Paul Dent, and Martin R. Graf. 2010. "The neuro-steroid, 5-androstene 3β,17α diol; induces endoplasmic reticulum stress and autophagy through PERK/eIF2α signaling in malignant glioma cells and transformed fibroblasts." *The International Journal of Biochemistry & Cell Biology* 42 (12):2019-2029. doi: https://doi.org/10.1016/j.biocel.2010.09.003.
Jin, Un-Ho, Keshav Karki, Yating Cheng, Sharon K. Michelhaugh, Sandeep Mittal, and Stephen Safe. 2019. "The aryl hydrocarbon receptor is a tumor suppressor–like gene in glioblastoma." *Journal of Biological Chemistry* 294 (29):11342-11353. doi: 10.1074/jbc.RA119.008882.
Johnson, Daniel E., Rachel A. O'Keefe, and Jennifer R. Grandis. 2018. "Targeting the IL-6/JAK/STAT3 signalling axis in cancer." *Nature Reviews Clinical Oncology* 15:234. doi: 10.1038/nrclinonc.2018.8.
Joo, Kyeung Min, Jinkuk Kim, Juyoun Jin, Misuk Kim, Ho Jun Seol, Johongir Muradov, Heekyoung Yang, Yoon-La Choi, Woong-Yang Park, Doo-Sik Kong, Jung-Il Lee, Young-Hyeh Ko, Hyun Goo Woo, Jeongwu Lee, Sunghoon Kim, and Do-Hyun Nam. 2013. "Patient-Specific Orthotopic Glioblastoma Xenograft Models Recapitulate the Histopathology and Biology of Human Glioblastomas In Situ." *Cell Reports* 3 (1):260-273. doi: https://doi.org/10.1016/j.celrep.2012.12.013.

Joshi, M., A. Kulkarni, and J. K. Pal. 2013. "Small molecule modulators of eukaryotic initiation factor 2alpha kinases, the key regulators of protein synthesis." *Biochimie* 95 (11):1980-90. doi: 10.1016/j.biochi.2013.07.030.

Kahlert, Ulf D., Abigail K. Suwala, Katharina Koch, Manabu Natsumeda, Brent A. Orr, Masanori Hayashi, Jarek Maciaczyk, and Charles G. Eberhart. 2015. "Pharmacologic Wnt Inhibition Reduces Proliferation, Survival, and Clonogenicity of Glioblastoma Cells." *Journal of Neuropathology & Experimental Neurology* 74 (9):889-900. doi: 10.1097/nen.0000000000000227.

Kaina, Bernd, Markus Christmann, Steffen Naumann, and Wynand P. Roos. 2007. "MGMT: Key node in the battle against genotoxicity, carcinogenicity and apoptosis induced by alkylating agents." *DNA Repair* 6 (8):1079-1099. doi: https://doi.org/10.1016/j.dnarep.2007.03.008.

Kawajiri, Kaname, Yasuhito Kobayashi, Fumiaki Ohtake, Togo Ikuta, Yoshibumi Matsushima, Junsei Mimura, Sven Pettersson, Richard S. Pollenz, Toshiyuki Sakaki, Takatsugu Hirokawa, Tetsu Akiyama, Masafumi Kurosumi, Lorenz Poellinger, Shigeaki Kato, and Yoshiaki Fujii-Kuriyama. 2009. "Aryl hydrocarbon receptor suppresses intestinal carcinogenesis in ApcMin/+ mice with natural ligands." *Proceedings of the National Academy of Sciences* 106 (32):13481-13486. doi: 10.1073/pnas.0902132106.

Kawanishi, Masanobu, Michiyo Sakamoto, Akihide Ito, Kyoko Kishi, and Takashi Yagi. 2003. "Construction of reporter yeasts for mouse aryl hydrocarbon receptor ligand activity." *Mutation Research/Genetic Toxicology and Environmental Mutagenesis* 540 (1):99-105. doi: 10.1016/s1383-5718(03)00174-8.

Kennedy, Benjamin C., Christopher R. Showers, David E. Anderson, Lisa Anderson, Peter Canoll, Jeffrey N. Bruce, and Richard C. E. Anderson. 2013. "Tumor-Associated Macrophages in Glioma: Friend or Foe?" *Journal of Oncology* 2013:11. doi: 10.1155/2013/486912.

Keunen, Olivier, Mikael Johansson, Anaïs Oudin, Morgane Sanzey, Siti A. Abdul Rahim, Fred Fack, Frits Thorsen, Torfinn Taxt, Michal Bartos, Radovan Jirik, Hrvoje Miletic, Jian Wang, Daniel Stieber, Linda Stuhr, Ingrid Moen, Cecilie Brekke Rygh, Rolf Bjerkvig, and Simone P. Niclou. 2011. "Anti-VEGF treatment reduces blood supply and increases tumor cell invasion in glioblastoma." *Proceedings of the National Academy of Sciences* 108 (9):3749-3754. doi: 10.1073/pnas.1014480108.

Kim, Soo-Hyun, Soo Jeong Choi, Yong-Chul Kim, and Hyo-Jeong Kuh. 2009. "Anti-tumor activity of noble indirubin derivatives in human solid tumor models In Vitro." *Archives of Pharmacal Research* 32 (6):915-922. doi: 10.1007/s12272-009-1614-2.

Kim, Yonghyun, Kang Ho Kim, Jeena Lee, Young-Ae Lee, Misuk Kim, Se Jeong Lee, Kernyu Park, Heekyoung Yang, Juyoun Jin, Kyeung Min Joo, Jeongwu Lee, and Do-Hyun Nam. 2012. "Wnt activation is implicated in glioblastoma

radioresistance." *Laboratory Investigation* 92 (3):466-473. doi: 10.1038/labinvest.2011.161.
Kirikoshi, H., S. Inoue, H. Sekihara, and M. Katoh. 2001. "Expression of WNT10A in human cancer." *Int J Oncol* 19 (5):997-1001. doi: 10.3892/ijo.19.5.997.
Kirikoshi, H., and M. Katoh. 2002. "Expression of WNT7A in human normal tissues and cancer, and regulation of WNT7A and WNT7B in human cancer." *Int J Oncol* 21 (4):895-900.
Knockaert, Marie, Marc Blondel, Stephane Bach, Maryse Leost, Cem Elbi, Gordon L. Hager, Scott R. Nagy, Dalho Han, Michael Denison, Martine Ffrench, Xiaozhou P. Ryan, Prokopios Magiatis, Panos Polychronopoulos, Paul Greengard, Leandros Skaltsounis, and Laurent Meijer. 2004. "Independent actions on cyclin-dependent kinases and aryl hydrocarbon receptor mediate the antiproliferative effects of indirubins." *Oncogene* 23 (25):4400-4412.
Köhle, Christoph, and Karl Walter Bock. 2007. "Coordinate regulation of Phase I and II xenobiotic metabolisms by the Ah receptor and Nrf2." *Biochem Pharmacol* 73 (12):1853-1862. doi: 10.1016/j.bcp.2007.01.009.
Kosuge, Yasuhiro, Hiroaki Saito, Tatsuki Haraguchi, Yoshimi Ichimaru, Sachiyo Ohashi, Hiroko Miyagishi, Shunsuke Kobayashi, Kumiko Ishige, Shinichi Miyairi, and Yoshihisa Ito. 2017. "Indirubin derivatives protect against endoplasmic reticulum stress-induced cytotoxicity and down-regulate CHOP levels in HT22 cells." *Bioorganic & Medicinal Chemistry Letters* 27 (23):5122-5125. doi: https://doi.org/10.1016/j.bmcl.2017.10.069.
Kuehn, Bridget M. 2010. "Genomics Illuminates a Deadly Brain Cancer." *JAMA* 303 (10):925-927. doi: 10.1001/jama.2010.236.
Kunikata, Toshio, Tomoki Tatefuji, Hajime Aga, Kanso Iwaki, Masao Ikeda, and Masashi Kurimoto. 2000. "Indirubin inhibits inflammatory reactions in delayed-type hypersensitivity." *European Journal of Pharmacology* 410 (1):93-100. doi: http://dx.doi.org/10.1016/S0014-2999(00)00879-7.
Leclerc, S., M. Garnier, R. Hoessel, D. Marko, J. A. Bibb, G. L. Snyder, P. Greengard, J. Biernat, Y. Z. Wu, E. M. Mandelkow, G. Eisenbrand, and L. Meijer. 2001. "Indirubins inhibit glycogen synthase kinase-3 beta and CDK5/p25, two protein kinases involved in abnormal tau phosphorylation in Alzheimer's disease. A property common to most cyclin-dependent kinase inhibitors?" *J Biol Chem* 276 (1):251-60. doi: 10.1074/jbc.M002466200.
Lim, Michael, Yuanxuan Xia, Chetan Bettegowda, and Michael Weller. 2018. "Current state of immunotherapy for glioblastoma." *Nature Reviews Clinical Oncology* 15 (7):422-442. doi: 10.1038/s41571-018-0003-5.
Lin, K. W., A. Liao, and A. A. Qutub. 2015. "Simulation predicts IGFBP2-HIF1alpha interaction drives glioblastoma growth." *PLoS Comput Biol* 11 (4):e1004169. doi: 10.1371/journal.pcbi.1004169.
Louis, David N., Arie Perry, Guido Reifenberger, Andreas von Deimling, Dominique Figarella-Branger, Webster K. Cavenee, Hiroko Ohgaki, Otmar D. Wiestler, Paul Kleihues, and David W. Ellison. 2016. "The 2016 World Health

Organization Classification of Tumors of the Central Nervous System: a summary." *Acta Neuropathologica* 131 (6):803-820. doi: 10.1007/s00401-016-1545-1.

Luo, B., and A. S. Lee. 2013. "The critical roles of endoplasmic reticulum chaperones and unfolded protein response in tumorigenesis and anticancer therapies." *Oncogene* 32 (7):805-818. doi: 10.1038/onc.2012.130.

Ma, J.-X., K. Park, K. Lee, T. Zhou, and B. Zhang. 2010. "Blocking Wnt Signaling, a Unifying Mechanism for the Anti-Angiogenic, Anti-Inflammatory and Anti-Fibrogenic Effect Of Pedf." *Investigative Ophthalmology & Visual Science* 51 (13):5094-5094.

Ma, Y., and L. M. Hendershot. 2004. "The role of the unfolded protein response in tumour development: friend or foe?" *Nat Rev Cancer* 4 (12):966-77. doi: 10.1038/nrc1505.

Mancinelli, Romina, Guido Carpino, Simonetta Petrungaro, Caterina Loredana Mammola, Luana Tomaipitinca, Antonio Filippini, Antonio Facchiano, Elio Ziparo, and Claudia Giampietri. 2017. "Multifaceted Roles of GSK-3 in Cancer and Autophagy-Related Diseases." *Oxidative Medicine and Cellular Longevity* 2017:14. doi: 10.1155/2017/4629495.

Mason, James J., and Bart O. Williams. 2010. "SOST and DKK: Antagonists of LRP Family Signaling as Targets for Treating Bone Disease." *Journal of osteoporosis* 2010:460120. doi: 10.4061/2010/460120.

Mathew, Lijoy K., Sumitra S. Sengupta, Jane LaDu, Eric A. Andreasen, and Robert L. Tanguay. 2008. "Crosstalk between AHR and Wnt signaling through R-Spondin1 impairs tissue regeneration in zebrafish." *The FASEB Journal* 22 (8):3087-3096. doi: 10.1096/fj.08-109009.

Mathew, Lijoy K., Michel T. Simonich, and Robert L. Tanguay. 2009. "AHR-dependent misregulation of Wnt signaling disrupts tissue regeneration." *Biochemical Pharmacology* 77 (4):498-507. doi: https://doi.org/10.1016/j.bcp.2008.09.025.

Matias, D., D. Predes, P. Niemeyer Filho, M. C. Lopes, J. G. Abreu, F. R. S. Lima, and V. Moura Neto. 2017. "Microglia-glioblastoma interactions: New role for Wnt signaling." *Biochimica et Biophysica Acta (BBA) - Reviews on Cancer* 1868 (1):333-340. doi: https://doi.org/10.1016/j.bbcan.2017.05.007.

Matias, Diana, Luiz Gustavo Dubois, Bruno Pontes, Luciane Rosário, Valeria Pereira Ferrer, Joana Balça-Silva, Anna Carolina Carvalho Fonseca, Lucy Wanjiku Macharia, Luciana Romão, Tania Cristina Leite de Sampaio e Spohr, Leila Chimelli, Paulo Niemeyer Filho, Maria Celeste Lopes, José Garcia Abreu, Flavia Regina Souza Lima, and Vivaldo Moura-Neto. 2019. "GBM-Derived Wnt3a Induces M2-Like Phenotype in Microglial Cells Through Wnt/β-Catenin Signaling." *Molecular Neurobiology* 56 (2):1517-1530. doi: 10.1007/s12035-018-1150-5.

Matsebatlela, Thabe M., Amy L. Anderson, Vincent S. Gallicchio, Howard Elford, and Charles D. Rice. 2015. "3,4-Dihydroxy-benzohydroxamic acid (Didox)

suppresses pro-inflammatory profiles and oxidative stress in TLR4-activated RAW264.7 murine macrophages." *Chemico-Biological Interactions* 233:95-105. doi: http://dx.doi.org/10.1016/j.cbi.2015.03.027.

MayoClinic. 2017. Viral Therapy in Treating Patients With Recurrent Glioblastoma Multiforme. edited by NCI National Cancer Institute.

McCord, Matthew, Yoh-suke Mukouyama, Mark R. Gilbert, and Sadhana Jackson. 2017. "Targeting WNT Signaling for Multifaceted Glioblastoma Therapy." *Frontiers in Cellular Neuroscience* 11 (318). doi: 10.3389/fncel.2017.00318.

McFarland, Braden C., Suk W. Hong, Rajani Rajbhandari, George B. Twitty, Jr., G. Kenneth Gray, Hao Yu, Etty N. Benveniste, and Susan E. Nozell. 2013. "NF-κB-Induced IL-6 Ensures STAT3 Activation and Tumor Aggressiveness in Glioblastoma." *PLOS ONE* 8 (11):e78728. doi: 10.1371/journal.pone.0078728.

McNamara, Mairéad G., and Warren P. Mason. 2012. "Antiangiogenic therapies in glioblastoma multiforme." *Expert Review of Anticancer Therapy* 12 (5):643-654. doi: 10.1586/era.12.35.

Meares, G. P., M. A. Mines, E. Beurel, T. Y. Eom, L. Song, A. A. Zmijewska, and R. S. Jope. 2011. "Glycogen synthase kinase-3 regulates endoplasmic reticulum (ER) stress-induced CHOP expression in neuronal cells." *Exp Cell Res* 317 (11):1621-8. doi: 10.1016/j.yexcr.2011.02.012.

Meares, Gordon P., Yudong Liu, Rajani Rajbhandari, Hongwei Qin, Susan E. Nozell, James A. Mobley, John A. Corbett, and Etty N. Benveniste. 2014. "PERK-Dependent Activation of JAK1 and STAT3 Contributes to Endoplasmic Reticulum Stress-Induced Inflammation." *Molecular and Cellular Biology* 34 (20):3911-3925. doi: 10.1128/mcb.00980-14.

Meijer, Laurent, Alexios-Leandros Skaltsounis, Prokopios Magiatis, Panagiotis Polychronopoulos, Marie Knockaert, Maryse Leost, Xiaozhou P. Ryan, Claudia Alin Vonica, Ali Brivanlou, Rana Dajani, Claudia Crovace, Cataldo Tarricone, Andrea Musacchio, S. Mark Roe, Laurence Pearl, and Paul Greengard. 2003. "GSK-3-Selective Inhibitors Derived from Tyrian Purple Indirubins." *Chemistry & Biology* 10 (12):1255-1266. doi: 10.1016/j.chembiol.2003.11.010.

Metidji, Amina, Sara Omenetti, Stefania Crotta, Ying Li, Emma Nye, Ellie Ross, Vivian Li, Muralidhara R. Maradana, Chris Schiering, and Brigitta Stockinger. 2018. "The Environmental Sensor AHR Protects from Inflammatory Damage by Maintaining Intestinal Stem Cell Homeostasis and Barrier Integrity." *Immunity* 49 (2):353-362.e5. doi: https://doi.org/10.1016/j.immuni.2018.07.010.

Miyoshi, Ken, Mikiro Takaishi, John DiGiovanni, and Shigetoshi Sano. 2012. "Attenuation of psoriasis-like skin lesion in a mouse model by topical treatment with indirubin and its derivative E804." *Journal of Dermatological Science* 65 (1):70-72. doi: http://dx.doi.org/10.1016/j.jdermsci.2011.10.001.

Molenaar, Remco J., Dagmar Verbaan, Simona Lamba, Carlo Zanon, Judith W. M. Jeuken, Sandra H. E. Boots-Sprenger, Pieter Wesseling, Theo J. M. Hulsebos, Dirk Troost, Angela A. van Tilborg, Sieger Leenstra, W. Peter Vandertop, Alberto Bardelli, Cornelis J. F. van Noorden, and Fonnet E. Bleeker. 2014. "The combination of IDH1 mutations and MGMT methylation status predicts survival in glioblastoma better than either IDH1 or MGMT alone." *Neuro-oncology* 16 (9):1263-1273. doi: 10.1093/neuonc/nou005.

Moon, Myoung Ju, Sang Kook Lee, Jong-Won Lee, Woo Keun Song, Si Wouk Kim, Jae Il Kim, Chunghee Cho, Soo Jeong Choi, and Yong-Chul Kim. 2006. "Synthesis and structure–activity relationships of novel indirubin derivatives as potent anti-proliferative agents with CDK2 inhibitory activities." *Bioorganic & Medicinal Chemistry* 14 (1):237-246. doi: http://dx.doi.org/10.1016/j.bmc.2005.08.008.

Motaln, Helena, Ana Koren, Kristina Gruden, Živa Ramšak, Christian Schichor, and Tamara T. Lah. 2015. "Heterogeneous glioblastoma cell cross-talk promotes phenotype alterations and enhanced drug resistance." *Oncotarget* 6 (38):40998-41017. doi: 10.18632/oncotarget.5701.

Murray, Iain A., Colin A. Flaveny, Brett C. DiNatale, Chris R. Chairo, Jennifer C. Schroeder, Ann Kusnadi, and Gary H. Perdew. 2010. "Antagonism of Aryl Hydrocarbon Receptor Signaling by 6,2',4'-Trimethoxyflavone." *Journal of Pharmacology and Experimental Therapeutics* 332 (1):135-144. doi: 10.1124/jpet.109.158261.

Murray, Iain A., Andrew D. Patterson, and Gary H. Perdew. 2014. "AH RECEPTOR LIGANDS IN CANCER: FRIEND AND FOE." *Nature reviews. Cancer* 14 (12):801-814.

Nam, Sangkil, Ralf Buettner, James Turkson, Donghwa Kim, Jin Q. Cheng, Stephan Muehlbeyer, Frankie Hippe, Sandra Vatter, Karl-Heinz Merz, Gerhard Eisenbrand, and Richard Jove. 2005. "Indirubin derivatives inhibit Stat3 signaling and induce apoptosis in human cancer cells." *Proceedings of the National Academy of Sciences* 102 (17):5998-6003. doi: 10.1073/pnas.0409467102.

National Brain Tumor Society, NBTS. "Quick Brain Tumor Facts." accessed 07/31/17. http://braintumor.org/brain-tumor-information/brain-tumor-facts/.

National Cancer Institute, NCI. "Cancer Stat Facts: Brain and Other Nervous System Cancer." accessed 07/31/2017. https://seer.cancer.gov/statfacts/html/brain.html.

Nduom, Edjah K., Michael Weller, and Amy B. Heimberger. 2015. "Immunosuppressive mechanisms in glioblastoma." *Neuro-Oncology* 17 (suppl_7):vii9-vii14. doi: 10.1093/neuonc/nov151.

Nebert, Daniel W., Amy L. Roe, Matthew Z. Dieter, Willy A. Solis, Yi Yang, and Timothy P. Dalton. 2000. "Role of the aromatic hydrocarbon receptor and [Ah] gene battery in the oxidative stress response, cell cycle control, and apoptosis." *Biochem Pharmacol* 59 (1):65-85. doi: 10.1016/s0006-2952(99)00310-x.

Nguyen, Chi D. L., Sebastian Malchow, Stefan Reich, Sascha Steltgens, Konstantin V. Shuvaev, Stefan Loroch, Christin Lorenz, Albert Sickmann, Christiane B. Knobbe-Thomsen, Björn Tews, Jan Medenbach, and Robert Ahrends. 2019. "A sensitive and simple targeted proteomics approach to quantify transcription factor and membrane proteins of the unfolded protein response pathway in glioblastoma cells." *Scientific Reports* 9 (1):8836. doi: 10.1038/s41598-019-45237-5.

Nicolaou, Katerina A., Vasilis Liapis, Andreas Evdokiou, Constantina Constantinou, Prokopios Magiatis, Alex L. Skaltsounis, Laura Koumas, Paul A. Costeas, and Andreas I. Constantinou. 2012. "Induction of discrete apoptotic pathways by bromo-substituted indirubin derivatives in invasive breast cancer cells." *Biochemical and Biophysical Research Communications* 425 (1):76-82. doi: https://doi.org/10.1016/j.bbrc.2012.07.053.

Niwa, Toshiro, Norie Murayama, Yurie Imagawa, and Hiroshi Yamazaki. 2015. "Regioselective hydroxylation of steroid hormones by human cytochromes P450." *Drug Metabolism Reviews* 47 (2):89-110. doi: 10.3109/03602532.2015.1011658.

Obacz, J., T. Avril, P. J. Le Reste, H. Urra, V. Quillien, C. Hetz, and E. Chevet. 2017. "Endoplasmic reticulum proteostasis in glioblastoma-From molecular mechanisms to therapeutic perspectives." *Sci Signal* 10 (470). doi: 10.1126/scisignal.aal2323.

Ojalvo, Laureen S., Charles A. Whittaker, John S. Condeelis, and Jeffrey W. Pollard. 2010. "Gene Expression Analysis of Macrophages That Facilitate Tumor Invasion Supports a Role for Wnt-Signaling in Mediating Their Activity in Primary Mammary Tumors." *The Journal of Immunology* 184 (2):702-712. doi: 10.4049/jimmunol.0902360.

Omuro, A., and L. M. DeAngelis. 2013. "Glioblastoma and other malignant gliomas: A clinical review." *JAMA* 310 (17):1842-1850. doi: 10.1001/jama.2013.280319.

Otvos, Balint, Daniel J. Silver, Erin E. Mulkearns-Hubert, Alvaro G. Alvarado, Soumya M. Turaga, Mia D. Sorensen, Patricia Rayman, William A Flavahan, James S. Hale, Kevin Stoltz, Maksim Sinyuk, Qiulian Wu, Awad Jarrar, Sung-Hak Kim, Paul L. Fox, Ichiro Nakano, Jeremy N. Rich, Richard M. Ransohoff, James Finke, Bjarne W. Kristensen, Michael A. Vogelbaum, and Justin D. Lathia. 2016. "Cancer Stem Cell-Secreted Macrophage Migration Inhibitory Factor

Stimulates Myeloid Derived Suppressor Cell Function and Facilitates Glioblastoma Immune Evasion." *STEM CELLS* 34 (8):2026-2039. doi: 10.1002/stem.2393.

Peterson, T. E., N. D. Kirkpatrick, Y. Huang, C. T. Farrar, K. A. Marijt, J. Kloepper, M. Datta, Z. Amoozgar, G. Seano, K. Jung, W. S. Kamoun, T. Vardam, M. Snuderl, J. Goveia, S. Chatterjee, A. Batista, A. Muzikansky, C. C. Leow, L. Xu, T. T. Batchelor, D. G. Duda, D. Fukumura, and R. K. Jain. 2016. "Dual inhibition of Ang-2 and VEGF receptors normalizes tumor vasculature and prolongs survival in glioblastoma by altering macrophages." *Proc Natl Acad Sci U S A* 113 (16):4470-5. doi: 10.1073/pnas.1525349113.

Prinz, Marco, and Josef Priller. 2014. "Microglia and brain macrophages in the molecular age: from origin to neuropsychiatric disease." *Nat Rev Neurosci* 15 (5):300-312. doi: 10.1038/nrn3722.

Procházková, Jiřina, Markéta Kabátková, Vítězslav Bryja, Lenka Umannová, Ondřej Bernatík, Alois Kozubík, Miroslav Machala, and Jan Vondráček. 2011. "The Interplay of the Aryl Hydrocarbon Receptor and β-Catenin Alters Both AhR-Dependent Transcription and Wnt/β-Catenin Signaling in Liver Progenitors." *Toxicological Sciences* 122 (2):349-360. doi: 10.1093/toxsci/kfr129.

Pukrop, Tobias, Faramarz Dehghani, Han-Ning. Chuang, Raphaela Lohaus, Kathrin Bayanga, Stephan Heermann, Tommy Regen, Denise Van Rossum, Florian Klemm, Matthias Schulz, Laila Siam, Anja Hoffmann, Lorenz Trümper, Christine Stadelmann, Ingo Bechmann, Uwe-Karsten Hanisch, and Claudia Binder. 2010. "Microglia promote colonization of brain tissue by breast cancer cells in a Wnt-dependent way." *Glia* 58 (12):1477-1489. doi: 10.1002/glia.21022.

Pyonteck, Stephanie M., Leila Akkari, Alberto J. Schuhmacher, Robert L. Bowman, Lisa Sevenich, Daniela F. Quail, Oakley C. Olson, Marsha L. Quick, Jason T. Huse, Virginia Teijeiro, Manu Setty, Christina S. Leslie, Yoko Oei, Alicia Pedraza, Jianan Zhang, Cameron W. Brennan, James C. Sutton, Eric C. Holland, Dylan Daniel, and Johanna A. Joyce. 2013. "CSF-1R inhibition alters macrophage polarization and blocks glioma progression." *Nat Med* 19 (10):1264-1272. doi: 10.1038/nm.3337

http://www.nature.com/nm/journal/v19/n10/abs/nm.3337.html - supplementary-information.

Pyrko, Peter, Axel H. Schönthal, Florence M. Hofman, Thomas C. Chen, and Amy S. Lee. 2007. "The Unfolded Protein Response Regulator GRP78/BiP as a Novel Target for Increasing Chemosensitivity in Malignant Gliomas." *Cancer Research* 67 (20):9809.

Qi, Tianjie, Haitao Li, and Shuai Li. 2017. "Indirubin improves antioxidant and anti-inflammatory functions in lipopolysaccharide-challenged mice." *Oncotarget* 8 (22):36658-36663. doi: 10.18632/oncotarget.17560.

Qian, Jiawen, Feifei Luo, Jiao Yang, Jun Liu, Ronghua Liu, Luman Wang, Chen Wang, Yuting Deng, Zhou Lu, Yuedi Wang, Mingfang Lu, Ji-Yang Wang, and Yiwei

Chu. 2018. "TLR2 Promotes Glioma Immune Evasion by Downregulating MHC Class II Molecules in Microglia." *Cancer Immunology Research*:canimm.0020.2018. doi: 10.1158/2326-6066.Cir-18-0020.
Ramirez, Yulian P., Jessica L. Weatherbee, Richard T. Wheelhouse, and Alonzo H. Ross. 2013. "Glioblastoma Multiforme Therapy and Mechanisms of Resistance." *Pharmaceuticals* 6 (12):1475-1506. doi: 10.3390/ph6121475.
Reed, Megan R, Leena Maddukuri, Emily Helm, April C.L. Bostian, Maroof K Zafar, and Robert L Eoff. 2017. "Inhibition of Kynurenine Signaling Decreases Glioblastoma Multiforme Genomic Instability and Sensitizes Cells to Chemotherapeutic Treatment." *The FASEB Journal* 31 (1_supplement):754.9-754.9. doi: 10.1096/fasebj.31.1_supplement.754.9.
Remmerie, Anneleen, and Charlotte L. Scott. 2018. "Macrophages and lipid metabolism." *Cellular immunology* 330:27-42. doi: 10.1016/j.cellimm.2018.01.020.
Ribas, J., K. Bettayeb, Y. Ferandin, M. Knockaert, X. Garrofe-Ochoa, F. Totzke, C. Schachtele, J. Mester, P. Polychronopoulos, P. Magiatis, A. L. Skaltsounis, J. Boix, and L. Meijer. 2006. "7-Bromoindirubin-3'-oxime induces caspase-independent cell death." *Oncogene* 25 (47):6304-18. doi: 10.1038/sj.onc.1209648.
Robertson, R. C., F. Guiheneuf, B. Bahar, M. Schmid, D. B. Stengel, G. F. Fitzgerald, R. P. Ross, and C. Stanton. 2015. "The Anti-Inflammatory Effect of Algae-Derived Lipid Extracts on Lipopolysaccharide (LPS)-Stimulated Human THP-1 Macrophages." *Mar Drugs* 13 (8):5402-24. doi: 10.3390/md13085402.
Roller, Corinna, and Danilo Maddalo. 2013. "The Molecular Chaperone GRP78/BiP in the Development of Chemoresistance: Mechanism and Possible Treatment." *Frontiers in pharmacology* 4:10-10. doi: 10.3389/fphar.2013.00010.
Roszman, Thomas, Lucinda Elliott, and William Brooks. 1991. "Modulation of T-cell function by gliomas." *Immunology Today* 12 (10):370-374. doi: https://doi.org/10.1016/0167-5699(91)90068-5.
Sajjad, M. U., B. Samson, and A. Wyttenbach. 2010. "Heat Shock Proteins: Therapeutic Drug Targets for Chronic Neurodegeneration?" *Current Pharmaceutical Biotechnology* 11 (2):198-215. doi: http://dx.doi.org/10.2174/138920110790909641.
Schneider, A. J., A. M. Branam, and R. E. Peterson. 2014. "Intersection of AHR and Wnt signaling in development, health, and disease." *Int J Mol Sci* 15 (10):17852-85. doi: 10.3390/ijms151017852.
Schulthess, Pascal, Alexandra Löffler, Silvia Vetter, Luisa Kreft, Michael Schwarz, Albert Braeuning, and Nils Blüthgen. 2015. "Signal integration by the CYP1A1 promoter — a quantitative study." *Nucleic Acids Research* 43 (11):5318-5330. doi: 10.1093/nar/gkv423.
Scobie, Micaela R., Haley R. Houke, and Charles D. Rice. 2019. "Modulation of glioma-inflammation crosstalk profiles in human glioblastoma cells by indirubin-3’-(2,3 dihydroxypropyl)-oximether (E804) and 7-bromoindirubin-3'-oxime

(7BIO)." *Chemico-Biological Interactions* 312:108816. doi: https://doi.org/10.1016/j.cbi.2019.108816.
Shan, Yongzhi, Xin He, Wei Song, Dong Han, Jianxing Niu, and Jianzhen Wang. 2015. "Role of IL-6 in the invasiveness and prognosis of glioma." *International Journal of Clinical and Experimental Medicine* 8 (6):9114-9120.
Shi, Yu, Olga A. Guryanova, Wenchao Zhou, Chong Liu, Zhi Huang, Xiaoguang Fang, Xiuxing Wang, Cong Chen, Qiulian Wu, Zhicheng He, Wei Wang, Wei Zhang, Tao Jiang, Qing Liu, Yaping Chen, Wenying Wang, Jingjing Wu, Leo Kim, Ryan C. Gimple, Hua Feng, Hsiang-Fu Kung, Jennifer S. Yu, Jeremy N. Rich, Yi-Fang Ping, Xiu-Wu Bian, and Shideng Bao. 2018. "Ibrutinib inactivates BMX-STAT3 in glioma stem cells to impair malignant growth and radioresistance." *Science Translational Medicine* 10 (443):eaah6816. doi: 10.1126/scitranslmed.aah6816.
Shin, E. K., and J. K. Kim. 2012. "Indirubin derivative E804 inhibits angiogenesis." *BMC Cancer* 12:164. doi: 10.1186/1471-2407-12-164.
Siegel, R. L., K. D. Miller, and A. Jemal. 2018. "Cancer statistics, 2018." *CA Cancer J Clin* 68 (1):7-30. doi: 10.3322/caac.21442.
Simmons, Grant W., Winnie W. Pong, Ryan J. Emnett, Crystal R. White, Scott M. Gianino, Fausto J. Rodriguez, and David H. Gutmann. 2011. "Neurofibromatosis-1 Heterozygosity Increases Microglia in a Spatially- and Temporally-Restricted Pattern Relevant to Mouse Optic Glioma Formation and Growth." *Journal of neuropathology and experimental neurology* 70 (1):51-62. doi: 10.1097/NEN.0b013e3182032d37.
Song, Libing, Liping Liu, Zhiqiang Wu, Yun Li, Zhe Ying, Chuyong Lin, Jueheng Wu, Bo Hu, Shi-Yuan Cheng, Mengfeng Li, and Jun Li. 2012. "TGF-β induces miR-182 to sustain NF-κB activation in glioma subsets." *The Journal of Clinical Investigation* 122 (10):3563-3578. doi: 10.1172/JCI62339.
Spink, B. C., M. M. Hussain, B. H. Katz, L. Eisele, and D. C. Spink. 2003. "Transient induction of cytochromes P450 1A1 and 1B1 in MCF-7 human breast cancer cells by indirubin." *Biochem Pharmacol* 66 (12):2313-21. doi: 10.1016/j.bcp.2003.08.019.
Springs, A. E., and C. D. Rice. 2006. "The Effects of Indirubin-3'-Monoxime, A Novel AHR Ligand, on Stress and Toxicity-Related Gene/Protein Expression in Human U937 Cells Undergoing Differentiation and Activation." *J Immunotoxicol* 3 (1):1-10. doi: 10.1080/15476910500468627.
Suwala, Abigail K., Allison Hanaford, Ulf D. Kahlert, and Jaroslaw Maciaczyk. 2016. "Clipping the Wings of Glioblastoma: Modulation of WNT as a Novel Therapeutic Strategy." *Journal of Neuropathology & Experimental Neurology* 75 (5):388-396. doi: 10.1093/jnen/nlw013.
Takenaka, Maisa C., Galina Gabriely, Veit Rothhammer, Ivan D. Mascanfroni, Michael A. Wheeler, Chun-Cheih Chao, Cristina Gutiérrez-Vázquez, Jessica Kenison, Emily C. Tjon, Andreia Barroso, Tyler Vandeventer, Kalil Alves de Lima, Sonja Rothweiler, Lior Mayo, Soufiene Ghannam, Stephanie Zandee, Luke Healy,

David Sherr, Mauricio F. Farez, Alexandre Prat, Jack Antel, David A. Reardon, Hailei Zhang, Simon C. Robson, Gad Getz, Howard L. Weiner, and Francisco J. Quintana. 2019. "Control of tumor-associated macrophages and T cells in glioblastoma via AHR and CD39." *Nature Neuroscience* 22 (5):729-740. doi: 10.1038/s41593-019-0370-y.

Thakkar, Jigisha P., Therese A. Dolecek, Craig Horbinski, Quinn T. Ostrom, Donita D. Lightner, Jill S. Barnholtz-Sloan, and John L. Villano. 2014. "Epidemiologic and molecular prognostic review of glioblastoma." *Cancer epidemiology, biomarkers & prevention : a publication of the American Association for Cancer Research, cosponsored by the American Society of Preventive Oncology* 23 (10):1985-1996. doi: 10.1158/1055-9965.EPI-14-0275.

Tu, Yanyang, Yuexia Zhong, Jianfang Fu, Yizhan Cao, Guoqiang Fu, Xiaoxi Tian, and Boliang Wang. 2011. "Activation of JAK/STAT signal pathway predicts poor prognosis of patients with gliomas." *Medical Oncology* 28 (1):15-23. doi: 10.1007/s12032-010-9435-1.

Tye, Hazel, Catherine L Kennedy, Meri Najdovska, Louise McLeod, William McCormack, Norman Hughes, Anouk Dev, William Sievert, Chia Huey Ooi, Tomo-o Ishikawa, Hiroko Oshima, Prithi S Bhathal, Andrew E Parker, Masanobu Oshima, Patrick Tan, and Brendan J Jenkins. 2012. "STAT3-Driven Upregulation of TLR2 Promotes Gastric Tumorigenesis Independent of Tumor Inflammation." *Cancer Cell* 22 (4):466-478. doi: https://doi.org/10.1016/j.ccr.2012.08.010.

Uckun, Fatih M., Sanjive Qazi, Zahide Ozer, Amanda L. Garner, Jason Pitt, Hong Ma, and Kim D. Janda. 2011. "Inducing apoptosis in chemotherapy-resistant B-lineage acute lymphoblastic leukaemia cells by targeting HSPA5, a master regulator of the anti-apoptotic unfolded protein response signalling network." *British Journal of Haematology* 153 (6):741-752. doi: 10.1111/j.1365-2141.2011.08671.x.

van der Vos, Kristan E., Erik R. Abels, Xuan Zhang, Charles Lai, Esteban Carrizosa, Derek Oakley, Shilpa Prabhakar, Osama Mardini, Matheus H. W. Crommentuijn, Johan Skog, Anna M. Krichevsky, Anat Stemmer-Rachamimov, Thorsten R. Mempel, Joseph El Khoury, Suzanne E. Hickman, and Xandra O. Breakefield. 2015. "Directly visualized glioblastoma-derived extracellular vesicles transfer RNA to microglia/macrophages in the brain." *Neuro-Oncology* 18 (1):58-69. doi: 10.1093/neuonc/nov244.

van Tellingen, O., B. Yetkin-Arik, M. C. de Gooijer, P. Wesseling, T. Wurdinger, and H. E. de Vries. 2015. "Overcoming the blood–brain tumor barrier for effective glioblastoma treatment." *Drug Resistance Updates* 19:1-12. doi: https://doi.org/10.1016/j.drup.2015.02.002.

Vandewynckel, Y. P., D. Laukens, A. Geerts, E. Bogaerts, A. Paridaens, X. Verhelst, S. Janssens, F. Heindryckx, and H. Van Vlierberghe. 2013. "The paradox of the unfolded protein response in cancer." *Anticancer Res* 33 (11):4683-94.

Vega, Eleanor A., Michael W. Graner, and John H. Sampson. 2008. "Combating immunosuppression in glioma." *Future oncology (London, England)* 4 (3):433-442. doi: 10.2217/14796694.4.3.433.

Verhaak, Roel G. W., Katherine A. Hoadley, Elizabeth Purdom, Victoria Wang, Yuan Qi, Matthew D. Wilkerson, C. Ryan Miller, Li Ding, Todd Golub, Jill P. Mesirov, Gabriele Alexe, Michael Lawrence, Michael O'Kelly, Pablo Tamayo, Barbara A. Weir, Stacey Gabriel, Wendy Winckler, Supriya Gupta, Lakshmi Jakkula, Heidi S. Feiler, J. Graeme Hodgson, C. David James, Jann N. Sarkaria, Cameron Brennan, Ari Kahn, Paul T. Spellman, Richard K. Wilson, Terence P. Speed, Joe W. Gray, Matthew Meyerson, Gad Getz, Charles M. Perou, D. Neil Hayes, and Network Cancer Genome Atlas Research. 2010. "Integrated genomic analysis identifies clinically relevant subtypes of glioblastoma characterized by abnormalities in PDGFRA, IDH1, EGFR, and NF1." *Cancer cell* 17 (1):98-110. doi: 10.1016/j.ccr.2009.12.020.

Wang, Qianghu, Baoli Hu, Xin Hu, Hoon Kim, Massimo Squatrito, Lisa Scarpace, Ana C. deCarvalho, Sali Lyu, Pengping Li, Yan Li, Floris Barthel, Hee Jin Cho, Yu-Hsi Lin, Nikunj Satani, Emmanuel Martinez-Ledesma, Siyuan Zheng, Edward Chang, Charles-Etienne Gabriel Sauvé, Adriana Olar, Zheng D. Lan, Gaetano Finocchiaro, Joanna J. Phillips, Mitchel S. Berger, Konrad R. Gabrusiewicz, Guocan Wang, Eskil Eskilsson, Jian Hu, Tom Mikkelsen, Ronald A. DePinho, Florian Muller, Amy B. Heimberger, Erik P. Sulman, Do-Hyun Nam, and Roel G. W. Verhaak. 2017. "Tumor Evolution of Glioma-Intrinsic Gene Expression Subtypes Associates with Immunological Changes in the Microenvironment." *Cancer Cell* 32 (1):42-56.e6. doi: https://doi.org/10.1016/j.ccell.2017.06.003.

Wang, Qin, Hisaka Kurita, Vinicius Carreira, Chia-I Ko, Yunxia Fan, Xiang Zhang, Jacek Biesiada, Mario Medvedovic, and Alvaro Puga. 2015. "Ah Receptor Activation by Dioxin Disrupts Activin, BMP, and WNT Signals During the Early Differentiation of Mouse Embryonic Stem Cells and Inhibits Cardiomyocyte Functions." *Toxicological Sciences* 149 (2):346-357. doi: 10.1093/toxsci/kfv246.

Wang, T. T. Y., Q. Pham, and Y. S. Kim. 2018. "Elucidating the Role of CD84 and AHR in Modulation of LPS-Induced Cytokines Production by Cruciferous Vegetable-Derived Compounds Indole-3-Carbinol and 3,3'-Diindolylmethane." *Int J Mol Sci* 19 (2). doi: 10.3390/ijms19020339.

Wang, Xian-Feng, Hong-Sheng Wang, Hao Wang, Fan Zhang, Ke-Fang Wang, Qiang Guo, Ge Zhang, Shao-Hui Cai, and Jun Du. 2014. "The role of indoleamine 2,3-dioxygenase (IDO) in immune tolerance: Focus on macrophage polarization of THP-1 cells." *Cellular Immunology* 289 (1):42-48. doi: https://doi.org/10.1016/j.cellimm.2014.02.005.

Weatherbee, Jessica L., Jean-Louis Kraus, and Alonzo H. Ross. 2016. "ER stress in temozolomide-treated glioblastomas interferes with DNA repair and induces apoptosis." *Oncotarget* 7 (28):43820-43834. doi: 10.18632/oncotarget.9907.

Wei, Xiaoli, Xishan Chen, Man Ying, and Weiyue Lu. 2014. "Brain tumor-targeted drug delivery strategies." *Acta Pharmaceutica Sinica B* 4 (3):193-201. doi: https://doi.org/10.1016/j.apsb.2014.03.001.

Weller, M., J. Rieger, C. Grimmel, E. G. Van Meir, N. De Tribolet, S. Krajewski, J. C. Reed, A. von Deimling, and J. Dichgans. 1998. "Predicting chemoresistance in human malignant glioma cells: the role of molecular genetic analyses." *Int J Cancer* 79 (6):640-4. doi: 10.1002/(sici)1097-0215(19981218)79:6<640::aid-ijc15>3.0.co;2-z.

Wu, Chenchun, Shuran Yu, Qianxia Tan, Peng Guo, and Huining Liu. 2018. "Role of AhR in regulating cancer stem cell–like characteristics in choriocarcinoma." *Cell Cycle* 17 (18):2309-2320. doi: 10.1080/15384101.2018.1535219.

Wu, Megan, Jennifer Guan, Chris Li, Simon Gunter, Labeeba Nusrat, Sheena Ng, Karan Dhand, Cindi Morshead, Albert Kim, and Sunit Das. 2017. "Aberrantly activated Cox-2 and Wnt signaling interact to maintain cancer stem cells in glioblastoma." *Oncotarget* 8 (47):82217-82230. doi: 10.18632/oncotarget.19283.

Yang, Li, and Yi Zhang. 2017. "Tumor-associated macrophages: from basic research to clinical application." *Journal of Hematology & Oncology* 10:58. doi: 10.1186/s13045-017-0430-2.

Yeung, YT, KL McDonald, T Grewal, and L Munoz. 2013. "Interleukins in glioblastoma pathophysiology: implications for therapy." *British Journal of Pharmacology* 168 (3):591-606. doi: 10.1111/bph.12008.

Yoshida, Hiderou, Toshie Matsui, Akira Yamamoto, Tetsuya Okada, and Kazutoshi Mori. 2001. "XBP1 mRNA Is Induced by ATF6 and Spliced by IRE1 in Response to ER Stress to Produce a Highly Active Transcription Factor." *Cell* 107 (7):881-891. doi: https://doi.org/10.1016/S0092-8674(01)00611-0.

Young, Richard M., Aria Jamshidi, Gregory Davis, and Jonathan H. Sherman. 2015. "Current trends in the surgical management and treatment of adult glioblastoma." *Annals of Translational Medicine* 3 (9):121. doi: 10.3978/j.issn.2305-5839.2015.05.10.

Zhan, T., N. Rindtorff, and M. Boutros. 2017. "Wnt signaling in cancer." *Oncogene* 36 (11):1461-1473. doi: 10.1038/onc.2016.304.

Zhang, Michael, Gregor Hutter, Suzana A. Kahn, Tej D. Azad, Sharareh Gholamin, Chelsea Y. Xu, Jie Liu, Achal S. Achrol, Chase Richard, Pia Sommerkamp, Matthew Kenneth Schoen, Melissa N. McCracken, Ravi Majeti, Irving Weissman, Siddhartha S. Mitra, and Samuel H. Cheshier. 2016. "Anti-CD47 Treatment Stimulates Phagocytosis of Glioblastoma by M1 and M2 Polarized Macrophages and Promotes M1 Polarized Macrophages In Vivo." *PLOS ONE* 11 (4):e0153550. doi: 10.1371/journal.pone.0153550.

Zhang, X., Y. Song, Y. Wu, Y. Dong, L. Lai, J. Zhang, B. Lu, F. Dai, L. He, M. Liu, and Z. Yi. 2011. "Indirubin inhibits tumor growth by antitumor angiogenesis via blocking VEGFR2-mediated JAK/STAT3 signaling in endothelial cell." *Int J Cancer* 129 (10):2502-11. doi: 10.1002/ijc.25909.

Zhou, Wenchao, Susan Q. Ke, Zhi Huang, William Flavahan, Xiaoguang Fang, Jeremy Paul, Ling Wu, Andrew E. Sloan, Roger E. McLendon, Xiaoxia Li, Jeremy N. Rich, and Shideng Bao. 2015. "Periostin secreted by glioblastoma stem cells recruits M2 tumour-associated macrophages and promotes malignant growth." *Nature Cell Biology* 17:170. doi: 10.1038/ncb3090.

Zhu, Huaiyang, Lina Leiss, Ning Yang, Cecilie B. Rygh, Siddhartha S. Mitra, Samuel H. Cheshier, Irving L. Weissman, Bin Huang, Hrvoje Miletic, Rolf Bjerkvig, Per Ø Enger, Xingang Li, and Jian Wang. 2017. "Surgical debulking promotes recruitment of macrophages and triggers glioblastoma phagocytosis in combination with CD47 blocking immunotherapy." *Oncotarget* 8 (7):12145-12157. doi: 10.18632/oncotarget.14553.

Zolezzi, Juan M., and Nibaldo C. Inestrosa. 2017. "Wnt/TLR Dialog in Neuroinflammation, Relevance in Alzheimer's Disease." *Frontiers in Immunology* 8 (187). doi: 10.3389/fimmu.2017.00187.

Zong, Hui, Luis F. Parada, and Suzanne J. Baker. 2015. "Cell of origin for malignant gliomas and its implication in therapeutic development." *Cold Spring Harbor perspectives in biology* 7 (5):a020610. doi: 10.1101/cshperspect.a020610.

Zong, Hui, Roel G. W. Verhaak, and Peter Canoll. 2012. "The cellular origin for malignant glioma and prospects for clinical advancements." *Expert review of molecular diagnostics* 12 (4):383-394. doi: 10.1586/erm.12.30.